09:13:33 OCA PAD INITIATION - PROJECT HEADER INFORMATION 08/07/89

Active

Project #: E-21-F51 Cost share #: Rev #: 0
Center # : 10/24-6-R6777-0A0 Center shr #: OCA file #:
Work type : RES
Contract#: 0120046 Mod #: Document : PO
Prime #: Contract entity: GTRC

Subprojects ? : Y
Main project #:

Project unit: EE Unit code: 02.010.118
Project director(s):
JOY E B EE (404)894-2936

Sponsor/division names: ITT GILFILLAN / VAN NUYS, CA
Sponsor/division codes: 208 / 034

Award period: 890714 to 891020 (performance) 891020 (reports)

Sponsor amount	New this change	Total to date
Contract value	10,000.00	10,000.00
Funded	10,000.00	10,000.00
Cost sharing amount		0.00

Does subcontracting plan apply ?: N

Title: ANTENNA CONCEPTS FOR RECEIVE-ONLY, UHF, SHIPBOARD RADAR

PROJECT ADMINISTRATION DATA

OCA contact: Don S. Hasty 894-4820

Sponsor technical contact

WALTER WEISS, EXT. 5257
(818)988-2600
ITT GILFILLAN

Sponsor issuing office

R.N. HISEY, S/C ADMINISTRATOR
(818)904-2461
ITT GILFILLAN
7821 ORION AVE., MAIL STOP 96
VAN NUYS, CA. 91409-7713

Security class (U,C,S,TS) : U ONR resident rep. is ACO (Y/N): N
Defense priority rating : N/A N/A supplemental sheet
Equipment title vests with: Sponsor GIT
NONE PROPOSED.

Administrative comments -
FIRM FIXED PRICE PURCHASE ORDER. SUBPROJECT IS A-8417/RYAN-ECSL FOR $[illegible],000
BUDGET FOR THIS MAIN PROJECT IS $5,000.

GEORGIA INSTITUTE OF TECHNOLOGY
OFFICE OF CONTRACT ADMINISTRATION

NOTICE OF PROJECT CLOSEOUT

SK, 003

Closeout Notice Date 03/30/90

Project No. E-21-F51 Center No. 10/24-6-R6777-0A0

Project Director JOY E B School/Lab EE

Sponsor ITT GILFILLAN/VAN NUYS, CA

Contract/Grant No. 0120046 Contract Entity GTRC

Prime Contract No.

Title ANTENNA CONCEPTS FOR RECEIVE-ONLY, UHF, SHIPBOARD RADAR

Effective Completion Date 900130 (Performance) 900130 (Reports)

Closeout Actions Required:	Y/N	Date Submitted
Final Invoice or Copy of Final Invoice	Y	
Final Report of Inventions and/or Subcontracts	N	
Government Property Inventory & Related Certificate	N	
Classified Material Certificate	N	
Release and Assignment	N	
Other	N	

Comments

Subproject Under Main Project No.

Continues Project No.

Distribution Required:

Project Director	Y
Administrative Network Representative	Y
GTRI Accounting/Grants and Contracts	Y
Procurement/Supply Services	Y
Research Property Managment	Y
Research Security Services	N
Reports Coordinator (OCA)	Y
GTRC	Y
Project File	Y
Other	N
	N

E-21-F51

ITT GILFILLAN Contract
ANTENNA CONCEPTS FOR RECEIVE-ONLY, UHF, SHIPBOARD RADAR

Monthly Progress Report
Georgia Tech Project E-21-F51
For the Period
July 14, 1989 through August 31, 1989

Prepared For

ITT GILFILLAN
7821 Orion Avenue
P.O. Box 7713
Van Nuys, California 91409-7713

Prepared By

Edward B. Joy
Antenna Laboratory
School of Electrical Engineering
Georgia Institute of Technology
Atlanta, Georgia 30332-0250

Progress

During the first report period of the contract telephone contacts were made to Mr. Dennis Tschudi to discuss the technical requirements for the antenna.

A literature search was begun to identify currently existing, UHF, Receive Only, Shipboard Radar Antennas.

A call was received from ITT to stop all work on the contract pending a possible funding problem.

E-21-F51

ITT GILFILLAN Contract
ANTENNA CONCEPTS FOR RECEIVE-ONLY, UHF, SHIPBOARD RADAR

Monthly Progress Report
Georgia Tech Project E-21-F51
For the Period
September 1, 1989 through September 30, 1989

Prepared For

ITT GILFILLAN
7821 Orion Avenue
P.O. Box 7713
Van Nuys, California 91409-7713

Prepared By

Edward B. Joy
Antenna Laboratory
School of Electrical Engineering
Georgia Institute of Technology
Atlanta, Georgia 30332-0250

Progress

No progress was made on the contract during the month of September 1989 pending resolution of the possible change in the project duration and funding.

A modification was made to the contract during September which extended the project to January 31, 1989. It was planned to defer all remaining effort on the project to the months of November 1989, December 1989 and January 1990.

E-21-F51

ITT GILFILLAN Contract
ANTENNA CONCEPTS FOR RECEIVE-ONLY, UHF, SHIPBOARD RADAR

Monthly Report
Georgia Tech Project E-21-F51
For the Period
October 1, 1989 through October 31, 1989

Prepared For

ITT GILFILLAN
7821 Orion Avenue
P.O. Box 7713
Van Nuys, California 91409-7713

Prepared By

Edward B. Joy
Antenna Laboratory
School of Electrical Engineering
Georgia Institute of Technology
Atlanta, Georgia 30332-0250

Progress

No progress was made on the contract during the month of October 1989 as per scheduled project extension.

E-21-F51

GEORGIA INSTITUTE OF TECHNOLOGY
SCHOOL OF ELECTRICAL ENGINEERING
ATLANTA, GEORGIA 30332

TELEPHONE: (404) 894-

February 20, 1990

Mr. R. N. Hisey
Subcontract Administrator
ITT Gilfillan
7821 Orion Avenue
M/S 96
Van Nuys, California 91409-7713

SUBJECT: Purchase Order No. 0120046
E21-F51

Dear Mr. Hisey:

Enclosed please find a copy of Monthly Progress Reports for the period November 1, 1989 to November 30, 1989 and December 1, 1989 to December 31, 1989.

If you have any questions, please feel free to contact me at (404) 894-7337.

Sincerely,

Kathy Knighton
Administrative Supervisor

KK/kcl
Enclosures

cc: Dr. E.B. Joy

ITT GILFILLAN Contract
ANTENNA CONCEPTS FOR RECEIVE-ONLY, UHF, SHIPBOARD RADAR

Monthly Progress Report
Georgia Tech Project E-21-F51
For the Period
November 1, 1989 through November 30, 1989

Prepared For

ITT GILFILLAN
7821 Orion Avenue
P.O. Box 7713
Van Nuys, California 91409-7713

Prepared By

Edward B. Joy
Antenna Laboratory
School of Electrical Engineering
Georgia Institute of Technology
Atlanta, Georgia 30332-0250

During the month of November various antennas were examined for suitability for the proposed broadband, UHF, circularly polarized phased array. The following antenna types were studied:

1) Planar Spiral
2) Conical Spiral
3) Crossed Log Periodic Dipole Array (LPDA)
4) Crossed Back Fire Log Periodic Dipole Array
5) Crossed Printed Circuit Board Notches
6) Dual Ridged Square Horn
7) Crossed Bow Tie Dipoles Above Ground Plane
8) Axial Mode Helix

These antennas are all circularly polarized and are in common use in the UHF region. The antennas are further subdivided according to achievable bandwidth:

A) 400 MHz to 2.6 GHz (6.5 to 1 Frequency Ratio)
   1) Planar Spiral
   2) Conical Spiral
   3) Crossed LPDA

B) 400 MHZ to 900 MHz (2.25 to 1 Frequency Ratio)
   1) Crossed Back Fire Log Periodic Dipole Array
   2) Crossed Printed Circuit Board Notches
   3) Dual Ridged Square Horn
   4) Crossed Bow Tie Dipoles Above Ground Plane

C) Less than a 2.25 to 1 Frequency Ratio
   1) Axial Mode Helix (1.6 to 1 Ratio)

The antenna types are next categorized by circularly polarized gain:

1) Axial Mode Helix (12 to 20 dBi)
2) Crossed LPDA (7 to 10 dBi)
3) Crossed Backfire LPDA (6 to 9 dBi)
4) Dual Ridged Square Horn (3 to 10 dBi)
5) Crossed Bow Tie Dipole Above Ground Plane (2 to 5 dBi)
6) Crossed Printed Circuit Board Notches (2 to 5 dBi)
7) Conical Spiral (3 dBi)
8) Planar Spiral (0 dBi)

The desirability of using the Crossed LPDA is apparent.

ITT GILFILLAN Contract
ANTENNA CONCEPTS FOR RECEIVE-ONLY, UHF, SHIPBOARD RADAR

Monthly Report
Georgia Tech Project E-21-F51
For the Period
December 1, 1989 through December 31, 1989

Prepared For

ITT GILFILLAN
7821 Orion Avenue
P.O. Box 7713
Van Nuys, California 91409-7713

Prepared By

Edward B. Joy
Antenna Laboratory
School of Electrical Engineering
Georgia Institute of Technology
Atlanta, Georgia 30332-0250

During the month of December various feed networks were examined for suitability. The key requirements for the feed networks are a) wideband operation (400 Mhz to 2.6 GHz preferable or 400 MHz to 900 MHz minimal), b) minimal switching, c) low loss, and d) single or multiple simultaneous beams. The following feed systems were studied:

1) Rotman Lens
2) R-2R Lens
3) R-KR Lens
4) Butler Matrix
5) Blass Matrix
6) Adaptations of 5) and 6) for Cylindrical Arrays

Lens feed systems have the advantage of not requiring the same number of array elements as beam positions, thus the array might have only 45 elements but could achieve say 60 discrete beams without variable phase shifters. This system would require only 60 SPST switches per receiver to connect the receiver(s) to one of the beam position ports of the lens.

Lens feed systems use electrical path length and geometry to insure the proper path length (phase shift) from the feed point to each element of a cylindrical array. Thus the lens size must be some multiplying constant times the size of the array. The array in this case will be on the order of 25 feet in diameter, thus the lens can be expected to be on this same order. The diameter of the R-2R lens for example is one half the size of the diameter of the array. The diameter of the R-KR lens, in its most used form, is 1.9 times the diameter of the lens, perhaps bigger than the ship's beam. The sizes of lens can be reduced for receiving applications through the use of frequency translation. The frequency of the signal passing through the lens need not be the same as the array frequency if a mixer, perhaps preceded by a low noise amplifier, is placed at the output of each array element and before the lens. Thus the frequency of the signal passing through the lens can be higher or lower than the frequency of the signal passing through the array elements. If the lens frequency is made higher than the array frequency, the lens must be smaller to produce the same phase shift.

Frequency translation will be required if the diameter of the array varies with frequency, as it would in a circular array of log periodic dipole arrays (LPDAs). The electrical diameter of a LPDA array decreases with increasing frequency. Thus the size of any lens feed system would likewise need to decrease with increasing frequency. Physical lens do not, however, decrease with increasing frequency. Frequency translation can be used again to provide a lens with decreasing electrical size with increasing frequency. The local oscillator frequency would be made to increase with increasing array frequency and the difference frequency, out of the array element mixers, would be passed through the lens. Thus the lens would look smaller as the array frequency increased. This is the case of a variable intermediate frequency. The receiver would

tune to the variable intermediate frequency, tuning to low intermediate frequencies to listen to high array frequencies.

Network type feed systems provide the required amplitude (normally constant for each element) and phase (normally a cylindrical phase front) for each element. The normal configuration is to provide excitation for N elements with N input ports of the network. The N by N networks have simpler realizations than N by M networks. The inputs to an N by N networks can be pre-phase shifted by variable phase shifters to obtain 360 degree scanning of a single beam without switching. Such networks and phase shifters must provide amplitude levels independent of frequency and phase shifts which are exactly linearly increasing with frequency. Often networks and incorporated power dividers and phase shifters do not meet this requirement. Frequency translation can again be used, this time to keep the intermediate frequency constant for the amplitude and power division networks. The phase shifting part of the network would use phase shifters in the base oscillator in a phase lock loop frequency generator circuit. Such a phase lock loop system producing the desired frequency through multiplication of the base frequency could produce a phase shift exactly linear with frequency.

The R-KR lens is the only lens which can produce beams in all 360 degrees using a single lens. The adaptations of the Butler matrix feed systems to cylindrical array configurations including the required fixed cylindrical phase shifts can also be used to produce 360 degree beams.

E-21-F51

ITT GILFILLAN Contract
ANTENNA CONCEPTS FOR RECEIVE-ONLY, UHF, SHIPBOARD RADAR

Final Report
Georgia Tech Project E-21-F51
For the Period
July 14, 1989 through January 31, 1989

Prepared For

ITT GILFILLAN
7821 Orion Avenue
P.O. Box 7713
Van Nuys, California 91409-7713

Prepared By

Edward B. Joy
Antenna Laboratory
School of Electrical Engineering
Georgia Institute of Technology
Atlanta, Georgia 30332-0250

ANTENNA CONCEPTS FOR RECEIVE-ONLY
UHF SHIPBOARD RADAR

This study addressed various antenna concepts and associated feed networks for receive-only, UHF (400 MHz to 2.6 GHz), shipboard radar. The participants in this study were Drs. Larry E. Corey, Edward B. Joy and Charles E. Ryan, Jr. all from the Georgia Institute of Technology. This study was aided by input from Mr. Dennis Tschudi and Mr. Walter Weiss of ITT Gilfillan.

UHF Shipboard Radar Antennas

Attached is a listing of UHF Shipboard Radar Antennas found in the book "Shipboard Antennas". Most of the antennas are rotating reflector or rotating flat panel phased arrays. None found covered the wide frequency range required and none were electronically scanned for 360 degree azimuth coverage.

Cylindrical Arrays

The horizontal (in the plane of the circular array or in the cone of a small angle conical array) 3 dB beamwidth in degrees for a cylindrical array is given approximately by:

$$BW_{az} = 59/D$$

where D is the diameter of the array in wavelengths. Thus a beamwidth of 5.9 degrees would require a diameter of 10 wavelengths, which at 400 MHz would be 24.6 feet in diameter. The corresponding elevation beamwidth in degrees is given by:

$$BW_{el} = 202/SQRT(D)$$

where SQRT is the square root operation. A 10 wavelength diameter circular array would then produce an elevation beamwidth of 64 degrees.

Gain of the circular array is approximated as:

$$\text{Gain} = 39{,}000/(BW_{az}\ BW_{el})$$

which for the above calculated beamwidths, is a gain of 20 dBi.

It is anticipated, based on the few existing cylindrical arrays, that side lobe levels approximately 20 dB below the main beam peak can be realized in an cylindrical array. Likewise, it is anticipated that beam cross over points will be in the range from 3 to 4 dB below the main beam peaks.

Broadband UHF Array Elements

Several circularly polarized, UHF, broadband, antenna types were considered for array application including: planar spiral, conical spiral, printed circuit board notch, double ridge horn, axial mode helix, log periodic dipole array and back fire log periodic dipole array. The axial mode helix can only achieve a bandwidth of 1.6 to one, the double ridge horn and the printed circuit board notch can achieve a bandwidth of 4 to one. The spirals and log periodic dipole array can achieve a bandwidth of 10 to one. The back fire log periodic is limited to a bandwidth of 2.5 to one. Sinuous antennas such as the Tecom Type 201600 described in the attached specification sheet have bandwidth capabilities similar to the spirals.

The back fire log periodic array is not a common antenna. The normal log periodic dipole array is an endfire array with main beam directed toward the short element end of the array. The short

elements, which are all less than one half wavelength at the operating frequency, produce very little scattering cross section to the forward propagating wave. The back fire, log periodic dipole array produces a main beam in the direction of the longer elements. The longer elements, which are all longer than one half wavelength at the operating frequency, achieve a large scattering cross section when they reach a length of approximately 1.4 wavelengths. This phenomena is shown in an attached figure from Harrington's Time-Harmonic Electromagnetic Fields book. Thus the back fire array is limited to frequency ranges such that the longer elements remain less than 1.4 wavelengths long for all operating frequencies. Several back fire log periodic arrays have been designed, constructed and tested at Georgia Tech with good gain and pattern over the limited 2.5 to one bandwidth. The gain is approximately 1 dB less than for the forward fire and the back lobe is only 10 dB down as compared to approximately 20 dB down for the forward fire configuration. The impedance variations are similar to the forward fire case, the VSWR typically remaining under 2 to one over the antenna operating bandwidth.

Array elements must also have physical size less than approximately one wavelength at the highest operating frequency to be used in an array in which it is desired to produce no grating lobes. The planar spiral has a diameter of approximately one third of a wavelength at the lowest operating frequency and is therefore limited to a frequency range of approximately 2.5 to one for use in a broadside broadband array. The frequency range is further reduced in a circular array as side elements will be steered to almost 90 degrees and thus will produce a grating lobe even with half wavelength spacing. It is estimated that the frequency range for planar spirals used in a circular array will be limited to 2 to one. The frontal size of a crossed notch element is approximately one fourth of a wavelength at the lowest operating frequency. Thus it might achieve a 4 to one frequency range in a

broadside planar array and approximately 2.5 to one in a circular array. The log periodic dipole array and backfire log periodic dipole array have frontal dimension of one half wavelength and require a minimum spacing of 0.7 wavelength spacing for good array performance. The center of radiation in a log periodic array moves toward the short element end of the array as the frequency increases. Thus if log periodic dipole arrays are arranged in a circle with the small element end of the arrays pointing toward the center of the circle, the 0.7 wavelength spacing between the centers of radiation is maintained at all frequencies. See an attached figure of such an array of log periodic dipole arrays from the Antenna Engineering Handbook. Grating lobes which might appear at wide angles are suppressed by the narrow beamwidth (typically 60 degree, 3dB beamwidth) of the log periodic dipole array.

Circular polarization is achieved naturally using a spiral. The sense of the spiral winding is the sense of the circular polarization. Spirals may be wound in either direction. The polarization sense of a spiral may also be reversed by feeding from the ends of the spiral arms instead of the normal center feed point. The printed circuit board notch requires two crossed notches, a power divider and an 90 degree frequency independent phase shifter to form circular polarization. Likewise the double ridged horn requires the power divider and phase shifter. The log periodic dipole array can be circularly polarized by mounting vertical dipoles on the same center twin lead transmission line as the horizontal dipole. The vertical dipoles are spaced with a tau factor equal to the square root of the tau factor for the horizontal dipoles, however. Thus a crossed dipole array is formed which produces circular polarization without the need for a power divider or phase shifter. Another way to produce circular polarization is through the use of a meander line polarizer grid placed in front of a linearly polarized antenna. Multilayer grids have produced acceptable performance over a frequency range as

large as 4 to one with some loss in gain. A multilayer polarizer grid will be large, thick and bulky at UHF, however.

The gain of the elements is also important in the overall gain of the array. The gain of the planar spiral, backed with a resistive cavity is approximately -1 dBi. The gain of a circular polarized notch, including losses in the power divider and phase shifter, is estimated to be 0 dBi. The gain of a circularly polarized, log periodic dipole array, of the large tau design, is 10 dBi. The gain of a similar, back fire, circularly polarized, log periodic dipole array is estimated to be 9 dBi.

Beamformer Networks

Several beamformer networks have been investigated to feed a circular array: The Rotman lens, the R-2R lens, the R-KR lens as well as the Butler, Blass and other matrix feed systems. The lens systems use the fact that the array is of constant radius. The corresponding lens size is related to the size of the constant radius antenna. The matrix systems, however, do not use geometry to create the proper cylindrical phasing, instead they employ fixed phase shifters to achieve the proper cylindrical phase, with additional variable amounts of phase shift for beam steering. The phase shift through the phase shifters must increase linearly with frequency for wide band operation.

The Rotman lens can be configured to work over a 90 degree sector with equal beamwidth beams. The R-2R lens is capable of full 360 degree coverage but when multiple simultaneous beams are required the coverage is reduced to 90 degrees. The R-2R lens diameter is one half the diameter of the array. The R-KR lens is capable of true 360 degree coverage with multiple simultaneous beams. A K value of 1.9 is chosen for best performance. This choice makes the diameter of the lens 1.9 times the diameter of the

array. The diameter of the lens can be reduced by using a lens with dielectric constant greater than air. The size of the lens can be reduced by the square root of the dielectric constant. Higher loss is normally associated with higher dielectric constant material, however. See the attached 1984 Microwave Journal article which discusses these various feed systems for circular arrays. The Rotman, R-2R and R-KR lenses are capable of wideband operation and could be configured in strip line or microstrip configuration at the UHF frequencies for lowest loss. Ohmic losses are expected to dominate over manufacturing and missmatch losses and could be as large as 3 dB for the size anticipated. There should be very little directivity loss, however.

Should the diameter of the cylindrical array vary with frequency, as is the case with a circular array of log periodic dipole arrays, the lens feed systems will not work unless the lens diameter varies in the same way. It is suggested that the electrical size of the lens could be made to vary by changing the frequency of the signal passing through the lens. The frequency can be changed by having a mixer at the output of each array element and adjusting the local oscillator frequency to produce the required frequency. The lens frequency should decrease with increasing array frequency for the case in which the array diameter decreases with increasing array frequency.

The Butler and Blass networks were originally developed for linear arrays, but have been applied to cylindrical arrays. These matrix networks with the addition of fixed cylindrical phase delays and commutating switches can be used to feed portions of a cylindrical array to produce single beam patterns, but with the power loss and cost associated with the required switching. Matrix methods of feeding circular symmetric arrays are discussed in an attached paper by Provencher. Another attached paper by Sheleg shows that a Butler matrix fed circular array can be steered by

variable phase shifters in addition to the fixed phase shifters. The matrix feed techniques require that the phase shift of the phase shifters vary linearly with frequency for wide band operation.

The phase shifters need only work at a single frequency if a mixer is employed at each array element. The local oscillator frequency is synthesized as multiples of some base frequency. The phase shifters shift the phase of the base frequency oscillator such that through the multiplying process the phase increases linearly proportional to frequency.

Array Configuration

It seems possible that a circular array of log periodic dipole arrays could produce a circular polarization, 20 dBi gain, constant pattern, and constant input impedance over the frequency range from 400 MHz to 2.6 GHz. The array would be a conical wedge array in which the lower surface of the conical wedge is at an angle of 28 degrees from horizontal and the upper surface of the conical wedge is at an angle of 12 degress from horizontal. The conical wedge would house two conical arrays of log periodic dipole arrays, the lower log periodic dipole array would be located at a cone angle of 24 degrees from horizontal and the upper conical array would be located at a cone angle of 16 degrees from horizontal. The center of the cone must be hollow, however, as the main beams of all the log periodic arrays would pass through this center point. Thus the array would have to be mounted at the top of a mast or the top of the deckhouse or gun turret, etc. The array would have a diameter of 24.6 feet plus any radome covering and would contain a phased array of 2 by 45 log periodic dipole arrays. Each log periodic dipole array would be approximately 12 feet in length. The cylindrical array would have two elements in elevation to form two beams in elevation and 45 elements in azimuth. A mixer (preceeded

by a low noise amplifier, perhaps) is attached to each log periodic dipole array and a local oscillator signal of the desired frequency supplied to each mixer. The difference output frequency of the mixer is fed into a R-KR feed network. Each output port of the R-KR lens is associated with an independent beam, each of which may be addressed separately or symultaneously. Each log periodic dipole array would occupy an eight degree sector in azimuth and an eight degree sector in elevation of the circular array. There would be two feed networks, one for the upper conical array and one for the lower conical array. One feed network can be eliminated if a switch is used to select the upper or lower array or perhaps the sum or differnce port of a hybrid tee connected to the upper and lower conical arrays. The feed network(s) would be located below the antenna cone. Some early work on a semi-circular array of log periodic dipole arrays was reported by DuHammel and Berry in an attached paper. One of their conclusions was that a frequency independent gain of 20 dBi was feasible.

A back fire configuration is also possible, but would require two arrays, one to cover the 400 to 1000 MHz band and one to cover the 1.0 to 2.6 GHz band. Each cylindrical array would again be in a two level conical arrangement with the same number of elements in each. The cone would be inverted, however, such that the long element end of the log periodic dipole array would be pointing up 20 degrees. This configuration has the advantage that the center of the cone can be metal such as a mast and possibly even small stacks for the 400 to 1000 MHz band. The diameter of the center hole for the low band array would be approximately six feet. The high band (1.0 to 2.6 GHz) array would have a diameter of approximately 9.8 feet. Another advantage of this configuration is that one side of the antenna is not receiving signals which must propagate through the other side of the array, which might distort the pattern and change the polarization of the array.

Shipboard Siting

The 20 dBi gain requirement means that the UHF array will be physically large. The diameter will be approximately 25 feet which is approximately one half of the typical warship beam of 50 to 60 feet. The large size thus presents definite problems in siting the antenna. Blockage effects due to the ships superstructure need to be minimized to avoid beam distortions and gain loss.

The UHF array antenna will require a volume which is approximately the volume swept by the rotating AN/SPS-49 radar antenna as mounted on the FFG-7 and CG-47 class ships. Such an antenna could be mounted on a tower or mast if this does not adversely affect the ships's topside moment. However, for the FFG-7 and CG-47 ships this might require the removal of the AN/SPS-49 air search radar.

A "stack" mounted configuration has been suggested. However, this does not appear to be feasible since the stacks are typically not "single" stacks, but come in intake/outlet pairs for the gas turbine engines. This is typical for the CG-47, DD-963 and DDG-51 class ships. The FFG-7 has a cylinder shrouding the stacks, but that location is low with respect to the superstructure resulting in unacceptable blockage.

It may be possible to mount "half arrays" outrigged from either the stack structure or from the deckhouse for the DD-963 and CG-47 ships which have the same "split" deckhouse topside. This is not particularly attractive due to possible damage from heavy seas. The array "halves" might be mounted on the deckhouse next to the stacks, with some blockage.

It is most likely that this large UHF array antenna will require its own mast or mast outrigger. This can be accomplished,

but will probably require extensive rearrangement of the existing topsides. See the attached information on the DDG-51, FFG-7, DD-963 and CG-47.

Prototype Development

The Georgia Institute of Technology would be most interested in the design, contruction and measurement of a prototype of such antenna system.

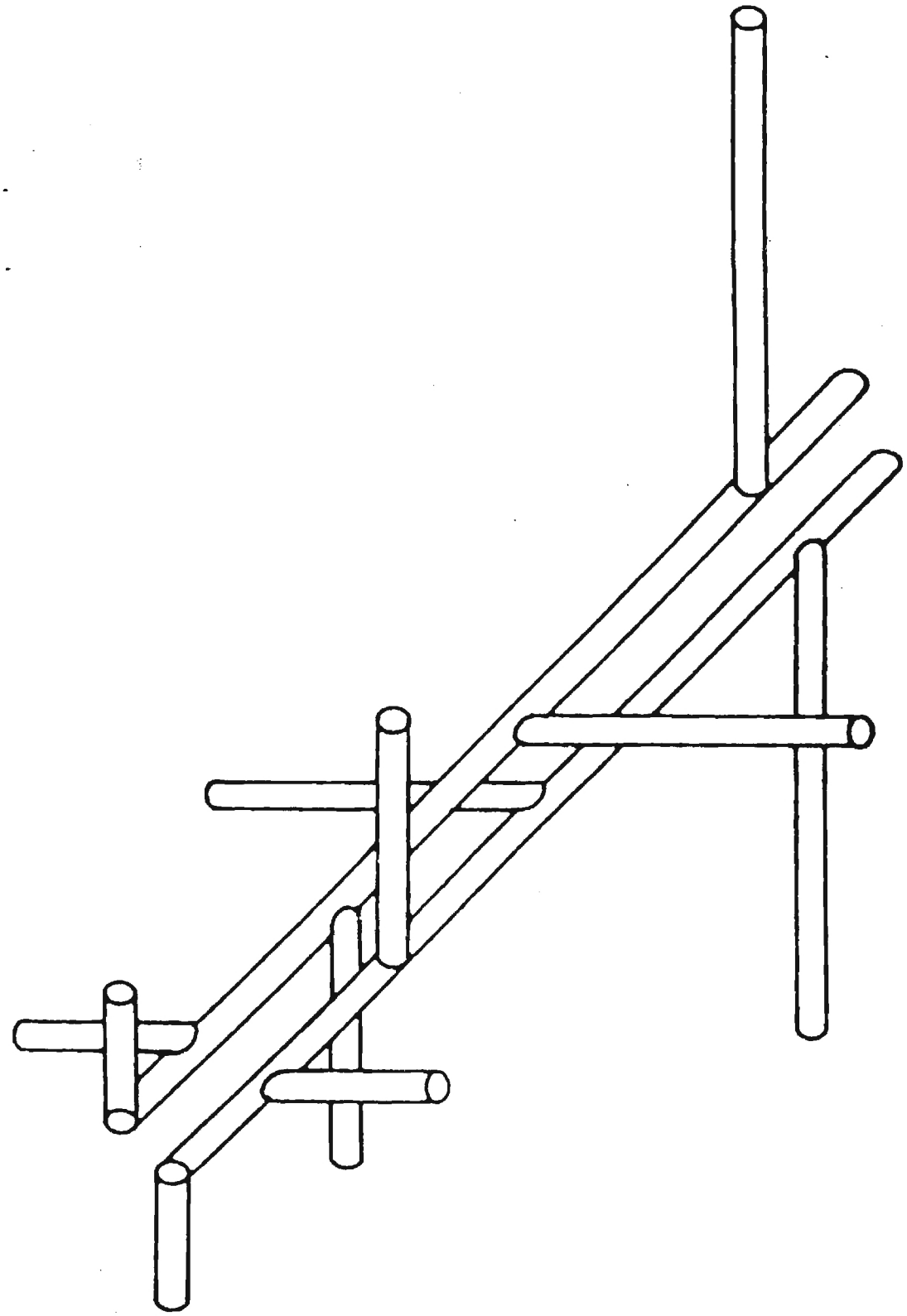

FIG. 14-37 View of circularly polarized crossed LP dipole arrays with a single feeder.

snow, *and* measuring the distance out to an object — doing far more than the human eye can do alone.[15] Moreover, during the forty years since becoming fully operational, radar development has never decreased in intensity, its design and application ever more sophisticated and complex. Higher transmitter power along with greatly improved antenna characteristics (higher gain, narrower beamwidths, lower sidelobes) allow vastly better resolution and accuracy than the now primitive equipment of World War II. But the tasks are tougher as the requirements levied upon radar in today's scenario have increased enormously. Whether it is civilian air traffic to be controlled or potential incoming anti-ship missiles to fend off, the demands for simultaneous detecting and tracking of closely spaced targets in all environments, from very great distances away to close in, strains the limits of imagination and technology. So fast must present-day reaction times be that in some applications radar sensors automatically activate other control systems, defensive weapons for example, completely by-passing human operators.

The U.S. Navy has over 1500 shipboard radars of nearly two dozen types in service, including long range 2-D and 3-D air search, surface search, aircraft control, harbor navigation, and weapons firing. By the mid-1980s the total number will increase to perhaps 2000, but with a refreshing decrease in the types, as projected by Figure 4-3.[17] As might be expected, there is a wide variety of radar antennas installed aboard Navy ships. Some are outmoded but still in use, many are of current inventory and some, such as the new AEGIS fixed, planar, phased-arrays, are representative of the latest antenna technology. Within the limits of non-classified information, examples of those types currently in service will be described.

4-1 SURVEILLANCE RADAR ANTENNAS

During the war years, as radar technology rapidly progressed, the varied equipment types resulted in categorization by primary function. There were radars used for long range air search, others for very close-in targets, some for covering high elevation angles, some for surface search, and still others needed principally for marine navigation. Gradually over the years, naval surveillance radars became segregated by purpose: two-dimensional air search, three-dimensional air search, surface search, and navigation.

4-1.1 2-D Air Search Radar Antennas

AN/SPS-6

The first of the improved, post-war long-range air search radars was the AN/SPS-6, a direct descendant of the models SR-3 and SR-6 which had been designed especially for high-angle detection of Kamikaze attacks in the Pacific theater.[16] Operating in the mid-UHF region (L-band), and originally procured in 1950, many of the later versions of the SPS-6 are still in service on older ships. A series of antennas has been used with equipment models of the SPS-6, beginning with the AS-402 (Figure 4-4), and followed by the AS-429 (Figure 4-5) and the AS-430A (Figure 4-6). All of these have since been replaced by the AS-430B shown in Figure 4-7 and described in detail below:

ANTENNA AS-430B/SPS-6C

a. TYPE/USE — The AS-430B is a directional transmit and receive antenna used with long-range air and surface search radar set AN/SPS-6C designed for shipboard operation to obtain target bearing and range information. Consisting of a dual-frequency feedhorn radiator, a wind balancing vane, and parabolic section reflector, the antenna has a 30° vertical beamwidth and a horizontal beamwidth of three and one-half degrees. The reflector assembly is a stainless steel frame which is ribbed and braced with fabricated stainless steel channel members and has a reflecting surface made of wire mesh. The dual feedhorn (radar and IFF) is silver plated stainless steel and has a fiberglass cover protecting the orifice. The entire assembly is supported by a pedestal which rotates the antenna at varying rpm's to supply target bearing data.
b. PHYSICAL CONFIGURATION — [See Figure 4-7].
c. DIMENSIONS — (1) Height: 95-⅞ inches (113-⅞ with pedestal); (2) Width: 204 inches; (3) Depth: 153-¾ inches; (4) Weight: 924 pounds (with pedestal).
d. FREQUENCY RANGE — 1250 to 1350 MHz (L-Band).
e. VSWR — Not to exceed 1.5:1 at the RF input.
f. POWER RATING — 750 kW peak.
g. POLARIZATION — Horizontal.
h. GAIN — 27 dB.
i. TYPE OF FEED — RG-132/W waveguide.
j. PRIMARY POWER REQUIRED — 115/230 vac, 60Hz.
k. REFERENCE — Technical Manual, Radar Set AN/SPS-6, NAVSEA 0967-114-8010.

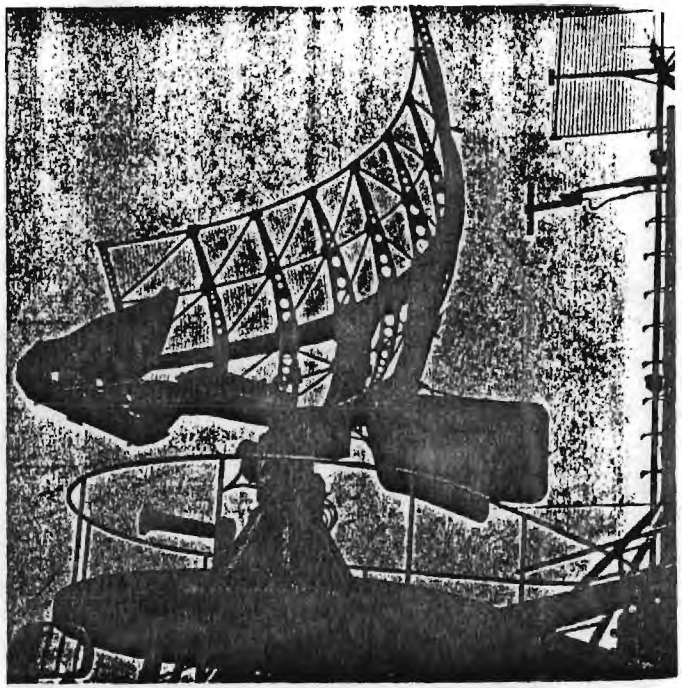

FIG. 4-7 AS-430B/SPS-6C 2-D Air Search

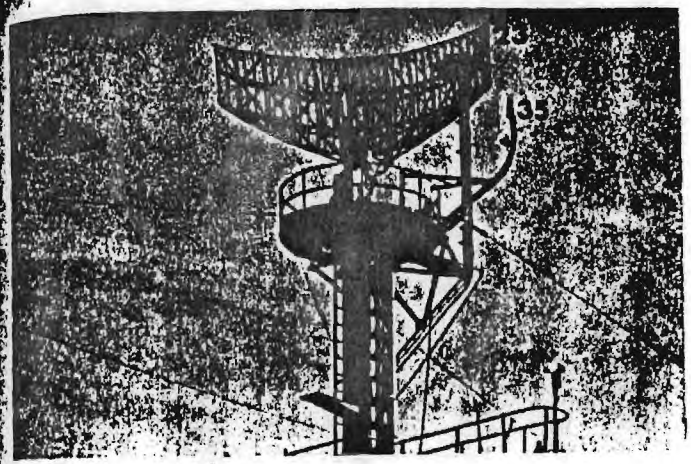

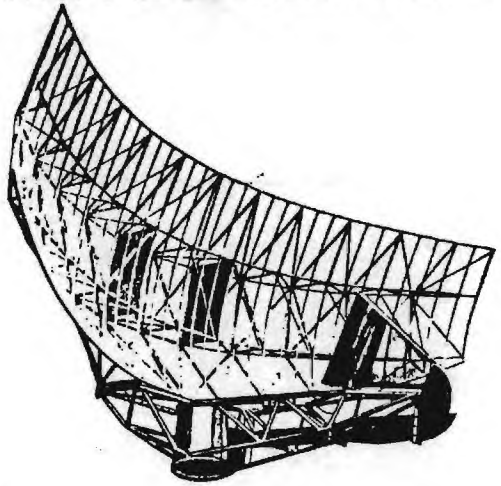

FIG. 4-8 AS-603/SPS-12 2-D Air Search Radar

AN/SPS-12

Shortly after the AN/SPS-6 equipment was purchased in the early 1950s, a second type of 2-D air search radar, the AN/SPS-12, was procured for fleet use. Operating at the same L-Band frequencies for long range target surveillance (out to 200 miles), the SPS-12, too, is now considered obsolete and being superseded by newer systems (refer to Fig. 4-3). Nevertheless, it is still found on a small number of naval ships. Its antenna, the AS-603 shown in shipboard configuration in Figure 4-8, has the following characteristics:

ANTENNA AS-603/SPS-12

a. TYPE/USE — The AS-603 is a directional, rotating, high gain antenna used with long range air and surface search radar set AN/SPS-12; designed for shipboard operation to obtain target bearing and range information. Consisting of a feedhorn exciter and parabolic section reflector, the antenna has a 30° cosecant-squared beam in the vertical plane and a three-degree beamwidth in the horizontal plane. The reflector assembly is an all-welded stainless steel frame of tubular construction with a reflector surface of welded wire mesh screening. The assembly rests on a tubular truss and drum support which bolts to the top of the rotary antenna pedestal. A vertically polarized antenna, the AT-388/SPS-12, is mounted in the mouth of the feedhorn for IFF use. To protect the dipole and horn interior from salt air and exhaust gas contaminates, a fiberglass cover is fitted over the front of the horn.
b. PHYSICAL CONFIGURATION — [See Figure 4-8].
c. DIMENSIONS — (1) Height: 92 inches (116 with pedestal); (2) Width: 205 inches; (3) Depth: 121 inches; (4) Weight: 990 pounds (with pedestal).
d. FREQUENCY RANGE — 1250 to 1350 MHz.
e. VSWR — Not to exceed 1.5:1 at RF input.
f. POWER RATING — 500 kW peak.
g. POLARIZATION — Horizontal.
h. GAIN — 25 dB.
i. TYPE OF FEED — CG-1027/U waveguide.
j. PRIMARY POWER REQUIRED — 440vac, 60Hz, three-phase.
k. REFERENCE — Technical Manual, Radar Set AN/SPS-12, NAVSEA-0967-069-2010.

AN/SPS-29

As reveiwed at the beginning of this chapter, the Navy, in its need for shipboard radar sets of manageable size (antennas in particular), had early centered its major research and development efforts around 200 MHz. Its first shipborne model, the XAF (Figure 4-2), operated at this frequency and from this experimental equipment came a long series of wartime successors including the CXAM, XAR, SA, SC-1, SK, and SR. Immediately following the war, the Navy was, for a time, required to give up the 200 MHz segment of the VHF band to the newly developing commercial television interests. By the mid-1950s, however, upon recognition of the merits of VHF radar for long range, high altitude detection, and the need for diversity of operation, the Navy won reassignment of the 200 MHz band for its uses.[19] Thereafter followed the development of the AN/SPS-17, which was superseded in turn by the AN/SPS-29 described below. The AN/SPS-29 is itself fast becoming obsolete (refer to Fig. 4-3).

ANTENNA AS-943/SPS-29

a. TYPE/USE — The AS-943 is a rotating planar array used with the shipborne AN/SPS-29 very long range air-search radar designed to detect the distance and bearing of remote targets. Arranged in four rows of seven horizontal radiators, there are 28 folded dipoles spaced one-half wavelength apart vertically and horizontally, and approximately 1/4 wavelength in front of a flat "bedspring" reflector, fabricated on an aluminum frame. The feed array leads from the rotating joint of the pedestal up to a tee assembly, where the power is divided equally to feed the top and bottom halves of the antenna. The power for each half of the antenna is further divided at the remainder of the dipoles on that branch of the feed array. The antenna input is tuned by a stub assembly between the input feed line and tee section. Internal construction of the dipoles provides for balun action and the impedance transformation necessary to obtain the proper current distribution for a highly directional beam. The antenna assembly is mounted on a rotatable pedestal and forms a radiation pattern having a 25.5° vertical beamwidth and 19° horizontal beamwidth. Provisions are made for installing a type AT-352/UPA IFF antenna above the radar reflector.
b. PHYSICAL CONFIGURATION — [See Figure 4-9].
c. DIMENSIONS — (1) Height: 102 inches (140 with pedestal); (2) Width: 210 inches; (3) Depth: 55 inches; (4) Weight: 1275 pounds (with pedestal).
d. FREQUENCY RANGE — 200 MHz VHF band.
e. INPUT IMPEDANCE — 50 ohms.
f. POWER RATING — 750 kW peak.
g. POLARIZATION — Horizontal.
h. GAIN — 18 dB.

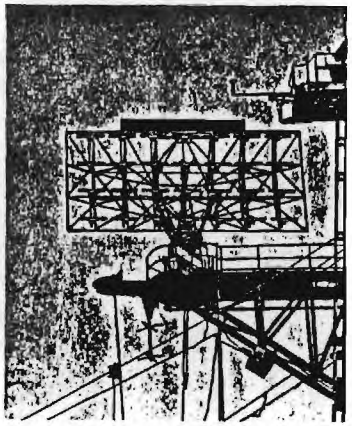

(a)

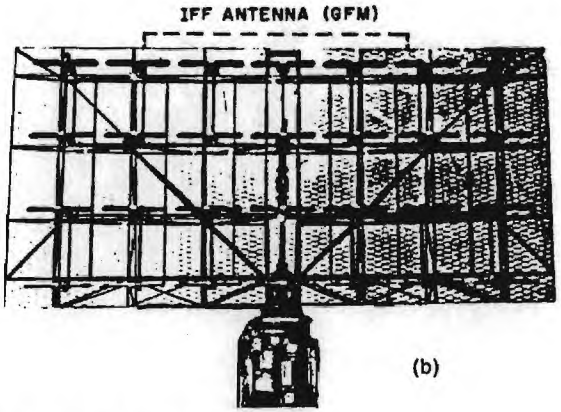

(b)

FIG. 4-9 AS-943/SPS-29 2-D Air Search Radar

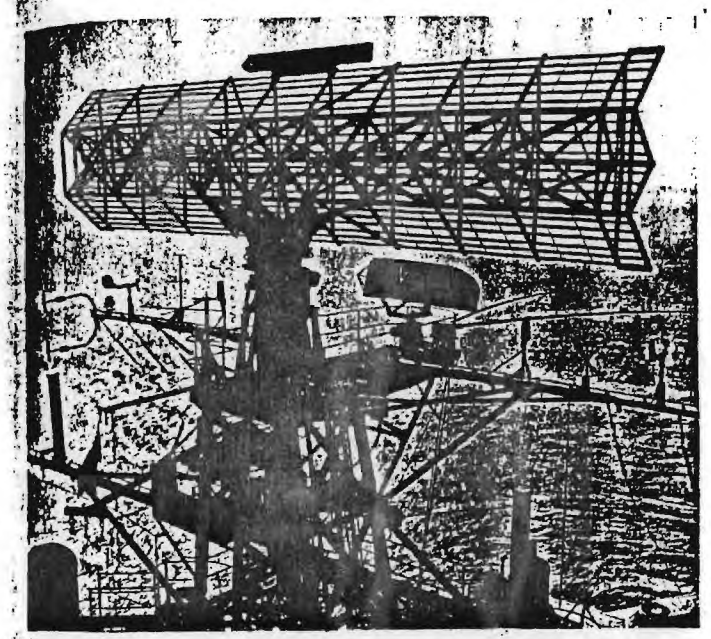

FIG. 4-10(a) AS-1092/SP 2-D Air Search Radar Top Of Mast Installation

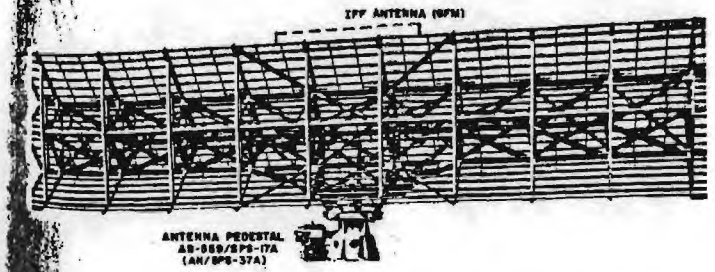

FIG. 4-10(b) AS-1092/SP 2-D Air Search Radar Physical Configuration

i. TRANSMISSION LINE TYPE — (1) Radar: RG-154/U; (2) IFF: RG-18/U.
j. PRIMARY POWER REQUIRED — 440 volt, three-phase, 60 Hz power for antenna drive motor. 115 volt, one-phase, 60 Hz for synchro reference and monitoring voltages.
k. INSTALLATION REQUIREMENTS — The antenna is secured to the turntable on the antenna pedestal, which is mounted to the ship's structure by four mounting pads each drilled for three ¾-inch bolts. The radar transmission line is pressurized with dry air from the system dehydrator unit.
l. SPECIAL CONSIDERATIONS — The area selected for the antenna installation must have 360° unobstructed clearance from ship's structures and rigging to accommodate the antenna swing circle. The location for the antenna should have maximum unobstructed azimuth coverage to limit shading or blind spots. Since the synchro system and ship's heading marker are adjustable through 360° the orientation of the antenna pedestal is not critical.
m. REFERENCES — (1) Technical Manual, AN/SPS-29 Radar Set, NAVSEA 0967-LP-057-0010. (2) NAVSEA Drawings RE-H2690237 and RE-H2690714. (3) AS-943/SPS-29, NAVSEA 0967-052-8280.

AN/SPS-37 and AN/SPS-43

Improvements in radar technology gave rise to development of the AN/SPS-37 and AN/SPS-43 as derivatives of the AN/SPS-29. Using a much wider pulse width, the SPS-37 and SPS-43 achieve a greater maximum detection range with one-third the peak RF power of the SPS-29. The antenna used with the SPS-37 and SPS-43 on most ships is the same as that used for the SPS-29, i.e., the AS-943 planar dipole array (broadbanded and redesignated the AS-1091 for the SPS-43, but otherwise identical to the AS-943). For very large ships, such as heavy cruisers and aircraft carriers, the SPS-37A and SPS-43A versions are used, both of which employ the larger (40-ft. long) AS-1092/SP shown in Figure 4-10 and described below:

ANTENNA AS-1092/SP

a. TYPE/USE — The AS-1092 is a rotating dipole array used with either the AN/SPS-27A or the AN/SPS-43A very long range air-search radars designed to detect the distance and bearing of remote targets. The antenna has a double corner reflector, one stacked upon the other, to form a W shaped cross-section. In front of the aluminum reflector, arranged in an array of two rows of ten evenly spaced pairs, the 20 dipoles, made of brass, are fed from a common coaxial transmission line branching out through various power dividers to feed each pair. Producing a radiaton pattern with a 20° vertical beamwidth and 7° horizontal beamwidth, the antenna assembly bolts to the turntable portion of the antenna pedestal. Provisions are made for mounting IFF antenna AT-352/UPA-22 atop the reflector.
b. PHYSICAL CONFIGURATION — [See Figures 4-10 (a) and (b)].
c. DIMENSIONS — (1) Height: 121 inches (161 with pedestal); (2) Width: 495 inches; (3) Depth: 63 inches; (4) Weight: 5720 pounds (with pedestal).
d. FREQUENCY RANGE — 200 MHz VHF band.
e. INPUT IMPEDANCE — 50 ohms.
f. POWER RATING — 180 kW peak.
g. POLARIZATION — Horizontal.
h. GAIN — 23 dB.
i. TRANSMISSION LINE TYPE — RG-154/U.
j. PRIMARY POWER REQUIRED — 440 volts, three-phase, 60 Hz.
k. REFERENCES — (1) Technical Manual, AN/SPS-37, NAVSEA 0967-052-7010. (2) AN/SPS-43, NAVSEA 0967-052-8010. (3) AS-1092/SPS-43A, NAVSEA 0967-LP-221-1010.

AN/SPS-40

While the 200 MHz AN/SPS-17 spawned the several VHF air search radars (AN/SPS-29, 37, 43) whose antennas are described above, a 400 MHz UHF version of the AN/SPS-17 was also produced. This resulted in an experimental AN/SPS-31, which was then followed by the procurement of a large number of AN/SPS-40 UHF air search radars. The earlier AN/SPS-40 equipment used an AS/1138/SP parabolic reflector antenna. Later models (i.e., the SPS-40B, C and D) use an AS-2782 model which is essentially identical to the AS-1138. Figure 4-11(a) is a shipboard view of the AS-2782/SPS-40B. As seen in Figure 4-3 and by Reference [20], the AN/SPS-40 is the current planned standard for naval long-range 2-D air search.

ANTENNA AS-2782/SPS-40B

a. TYPE/USE — The AS-2782 is a rotating, directional, high gain antenna used with the AN/SPS-40B long-range air-search radar designed for ships to detect distance and bearing of remote targets. A dual feedhorn and truncated paraboloid reflector, covered with a wire screen to reduce weight and wind resistance, comprises the antenna. The dual feed includes the radar section and an integral IFF. A slot type, the radar feed has a tuned cavity and flared shape to ensure proper illumination of the reflector. The reflector then forms the RF energy into a fan shaped beam with a 19° vertical beamwidth and 11° horizontal beamwidth.

The integral IFF feed is composed of two full-wave dipoles inserted in the feedhorn to simulate a corner reflector. This arrangement radiates vertically polarized IFF signals to effectively eliminate any interference with the horizontally polarized radar energy. A fiberglass cover is placed over the feed assembly to protect the opening from weather and corrosive contaminates.

b. PHYSICAL CONFIGURATION — [See Figure 4-11(b)].
c. DIMENSIONS — (1) Height: 140 inches (191 with pedestal); (2) Width: 213½ inches; (3) Depth: 108½ inches; (4) Weight: 1725 pounds (with pedestal).
d. FREQUENCY RANGE — 400 MHz UHF band.
e. VSWR — 1.5:1 or less into 50 ohms.
f. RF POWER RATING — 200 kW peak.
g. POLARIZATION — Horizontal.
h. GAIN - 21 dB.
i. TRANSMISSION LINE TYPE — (1) RG-153/U (radar); (2) RG-219/U (IFF).
j. PRIMARY POWER REQUIRED — 400 volts, three-phase, 60 Hz power for antenna drive motor. 115 volts, one-phase, 60Hz for synchro reference, and monitoring voltages.
k. INSTALLATION REQUIREMENTS — The base of the antenna pedestal has 16 bolt holes drilled for clearance for ¾-inch bolts spaced 20° apart on a 33-inch diameter bolt circle. The mounting base must provide a cutout access to permit removal of the rotary joint. The radar transmission line is pressurized with dry air by the radar dehydrator unit. The pedestal must be oriented fore and aft along the ship's centerline in accordance with the marking on the pedestal base.
l. SPECIAL CONSIDERATIONS — The area selected for the antenna installation must have a 360° unobstructed clearance to accommodate the antenna swing circle. The location of the antenna should have maximum unobstructed azimuth coverage to limit shading or blind spots.
m. REFERENCES — (1) Technical Manual, AN/SPS-40 Radar Set, NAVSEA 0967-LP-441-9010. (2) NAVSEA Drawing RE-D2699234.

AN/SPS-49

As a means of diversifying its radar operation frequencies, the Navy began production of an 800 MHz system, its modern-day, high performance, very long range, 2-D air-search radar equipment: the AN/SPS-49. A medium power system, the SPS-49 provides high resolution surveillance in varying environments, including severe clutter and jamming. Its antenna, the AS-3263/SPS-49, is pictured installed in Figure 4-12, and is described in detail below:

ANTENNA AS-3263/SPS-49

a. TYPE/USE — The AS-3263 is a high gain, rotating antenna used with the AN/SPS-49 radar system to provide target range and bearing information. Three major sections comprise the antenna: the feedhorn and its support boom; the reflector; and the antenna pedestal assembly. The reflector is 24 feet wide and has a double curved parabolic section composed of horizontal members to form the horizontally polarized RF energy into a 9° vertical and 3.3° horizontal beamwidth. RF energy is routed to the feedhorn via waveguide through elevation and azimuth rotary joints located within the pedestal.

The antenna is provided with two azimuth drive speeds. Optimum long range is obtained at the lower speed, 6 rpm. A higher speed, 12 rpm, is used if the operator desires to increase the data rate (at the expense of long range performance). To hold the radar beam near the horizon for stabilized long range detection as the ship rolls and pitches, the antenna is mounted on a trunion so that the elevation angle can be controlled by means of a jackscrew located behind the reflector. The jackscrew is turned by a motor-driven gearbox assembly whereby rotating threads cause the antenna to tilt up or down with varying ship attitude.

Four omnidirectional auxiliary antennas are used with special versions of the SPS-49 to provide coherent sidelobe cancelling (CSLC) in the presence of jamming. The antennas, types AS-3077/SP, AS-3078/SP, and AS-3079/SP shown in Figure 4-13, are mounted in an approximate 20-foot diameter circle. Two of the antennas are placed above the radar antenna on platforms attached to booms extending from the adjacent mast, and the other two are mounted below the radar antennas. The sidelobe canceller circuitry generates a signal equal in amplitude but opposite in phase to the jamming energy in order to effectively cancel it.

Provisions are made for mounting an IFF antenna at the extreme end of the feedhorn support. However, the IFF antenna is not part of the SPS-49 radar set.

b. PHYSICAL CONFIGURATION — [See Figure 4-12(b)].
c. DIMENSIONS — (1) Height: 171 inches (with pedestal); (2) Width: 288 inches; (3) Depth: 189 inches; (4) Weight: 3040 pounds (with pedestal).
NOTE — The CSLC antennas are 17 inches high, 8 inches in diameter, and weigh 10 pounds each.
d. FREQUENCY RANGE — 851 to 942 MHz.
e. VSWR — Not greater than 2.0:1.
f. RF POWER RATING — 280 kW peak.
g. POLARIZATION — Horizontal.
h. GAIN — 29 dB.

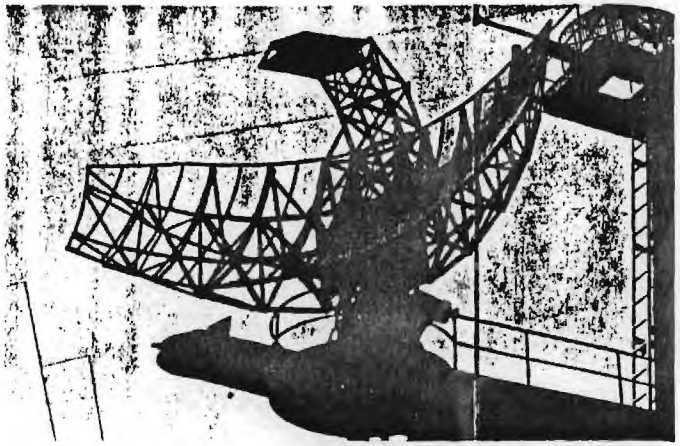

FIG. 4-11(a) AS-2782/SPS-40B 2-D Air Search Radar Shipboard Installed

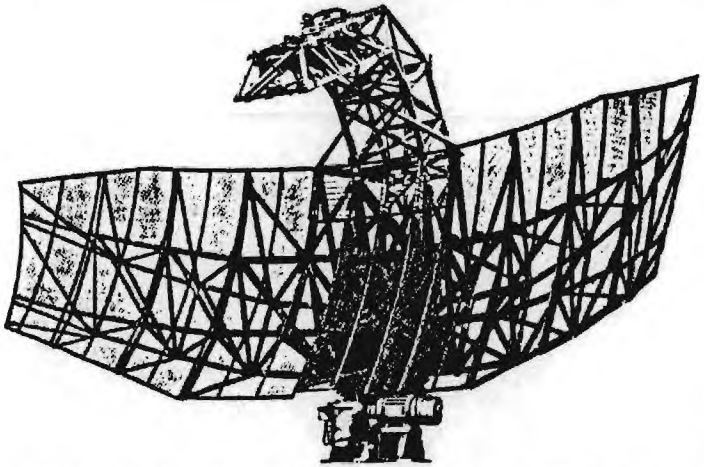

FIG. 4-11(b) AS-2782/SPS-40B 2-D Air Search Radar Physical Configuration

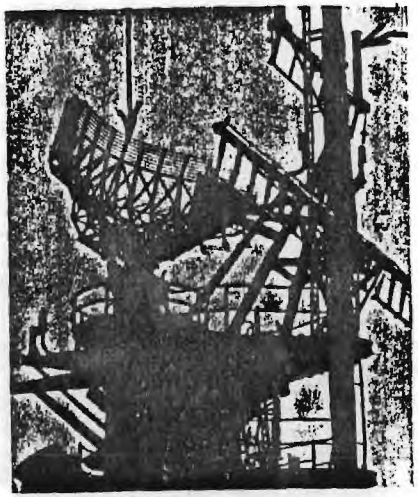

(a)

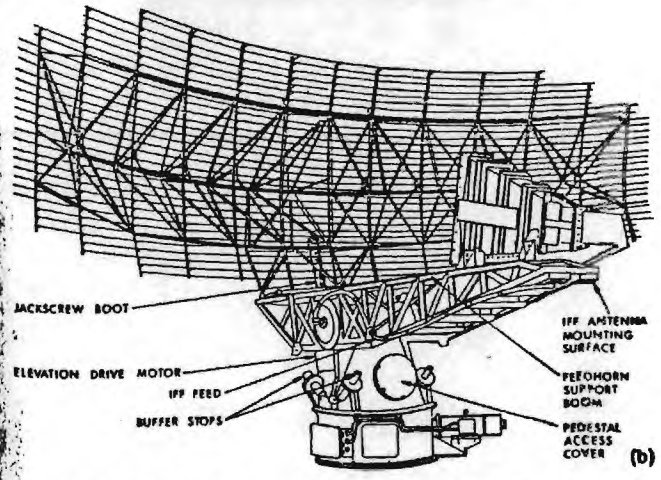

(b)

FIG. 4-12 AS-3263/SPS-49 2-D Air Search Radar Antenna

i. TRANSMISSION LINE TYPE — (1) 9-¾ x 2.4-inch waveguide P/N WR975 (for radar antenna); (2) MS22931 Coax (for CSLC antennas).
j. PRIMARY POWER REQUIRED — 440 volts, three-phase, 60 Hz; 115 volts, one-phase, 60 Hz.
k. REFERENCE — Technical Manual, AN/SPS-49(V), NAVSEA 0967-LP-584-8010.

AN/SPS-58, AN/SPS-62, AN/SPS-65 Series

The AN/SPS-58 is the air surveillance portion of the shipboard acquisition and designation system known as the Basic Point Defense Surface Missile System (BPDSMS). This equipment is intended for rapid designation of high speed, low altitude radar-detected targets, at very short range, to the ship weapons control systems even in a severe clutter-environment. Early models of the SPS-58 used the AS-2607 antenna depicted in Figure 4-14. However, subsequent versions (i.e., the AN/SPS-58A and then the AN/SPS-62), incorporated a modification to the ship's SPS-10 antenna, the AS-936, by replacing the single feedhorn of the SPS-10 with the dual-feed AS-4022/SPS-58A waveguide horn. Since the SPS-10 is basically a C-band surface search radar, while the SPS-58 is an L-band air search acquisition system with target designation capability, this unified dual antenna affords an overall ship sensor system featuring independent, but simultaneous, operation of both air and surface surveillance within a 25-mile range.

A further improved variant of the SPS-58 is the AN/SPS-65, which offers enhanced performance in an ECM environment, an automatic target detection interface, and higher reliability.[21] The SPS-65 also uses the modified SPS-10 antenna with the dual-feed waveguide horn, redesignated the AS-936C as shown in Figure 4-15 and described below. (Only the L-band air search characteristics will be detailed here. The C-band portion is given later under the Surface Search radar section of this chapter.)

ANTENNA AS-936C/SPS-10B

a. TYPE/USE — The AS-936C is an antenna assembly consisting of an SPS-10 antenna altered to operate with the very short range SPS-65 air surveillance radar for BPDSMS and NATO Sea Sparrow systems. The SPS-10 antenna modification is accomplished by replacing the existing C-band horn of an AS-936B antenna with the dual-feed AS-4022/SPS-58A waveguide horn. The resultant integrated L and C band antenna is fed from a rotary joint incorporated within the existing SPS-10 pedestal, and, for the air search portion, has a 16° vertical beamwidth and a 6° horizontal beamwidth. The 16° elevation beam ensures horizon detection capability for all but extreme ship roll conditions with no antenna stabilization feature.
b. PHYSICAL CONFIGURATION — [See Figure 4-15].
c. DIMENSIONS — (1) Height: 76 inches (with pedestal); (2) Width: 126 inches (swing circle); (3) Depth: 126 inches (swing circle); (4) Weight: 440 pounds (with pedestal).
d. FREQUENCY RANGE — L-band.
e. POWER RATING — 20 kW peak.
f. POLARIZATION — Vertical.
g. GAIN — 23 dB minimum.
h. TRANSMISSION LINE — Waveguide.
i. REFERENCE — Technical Manual, Radar Set AN/SPS-65, NAVSEA 0967-609-5010.

4-1.2 3-D AIR SEARCH RADAR ANTENNAS

Toward the end of World War II, as radar devices capable of handling much greater power at increasingly higher operating frequencies were developed, several S-band (2 to 4 GHz) radar systems were manufactured and rushed into service. Among these were the Navy's 700 kW models SM and SP, the first radars designed specifically for three-dimension detection and interception of figher planes. Using parabolic dish antennas having an extremely narrow conical beam to provide simultaneous azimuth and elevation information, these radars were, therefore, restricted to covering only one airplane at a time. This necessitated continual switching back and forth between an enemy aircraft and the Allied plane being guided to intercept.

To overcome this limitation, the model SX multiple-intercept 3-D radar was introduced into the fleet at the end of the war and used extensively thereafter. As is evident in Figure 4-16, the SX antenna was actually composed of two separate antennas, one for routine air search and the other working independently as a height-finder. That is, while the total assembly rotated 360° in azimuth, the height-finder scanned angular sectors in elevation to achieve three-dimensional coverage.

By the early 1950s, however, the 3-D fighter director function was being accomplished by use of a single integrated antenna. Initially, this had been done at L-band, on a limited basis aboard ship, with the AN/SPS-2. Having an output of 7 megawatts to provide very long range detection (out to 300 miles) at altitudes of 100,000 feet,

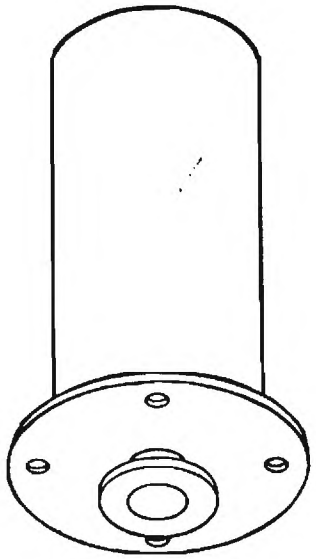

FIG. 4-13 AS-3077, 3078, 3079 Coherent Sidelobe Canceller Antenna

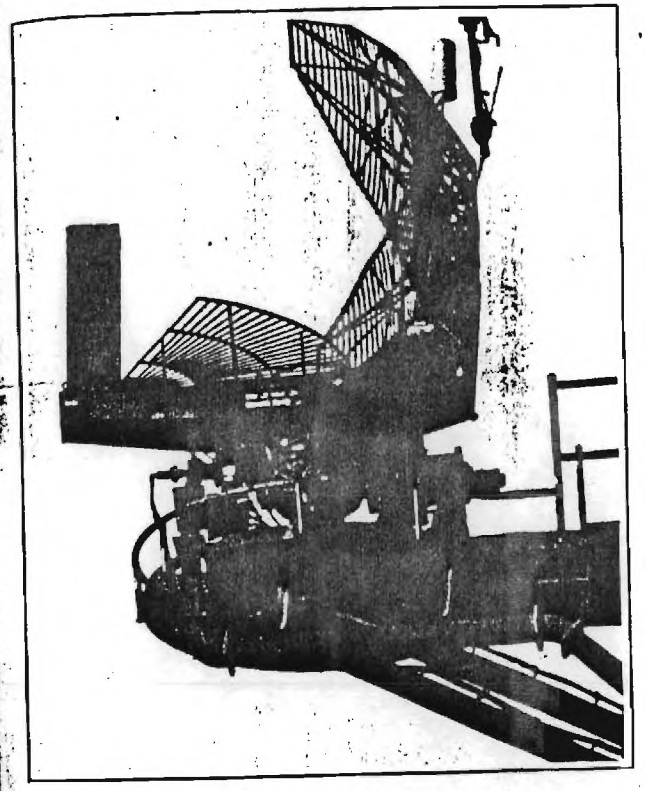

FIG. 4-14 AS-2607/SPS-58 2-D Air Search Radar Antenna

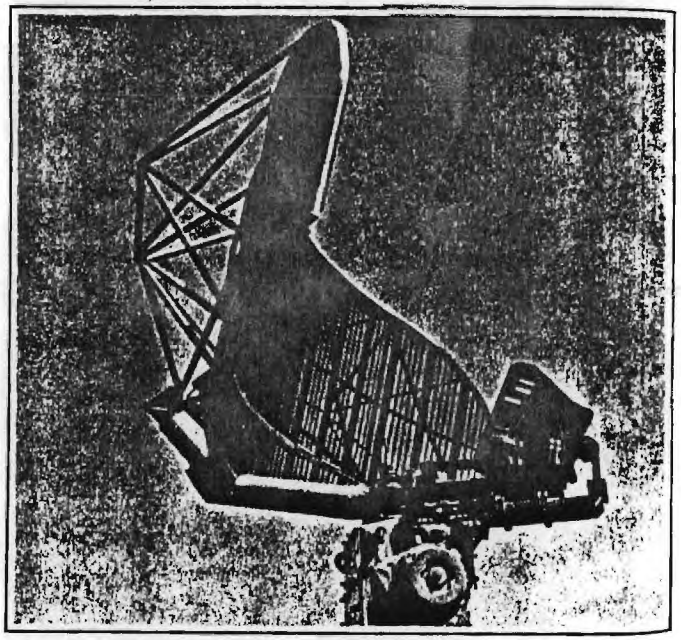

FIG. 4-15 AS-936C/SPS-10B Radar Antenna Used With AN/SPS-65 2-D Air Search Antenna

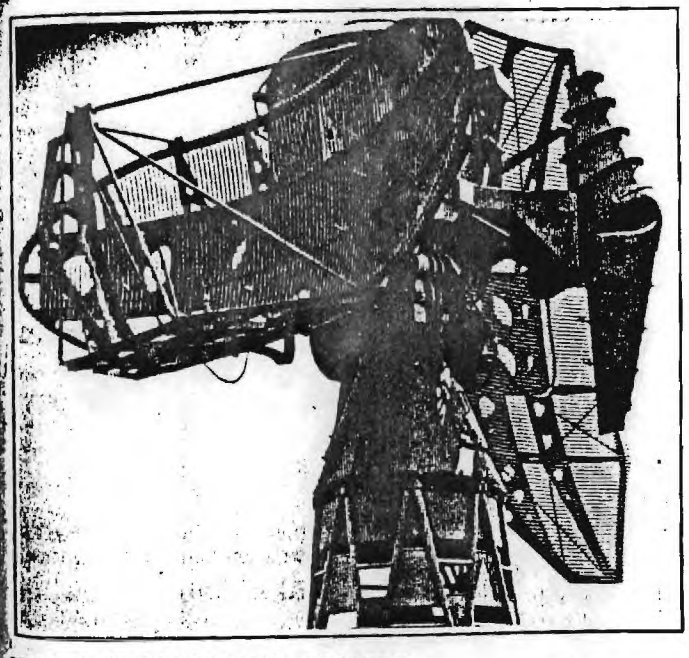

FIG. 4-16 Model SX 3-D Air Search Antenna

c. DIMENSIONS — (1) Height: 96 inches, radius (total director); (2) Width: 50 inches, radius (total); (3) Depth: 50 inches, radius (total); (4) Weight: 3,315 pounds (total).
d. FREQUENCY RANGE — X-band.
e. RF POWER RATING — 2kW.
f. POLARIZATION — [Classified].
g. GAIN — [Classified].
h. TRANSMISSION LINE TYPE — Waveguide.
i. REFERENCES — (1) NATO Seasparrow Surface Missile System MK57, MODS 0 and 1, NAVSEA OP-4004. (2) Guided Missile Fire Control System MK91 MODS 0 and 1, NAVSEA OP-4005.

Target Acquisition System MK 23

The MK 23 Target Acquisition System (TAS) is a major component of what is termed the Improved Point Defense Surface Missile System (IPDSMS). TAS itself is comprised of five integrated subsystems: (1) a range-gated pulse-doppler radar; (2) a computer unit; (3) a display unit; (4) an IFF system; and (5) a combination radar/IFF antenna to be described later. Designed for use in conjunction with shipboard fire control systems and weapons, TAS locates, acquires, tracks, classifies, and designates high speed, small radar cross-section hostile threats which dive from high altitudes or "pop up" off the horizon just 30 to 60 seconds before intended impact. TAS, therefore, must automatically identify, react, and designate such targets to the NATO Seasparrow Surface Missile System (NSSMS) in a matter of a very few seconds, and it must do so with precision in all sea environments, including clutter and jamming. To be successful in countering, the corresponding point defense weapon systems (e.g., NSSMS, CIWS, RAM, five-inch guns), of course, must also be highly automatic so as to minimize lock-on-time, firing, and guiding to intercept.

In its operation, TAS offers a selection of four modes:

(*a*) *Normal* — this is the routine, automatic, point defense mode with instrumented range of 20 nautical miles.
(*b*) *Medium Range* — offering radar surveillance and air control beyond 90 nautical miles.
(*c*) *Mixed* — combining Normal and Medium Range to enable the ship to perform simultaneous multiple operation, such as point defense and air operation, from a single radar.
(*d*) *EMCON* — allowing selectable sector scanning to minimize hostile detection of the ship.

ANTENNA TAS

a. TYPE/USE — As seen in Figure 4-70, the TAS antenna is a combined rotating sensor with radar and IFF functions mounted back-to-back on a common, stabilized pedestal. Coverage is 360° continuous in azimuth, and from 0 to 75 degrees in elevation. The radar is a 2-D, L-band, fan beam (3.3° horizontal beamwidth) radiator used for search, detection, and acquisition. It is composed of 26 horns with evenly distributed corporate feed. Associated with the radar antenna, located one at each end, are two small backfill horn antennas; one for sidelobe blanking and one for coherent sidelobe cancellation. Physically mounted 180° behind the radar antenna is the AS-2189/UPX IFF antenna. A small IFF backfill radiator is located on top for IFF sidelobe cancellation.
b. PHYSICAL CONFIGURATION — [See Figure 4-70].
c. DIMENSIONS — (1) Height: 129 inches (with pedestal); (2) Width: 231 inches; (3) Depth: 76 inches; (4) Weight: 2000 pounds (total).
d. FREQUENCY RANGE — L-band.
e. RF POWER RATING — 200 kW peak.
f. POLARIZATION — Vertical (radar antenna).
g. GAIN — 21 dB (radar antenna).
h. TRANSMISSION LINE TYPE — Waveguide.
i. PRIMARY POWER REQUIREMENTS — (1) 115 vac, 60 Hz, three-phase; (2) 115 vac, 400 Hz, three-phase; (3) 440 vac, 400 Hz, three-phase.
j. REFERENCES — (1) Target Acquisition System MK 23, NAVSEA OP-4199. (2) Installation Guidance Notebook for Target Acquisition System MK 23, NAVSEA SW230-AO-INS-010. (3) *Surface Warfare Magazine*, May 1980, p. 15.

Phalanx Close-in Weapon System

The final shipboard self-defense weapon employed as part of the Navy's defense-in-depth protection against anti-ship missiles is the Phalanx Close-in Weapon System (CIWS). That is to say, it is CIWS which is relied upon to, without any assistance from other ship systems, automatically engage and destroy any missiles which penetrate the ship's primary defense screen. CIWS will, in a secondary role, accept targets designated from other sources and engage them up to 80-degree elevation relative to the deck. Additionally, CIWS can operate against small surface targets as directed by optical designators.

CIWS is a self-contained weapon system, consisting of a search radar, a track radar, and a six-barrel 20 mm Gatling gun firing 3000

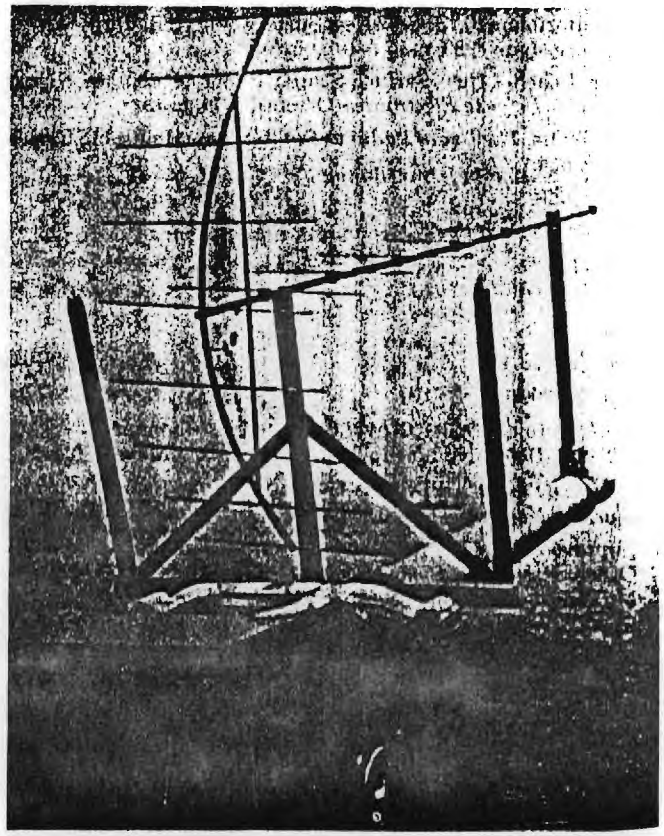

FIG. 4-1 First Shipboard Radar Antenna 200 MHz Experimental Equipment

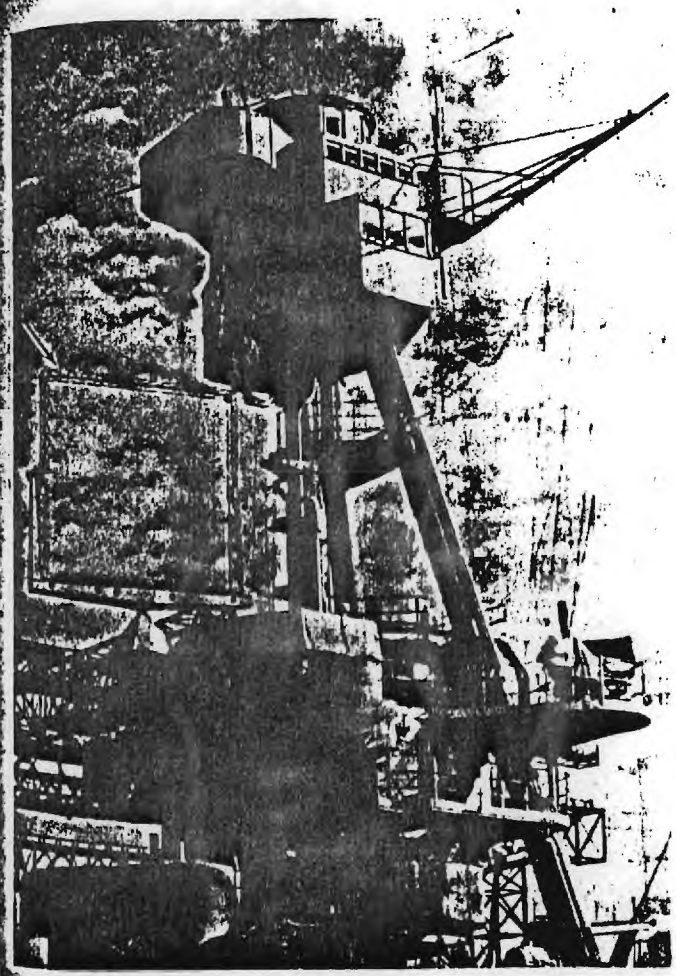

FIG. 4-2 Model XAF Early Navy Shipboard Radar Antenna *USS New York*

HARRINGTON

For a stationary formula, we assume a current $\mathbf{J}^a$ on S and approximate $\langle c,c\rangle$ by $\langle a,a\rangle$, subject to the constraint

$$\langle a,a\rangle = \langle c,a\rangle = -\langle i,a\rangle \tag{7-112}$$

The last equality results from Eq. (7-110). To express this constraint in a form for which $\langle a,a\rangle$ is insensitive to the amplitude of $\mathbf{J}^a$, we take

$$\langle a,a\rangle = \frac{\langle i,a\rangle^2}{\langle a,a\rangle}$$

and, replacing $\langle c,c\rangle$ by $\langle a,a\rangle$ in Eq. (7-111), we have

$$\text{Echo} \approx \frac{-\langle i,a\rangle^2}{(Il)^2\langle a,a\rangle} = -\frac{\left(\oint\!\!\oint \mathbf{E}^i \cdot \mathbf{J}^a\, ds\right)^2}{(Il)^2 \oint\!\!\oint \mathbf{E}^a \cdot \mathbf{J}^a\, ds} \tag{7-113}$$

where $\mathbf{E}^a$ is the field produced by the assumed currents $\mathbf{J}^a$. This is the variational formulation of the problem. Note the close similarity of the echo problem to the impedance problem of the preceding section. The impedance problem is essentially an echo problem for which the source is at the obstacle. A more general formulation of the echo problem can be made by replacing Il with an arbitrary source.

The tensor Green's functions of Sec. 3-10 can be used to put Eq. (7-113) into a more descriptive form. Define $[\Gamma(\mathbf{r},\mathbf{r}')]$ as the tensor of proportionality between a current element $d\mathbf{J}^a$ at $\mathbf{r}'$ and the field $d\mathbf{E}^a$ that it produces at $\mathbf{r}$, that is,

$$d\mathbf{E}^a(\mathbf{r}) = [\Gamma(\mathbf{r},\mathbf{r}')]\, d\mathbf{J}^a(\mathbf{r}')$$

Then Eq. (7-113) can be written as

$$\text{Echo} \approx \frac{-\left[\frac{1}{Il}\oint\!\!\oint \mathbf{E}^i(\mathbf{r}) \cdot \mathbf{J}^a(\mathbf{r})\, ds\right]^2}{\oint\!\!\oint ds \oint\!\!\oint ds'\, \mathbf{J}^a(\mathbf{r}) \cdot [\Gamma(\mathbf{r},\mathbf{r}')]\, \mathbf{J}^a(\mathbf{r}')}$$

This equation is in a form characteristic of variational solutions in general.

A commonly calculated parameter is the echo area, defined by Eq. (3-30). For linearly polarized fields, the echo area is given by

$$A_e = \lim_{r\to\infty}\left(4\pi r^2 \left|\frac{E^s}{E^i}\right|^2\right) \tag{7-114}$$

If, in Fig. 7-14, we let Il be z-directed and located on the x axis, and then let $r = x \to \infty$, we have, in the vicinity of the obstacle,

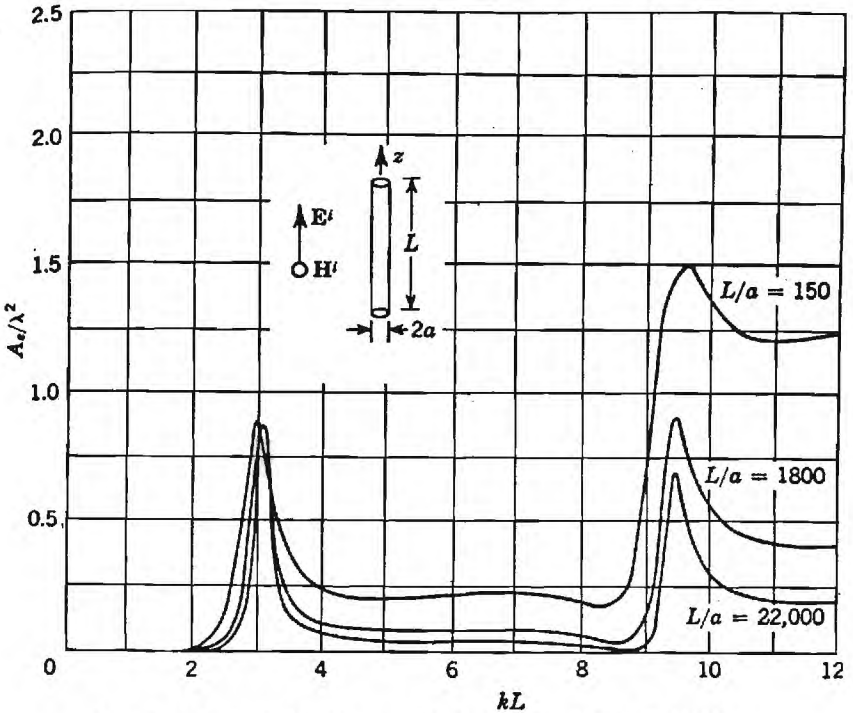

FIG. 7-15. Broadside echo area A_e of a wire. (*After Y. Y. Hu.*)

Also, by definition, we have echo $= E_z^s/Il$; hence from Eq. (7-113)

$$E_z^s = \frac{\eta E_0 \left(\oint\!\!\oint \mathbf{u}_z \cdot \mathbf{J}^a e^{jkz}\, ds\right)^2}{j2\lambda r \oint\!\!\oint \mathbf{E}^a \cdot \mathbf{J}^a\, ds}$$

Therefore, by Eq. (7-114), our stationary formula for echo area is

$$A_e = \pi\left|\frac{\eta}{\lambda}\frac{\left(\oint\!\!\oint J_z^a e^{jkz}\, ds\right)^2}{\oint\!\!\oint \mathbf{E}^a \cdot \mathbf{J}^a\, ds}\right|^2 \tag{7-115}$$

when the incident plane wave is z-polarized and $-x$ traveling.

As an example, consider the scattering of a plane wave by a thin conducting wire, as represented by the insert of Fig. 7-15. The integral in the denominator of Eq. (7-115) is just the self-reaction of the assumed current on the wire. This is the same type of reaction that we encountered in the linear-antenna problem, approximated by Eq. (7-105). Defining A as the self-reaction, we have

$$A = \oint\!\!\oint \mathbf{E}^a \cdot \mathbf{J}^a\, ds \approx \frac{1}{\quad}\int^{L/2} dz \int^{L/2} dz'\, I^a(z) I^a(z')\left(k^2 + \frac{\partial^2}{\partial z^2}\right) G$$

ure has a characteristic impedance somewhat higher than that for a sheet struc- with the same values of α and τ. There does not appear to be a definite trend in ion of impedance with the τ ratio. For example, increasing τ for the wire struc- ncreases the characteristic impedance, whereas it decreases the characteristic dance for the circular tooth sheet structure.

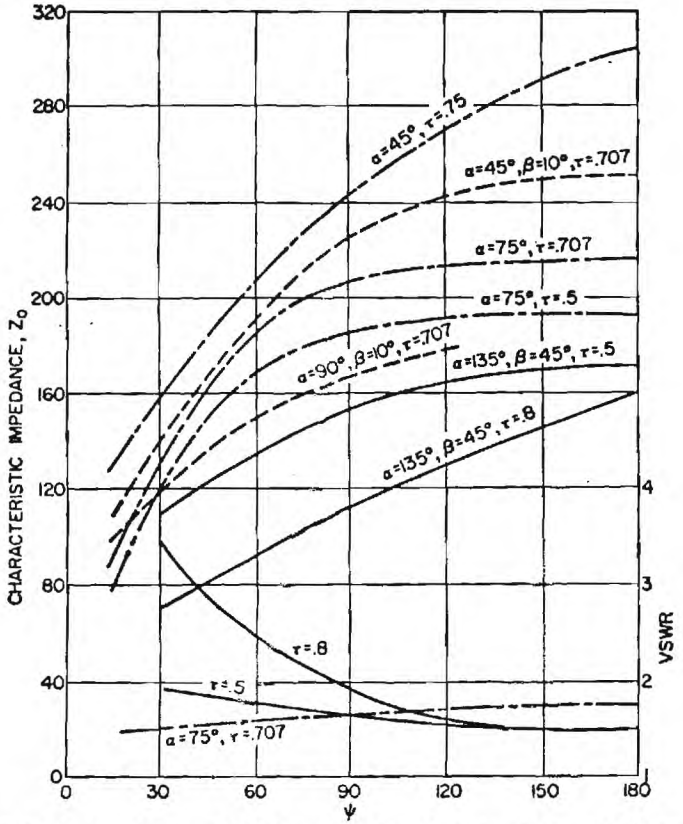

. 18-20. Variation of Z_0 and VSWR with ψ for sheet structures with: Circular teeth — —). Trapezoidal teeth (– – – –). Wire structure with trapezoidal teeth (— – —).

few curves of the VSWR referred to the characteristic impedance are also given on plot. It will be noticed that the VSWR increases, especially for the circular tooth et structure, with $\tau = 0.8$, as ψ is decreased. For all the other structures, the WR remains less than 2:1 over the range of ψ values considered. In some, but not cases it has been found that the VSWR rises rapidly as ψ approaches zero for the e structures.

The impedance variation for E-plane arrays is similar to that for H-plane arrays ept that the angular spacing must be greater than $\frac{3}{2}\alpha$ in order to avoid excessive WR's.

For the ψ values of most interest, that is, from 15 to about 90°, it is noticed that the racteristic impedance ranges from approximately 70 to 240 ohms. Thus it is essary to use a wideband technique to match this impedance to a coaxial or a balanced line. The tapered-line transformers described in Refs. 13 and 14 are ideally suited for matching this impedance over theoretically unlimited bandwidths. These transformers usually require a length on the order of 0.4 to 0.5 wavelength at their lowest frequency of operation.

The impedance behavior of the dipole structure of Fig. 18-11 is illustrated in Fig. 18-21. These results were obtained with a balanced-line characteristic impedance of 105 ohms.

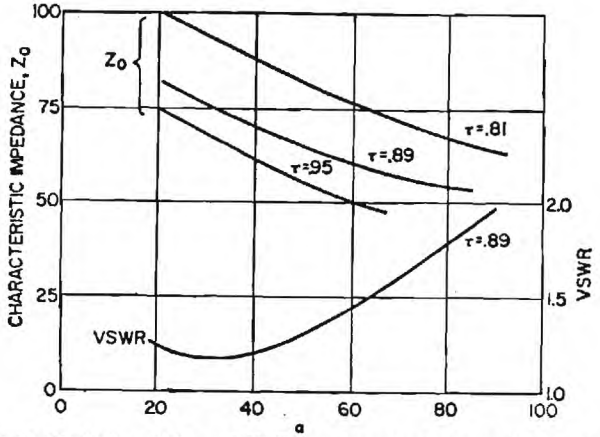

FIG. 18-21. Variation of Z_0 and VSWR with α for log-periodic dipole array.

In designing log-periodic antennas for bandwidths of 10:1 or greater, it is usually found that the characteristic impedance decreases gradually as the frequency is increased over this range. This variation is due to improper construction of the antenna; that is, it is usually not practical to taper the diameter of wires or thickness of the sheets according to theory because of mechanical limitations. However, this variation is not serious since many types of log-periodic antennas have been built with a tapered-line input transformer such that the complete system covers a 10:1 frequency range with a VSWR less than 2:1.

Several wire-trapezoidal-tooth unidirectional structures were built with $\alpha = 67\frac{1}{2}°$, $\tau = 0.6$, and $\psi = 37°$, but with the wire sizes varying over a 10:1 range. It was found that the wire size had a negligible effect on the patterns but that the characteristic impedance decreased about 30 per cent as the wire sizes increased by a factor of 10:1.

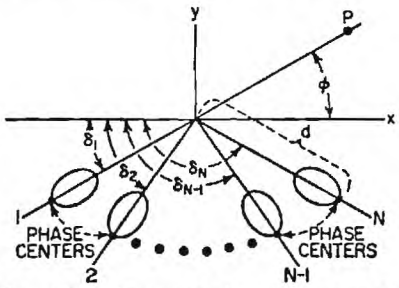

FIG. 18-22. Geometry for array of end-fire elements.

Multielement Arrays. A schematic representation of an array of N elements as viewed from the top is illustrated in Fig. 18-22. The radial lines defined by δ_n represent the elements of the array. The α and τ parameters for the N elements are made identical so as to assure identical element patterns. The xy-plane radiation pattern of the array is given by

$$E(\phi) = \sum_{n=1}^{N} A_n f(\phi - \delta_n) e^{-j[\beta d \cos(\phi - \delta_n) - \gamma_n]} \qquad (18\text{-}18)$$

ANTENNA ENGINEERING HANDBOOK, ed. JASIK

$f(\phi)$ is the element pattern and $\beta d \cos(\phi - \delta_n)$ represents the phase advance of ...se center relative to the origin. The function f may take the same form as that ...reviously, that is, $f(\phi) = \cos^n(\phi/2)$. The value of the feed-point current for ... element is given by A_n. In nearly all practical cases, $A_n = 1$ for all n. This is ...olished in practice by connecting half of the elements together and feeding them ...t the other half. The parameter γ_n is the relative phase of the field radiated ...he nth element. It may be controlled by expanding or contracting the element ...ing to the phase-rotation principle to be described later.

... assumptions made in Eq. (18-18) are that the element patterns and input ...ances are identical. Although mutual effects can make these assumptions invalid, good correlation between theory and experiment has been obtained. Cut-and-try synthesis procedures may be used with Eq. (18-18).

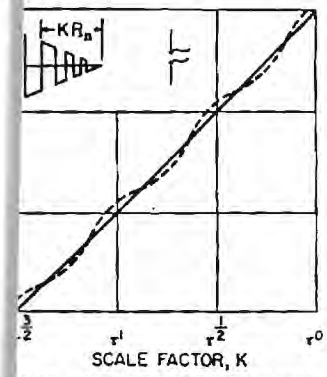

...8-23. Illustration of phase-rota-...henomena for log-periodic an-...s.

A basic characteristic of logarithmically periodic antennas is the phase-rotation phenomenon. It has been verified experimentally that if the phase of the electric field received at a distant dipole (Fig. 18-23) is measured relative to the phase of the current at the feed point of the structure, the phase of the received signal will be delayed 360° as the structure is expanded through a period. In Fig. 18-23 the distance to an arbitrary transverse element is given by KR_n. The expansion of the structure through a period is accomplished by letting K increase from 1 to $1/\tau$. During this expansion all lengths ...ved in the structure are multiplied by K. In Fig. 18-23 the phase delay in ...as is plotted vs. the logarithm of K. The ideal phase variation is given by the ...straight line. Measurements have indicated that the actual phase variation is ...what like the dashed line. The approximate measurements made to date indi-...hat the deviation of the dashed line from the straight line is not more than 15°. ...elation between γ_n and K_n is given by

$$K_n = \exp\left[\frac{\gamma_n}{2\pi} \ln \tau\right] \tag{18-19}$$

...nately, the phase center and the element patterns are independent of the expan-...r contraction of a logarithmically periodic element.

...e information given above in Figs. 18-14, 18-15, and 18-23 is sufficient for pre-...g the pattern of an array of similar end-fire elements. The method can be ...ded to cover a combination of E- and H-plane arrays. The phase-rotation ...omenon is extremely important since it allows a frequency-independent method of ...ng the elements of the array.

...perimental and theoretical patterns for a six-element phased-H-plane array of ... trapezoidal tooth elements are given in Fig. 18-24. The values of the design ...meters for this array were $\alpha = 9.5°$, $\tau = 0.88$, $N = 6$, $\delta_n - \delta_{n-1} \approx 17°$ for all n, ...$d/\lambda = 1.95$. The elements were phased to produce a beam-cophasal condition. ...gain of the array was 14 db over a dipole.

...though gains up to 18 db are feasible by using a combined E- and H-plane array, ...ize and complexity of the antenna become great since it is necessary to use very ...l α angles and τ values near unity.

Design Procedure. In designing an array, a judicious choice of the parameters N, α, τ, and δ_n should be made so as to achieve a minimum amount of space and material and number of elements. Although the design method is cut and try, a rough approximation to an optimum design may be obtained by the following procedure. The procedure is the same for arrays in the E plane and H plane. Given a desired beamwidth, the equivalent broadside aperture D may be calculated from

$$\frac{D}{\lambda} = \frac{40}{\bar{\varphi}} \tag{18-20}$$

where $\bar{\varphi}$ is the half-power beamwidth in degrees. The number 40 instead of 50 (which

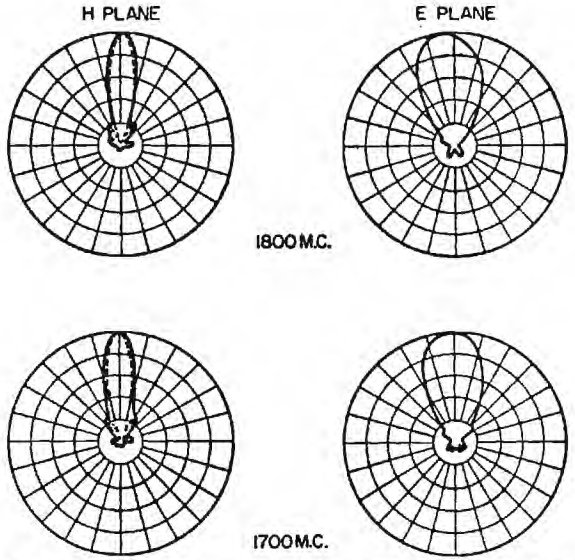

FIG. 18-24. Predicted (- - - -) and measured (———) patterns of six-element phased array.

is for a uniform aperture) is used because the end-fire directivity of the elements tends to enhance the effective aperture. The distance between the phase centers of the two outer elements must be approximately D. Results indicate that a reasonable maximum spacing between the phase centers of adjacent elements is 0.7 wavelength. Thus the number of elements may be determined approximately from

$$N - 1 \approx \frac{D}{0.7\lambda} = \frac{57.1}{\bar{\varphi}} \tag{18-21}$$

For a one-dimensional array N must be even in order to present a balanced load to the feed line. The maximum value of the angle $\delta_N - \delta_1$, which defines the sector occupied by the array, depends on the beamwidth of the element pattern. If $\delta_N - \delta_1$ is greater than the element beamwidth, then elements 1 and N will contribute little to the formation of the main beam. An examination of Fig. 18-14 indicates that reasonable maximum values of $\delta_N - \delta_1$ are 60° for an E-plane array and 70 to 130° for an H-plane array. If low first side lobes are desired, values somewhat smaller than the maximum should be chosen.

The distance d to the phase center is equal to

$$\frac{d}{\lambda} = \frac{D}{2\lambda \sin\left(\frac{\delta_N - \delta_1}{2}\right)} = \frac{20}{\varphi \sin\left(\frac{\delta_N - \delta_1}{2}\right)} \tag{18-22}$$

The angle α is then determined from Fig. 18-15 since d/λ is known. The minimum value of τ is then determined from Fig. 18-14. It is usually desirable to use the minimum value of τ since the element beamwidth has little influence on the array pattern for $N \geq 4$.

Since A_n and $(\delta_n - \delta_{n-1})$ are usually made independent of n, the remaining parameter to determine is K_n. If high gain and a beam direction of ϕ_0 are desired, then K_n is chosen so that $[\beta d \cos(\phi_0 - \delta_n) - \gamma_n]$ has the same value for all n. Equation (18-19) gives the relation between K_n and γ_n.

For shaped beams γ_n, and hence K_n, would be determined on a cut-and-try basis. After the approximate synthesis given above, the array pattern may be calculated by the method of the preceding section.

The above procedure determines the parameters α, τ, δ_n, K_n, and N. It remains to determine the type and size of the elements. For frequencies above about 500 Mc, a sheet structure should be used, and for ranges below that, wire structures should be used. If it is desired to cover a frequency range which overlaps 500 Mc, it may be necessary, because of mechanical considerations, to use wire construction for the back of the structure and a sheet or printed-circuit construction for the front of the structure. A gradual transition between the two types of structures may be made with only a small effect upon the electrical characteristics.

If minimum antenna size is important, rectangular or trapezoidal teeth should be used. If not, triangular teeth may be used or other similar versions. Curved teeth may also be used if the α angle is not too large.

The size of the element is determined from the lowest frequency required. Approximately, the largest tooth for a sheet structure should be about a quarter wavelength long at the lowest frequency and the longest transverse wire for the wire structure should be approximately a half wavelength long. The highest frequency determines the length of the shortest teeth and wires in a similar manner. For high-power or microwave applications, the size of the input cable or transmission line may limit the upper frequency.

The preceding theory and curves may be used to predict the performance of the initial design. If it is close, then the antenna model should be constructed and a pattern and impedance investigation should be performed over a period so as to determine the exact parameters. Once this is done, then the antenna should be checked over the complete frequency range, including measurement of the input impedance. It is then possible to design the tapered-line transformer for feeding the antenna.

For applications which demand minimum antenna size, it is possible to use end loading on the tips of a few of the largest teeth. The lower-frequency cutoff may be lowered 15 or 20 per cent by this means.

18.5. SPECIAL APPLICATIONS

Arrays over Ground. Although the above antennas have radiation patterns which are essentially independent of frequency, many applications demand that the antenna be placed near ground. If one of these antennas is placed with its feed point above ground, then it is apparent that the resultant pattern will be frequency-dependent since its electrical height above ground changes with frequency. However, the above array theory suggests that if log-periodic elements are inclined with respect to ground and

with their feed points at ground level, then the resultant radiation pattern will be frequency-independent. The elements can be placed so that with their images they form either H-plane or E-plane arrays or a combined E- and H-plane array. For an equivalent H-plane array there will, of course, be a null in the resultant pattern on the horizon. The array theory above may be used to calculate the resultant pattern by adjusting the phase of the image elements. For an H-plane array, the phase of the image element will be 180° different from that of the element above ground, whereas for an E-plane array, the phase of the image element would be the same as that of the element.

A very important application for this type of an antenna is for point-to-point communication circuits.[16] Figure 18-25 shows a two-element array above ground

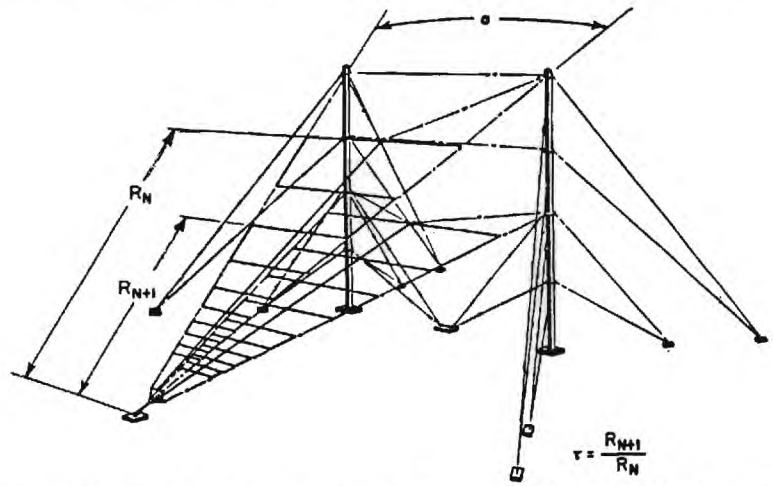

FIG. 18-25. Log-periodic H-F antenna with frequency-independent elevation pattern.

oriented so that they and their image elements form an H-plane array. Theoretically, the feed point of the antenna should be at ground level, but in practice the feed point is placed a small height above ground to protect personnel from high r-f voltages. Except for very short distances, high-frequency point-to-point communication is accomplished by reflection of the radio waves from the ionosphere. The vertical angle of arrival or departure (from the ground) depends upon the distance between the points and the height of the reflecting layer. Although its value ranges from 70° down to a few degrees for various circuits, its value for a particular circuit is relatively constant since the height of the reflecting layer does not change by a great amount. However, because of changing ionospheric conditions during the sunspot cycle and from night to day, it is necessary to change the operating frequency over bandwidths of 4 or 6:1. Thus it is most desirable to have an antenna for which the vertical angle of the main lobe is independent of frequency. Present-day antennas, such as the dipole, rhombic, billboard, discone, etc., do not satisfy this requirement.

The direction of the main lobe for the structure of Fig. 18-25 may be controlled by the α angle of the individual element and the angles of the elements with respect to ground. The size of the structure is determined by the lower-frequency limit. Figure 18-26 shows the vertical-plane pattern for a structure with $\alpha = 14°$ and $\tau = 0.75$. The two half structures are oriented at angles of 32 and 48° with respect to ground. The dimensions of the antenna at the lowest frequency are given in wavelengths in the figure. The lower half structure is scaled so that its radiation leads that of the upper

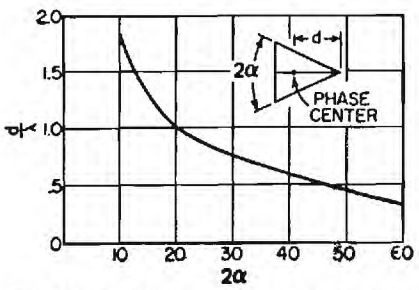

FIG. 14-30 Distance from vertex to phase center as a function of 2α.

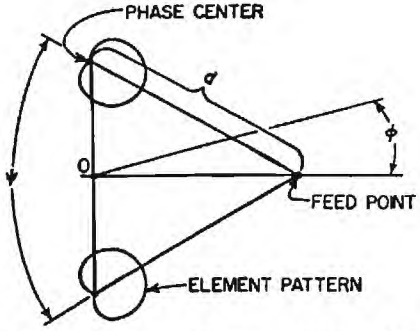

FIG. 14-31 Schematic representation of a two-element array.

where $\cos^n(\phi/2)$ is an assumed functional form for the element pattern. The exponent n is related to the half-power beamwidth BW by

$$n = -0.35/\ln\left(\cos\frac{\mathrm{BW}}{2}\right)$$

For an H-plane array (like Fig. 14-23) the H-plane beamwidth is used, and for an E-plane array the E-plane beamwidth is used to determine n. The beamwidths may be obtained from Fig. 14-29. Although this procedure neglects the effect of the presence of one half structure on the pattern of the other, it will give fairly accurate results, especially for values of α smaller than 60°.

Figure 14-32 shows the variation of the H-plane beamwidth, gain, and front-to-back ratio with the angle ψ for a wire trapezoidal-tooth H-plane array with $2\alpha = 60°$ and $\tau = 0.77$. The E-plane beamwidth is nearly independent of the angle ψ, and its value is approximately 63°. Of course, for $\psi = 180°$ a bidirectional beam is produced.

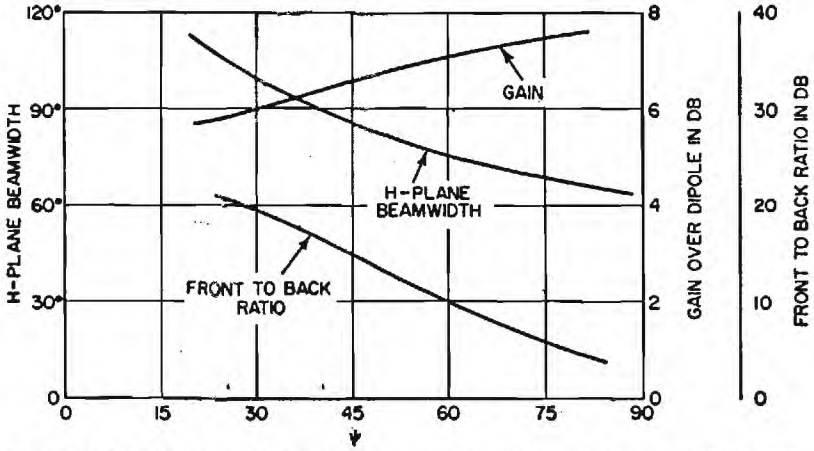

FIG. 14-32 Effect of angle ψ on pattern characteristics for an antenna with $2\alpha = 60°$ and $\tau = 0.77$.

ANTENNA ENGINEERING HANDBOOK, 1984, eds Johnson + Jasik

Notice that if both high gain and high front-to-back ratio are desired, a comp value of ψ must be chosen. As is to be expected, the H-plane beamwidth de rapidly with increasing ψ since this increases the H-plane aperture of the ante

The characteristic impedance increases as the angle between the two el increases; it will be in the range of about 100 to 300 Ω and will also depend u type of element. Thus, it may be necessary to use broadband transformers to to the transmission-line feed.

Multielement Arrays A schematic representation of an array of N elem viewed from the top is illustrated in Fig. 14-33. The radial lines defined by δ_n re the elements of the array. The α and τ parameters for the N elements are ma tical so as to assure identical element patterns. The xy-plane radiation patter array is given by

$$E(\phi) = \sum_{n=1}^{N} A_n f(\phi - \delta_n)\exp[-j(\beta d\cos(\phi - \delta_n) - \gamma_n)] \quad (1$$

where $f(\phi)$ is the element pattern and $\beta d\cos(\phi - \delta_n)$ represents the phase of the phase center relative to the origin. The function f may take the same that used previously, that is, $f(\phi) = \cos^n(\phi/2)$. The value of the feed-point for the nth element is given by A_n. In nearly all practical cases, $A_n = 1$ for all is accomplished in practice by connecting half of the elements together and them against the other half. The parameter γ_n is the relative phase of the field from the nth element. It may be controlled by expanding or contracting the according to the phase-rotation principle to be described later.

The assumptions made in Eq. (14-18) are that the element patterns ar impedances are identical. Although mutual effects can make these assu invalid, good correlation between theory and experiment has been obtained. C try synthesis procedures may be used with Eq. (14-19).

A basic characteristic of logarithmically periodic antennas is the phase- phenomenon. It has been verified experimentally that if the phase of the elec received at a distant dipole (Fig. 14-34) is measured relative to the phase of

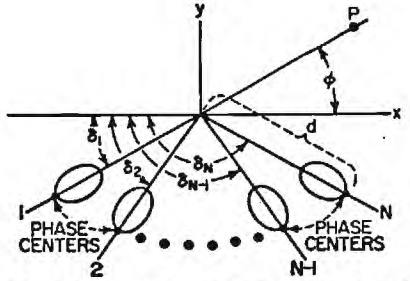

FIG. 14-33 Geometry for an array of end-fire elements.

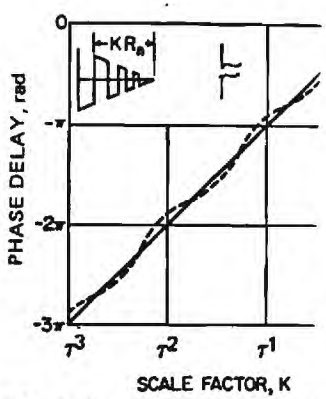

FIG. 14-34 Illustration of the pl tion phenomenon for log-periodic

rent at the feed point of the structure, the phase of the received signal will be delayed by 180° as the structure is expanded through a period. In Fig. 14-34, the distance to an arbitrary transverse element is given by KR_n. The expansion of the structure through a period is accomplished by letting K increase from 1 to $1/\tau$. During this expansion all lengths involved in the structure are multiplied by K. In Fig. 14-34 the phase delay in radians is plotted versus K on a logarithmic scale. The ideal phase variation is given by the solid straight line. Measurements have indicated that the actual phase variation is somewhat like the dashed line. The approximate measurements made to date indicate that the deviation of the dashed line from the straight line is not more than 15°. The relation between the phase γ_n and K_n is given by

$$K_n = \tau^{\gamma_n/\pi} \qquad (14\text{-}20)$$

Fortunately, the phase center and the element patterns are independent of the expansion or contraction of a logarithmically periodic element.

This phase rotation appears not only in the radiation field but also in the reflected wave on the feeder for log-periodic antennas and log-periodic transmission-line circuits.[51] It produces dispersion of transmitted or received signals, and the dispersion increases as τ approaches unity.

The information given in Figs. 14-29, 14-30, and 14-34 is sufficient for predicting the pattern of an array of similar end-fire elements. The method can be extended to cover a combination of E- and H-plane arrays. The phase-rotation phenomenon is extremely important since it allows a frequency-independent method of phasing the elements of the array.

Experimental and theoretical patterns for a six-element phased H-plane array of wire trapezoidal-tooth elements are given in Fig. 14-35. The values of the design

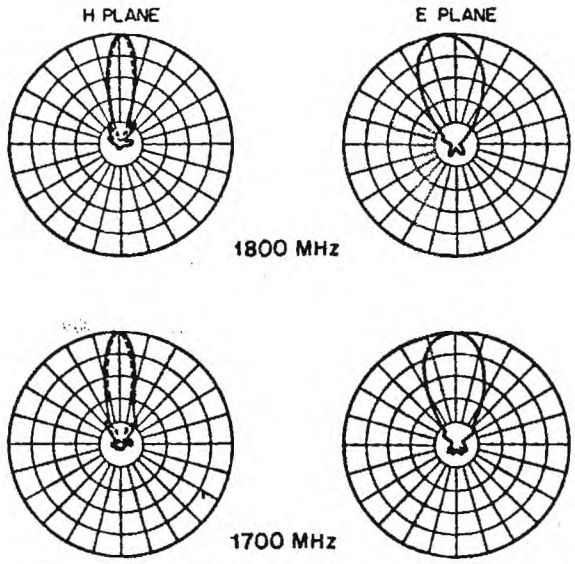

FIG. 14-35 Predicted (-----) and measured (———) patterns of a six-element phased array.

parameters for this array were $\alpha = 19°$, $\tau = 0.94$, $N = 6$, $\delta_n - \delta_{n-1} \approx 17°$ n, and $d/\lambda = 1.95$. The elements were phased to produce a beam-cophasal con The gain of the array was 14 dβ over a dipole.

Although gains of up to 18 dβ are feasible by using a combined E- and H array, the size and complexity of the antenna become great since it is necessary very small α angles and τ values near unity.

An approximate design procedure for arrays is given in Ref. 7.

14-5 CIRCULARLY POLARIZED STRUCTURES

Circular polarization may be obtained by using crossed LP dipole arrays. Fig 36 is a front view of a practical configuration. Feeders 1 and 2 are used to ex vertical and horizontal dipoles respectively. The solid lines represent the dipole cell and the dashed lines the dipoles in the next cell. It is desirable to make the between the feeder lines as small as practicable in order to simulate planar ar the two crossed arrays are identical, it is necessary to excite the two feeders broadband 90° phase difference circuit or a broadband quadrature hybrid. In ter case, both left and right circularization are obtained simultaneously. Altern one dipole array may be scaled by $\tau^{1/2}$ with respect to the other, producing a 90 shift of the radiated field. The two feeders may be fed in or out of phase for o of circular polarization or by a broadband 0–180° hybrid for both senses of polarization.

Another approach is to use two crossed dipole arrays, one scaled by τ excite them by a single feeder as illustrated in Fig. 14-37. It is quite surpris this gives the 90° phasing between the two arrays. Of course, only one sense of polarization may be obtained.

Since the H-plane beamwidth is usually about 50 percent greater than plane beamwidth, the axial ratio is low only for directions close to the axis of th To obtain low axial ratios over wide angles, a traveling-wave ring-type ra desired rather than crossed dipoles. The simplest solution is a spiral antenna. approach is to use four LP elements placed on the sides of a pyramid. Because of the asymmetrical-coupling problems between adjacent elements, the shunt-loaded LP elements of Fig. 14-27 do not work unless the spacing between the tips of adjacent elements is large. In this case the ψ angle is large, and in turn the back radiation is large. The traveling-wave structures of Fig. 14-27 may be used since they are much less susceptible to the asymmetrical coupling. However, these structures are limited to small α angles, which leads to a long antenna.

Some LP monopulse antennas have been used as feeds for reflectors. They consist of a circular array of six or eight

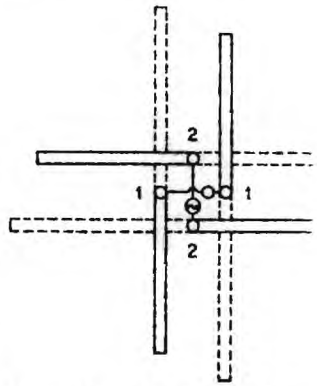

FIG. 14-36 Feeder configur crossed LP dipole antennas.

John Thomas F.I.
John Sutton

TECOM
TECHNICAL EXCELLENCE COMMITTED TO QUALITY

TYPE 201600 DUAL POLARIZED CAVITY BACKED ANTENNA

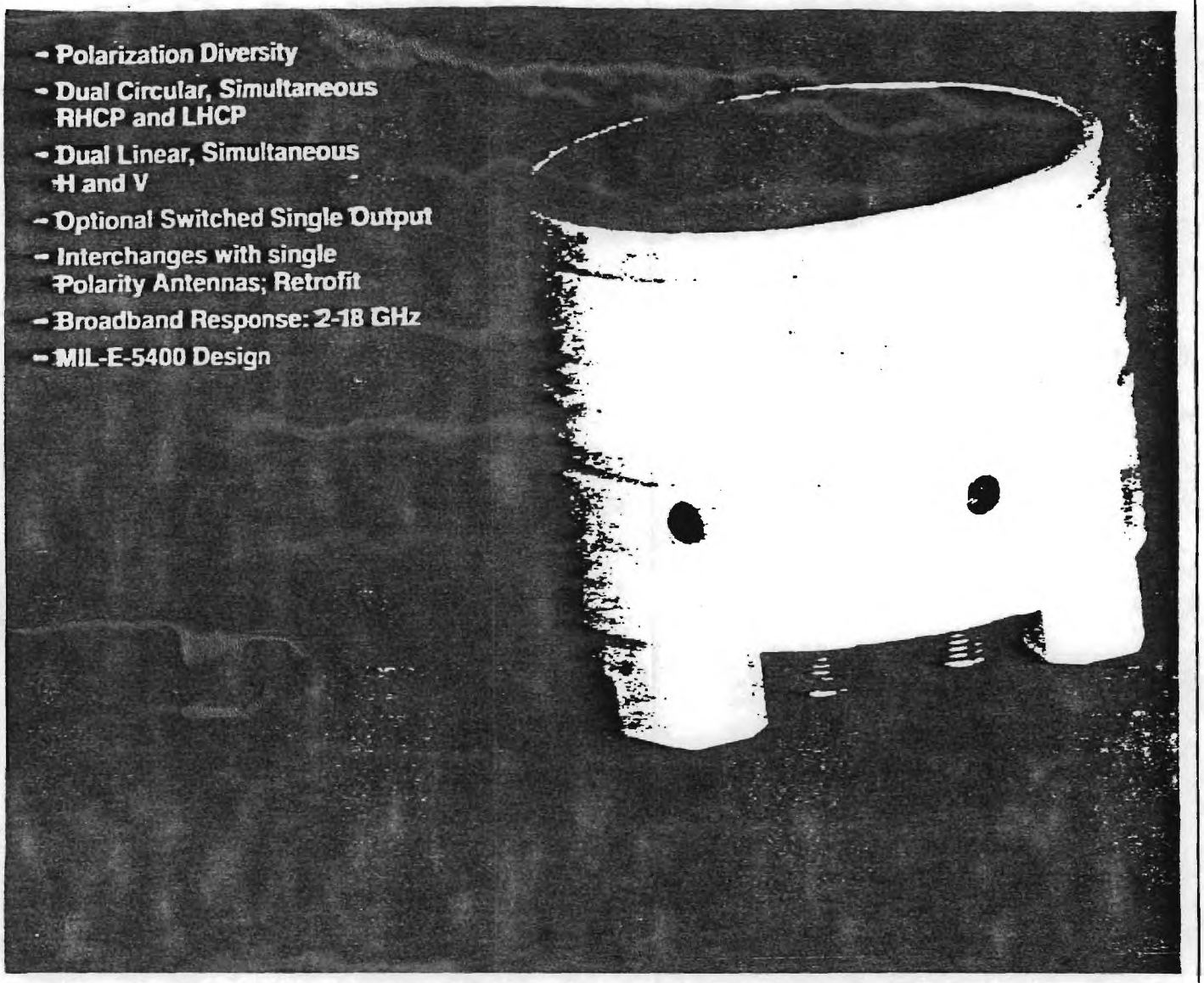

PERFORMANCE SPECIFICATIONS

CHARACTERISTICS	201600-1	201600-2
Polarization:	Dual Linear Simultaneous H & V	Dual Circular, Simultaneous RHCP & LHCP
Frequency:	2 to 18 GHz	2 to 18 GHz
VSWR:	See Figure 1	See Figure 2
Half Power Beamwidth:	115° to 65°	115° to 65°
Ellipticity At 0°:	N/A	2.0 Nominal (3 dB Max.)
At ±45°:	N/A	≤ 4 dB

CHARACTERISTICS	201600-1	201600-2
Power Handling Capacity:	1.0 W/CW	1.0 W/CW
Gain:	See Figure 3	See Figure 4
Amplitude Tracking		
At 0°	≤ ± 1.25 dB	≤ ± 1.25 dB
At ±45°	< ± 1.50 dB	< ± 1.50 dB
At ±60°	< ± 2.00 dB	< ± 2.00 dB
Connectors:	(2) SMA Female (Option: 1 Switched SMA)	(2) SMA Female

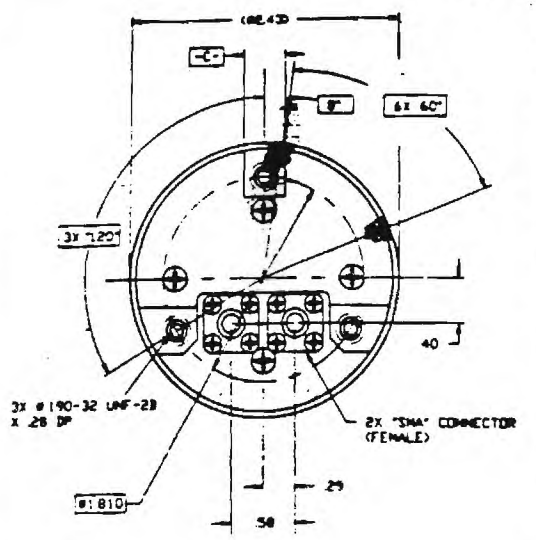

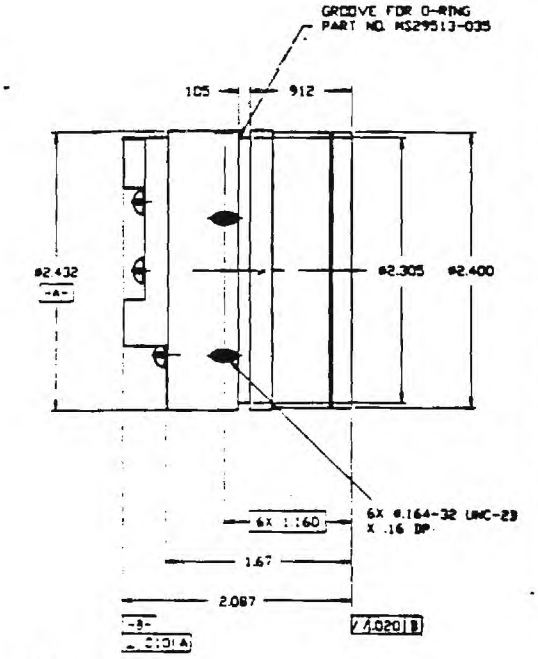

Weight: 9.0 Ozs.

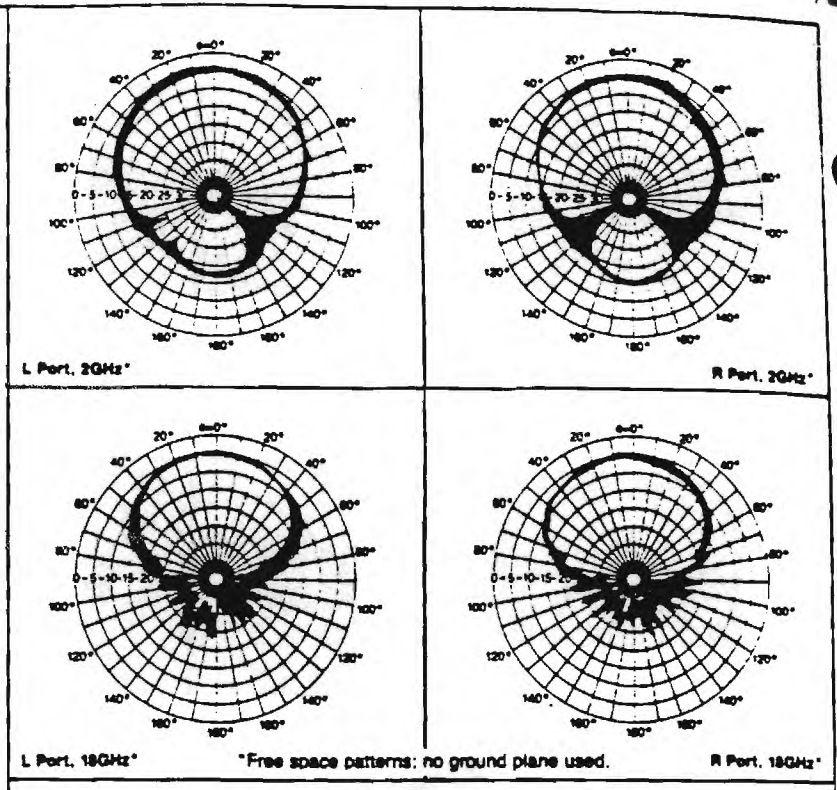

*Free space patterns: no ground plane used.

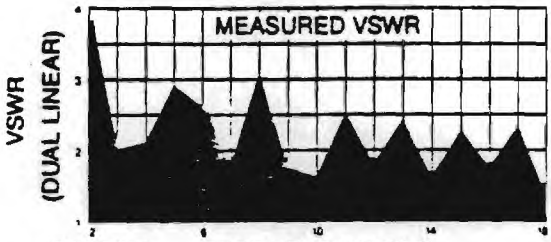

FIGURE 1

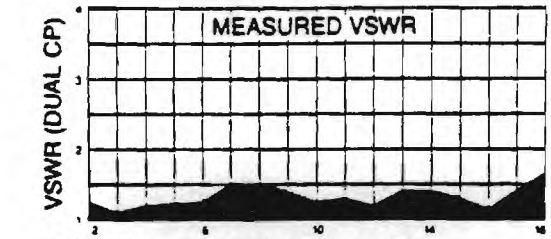

FIGURE 2

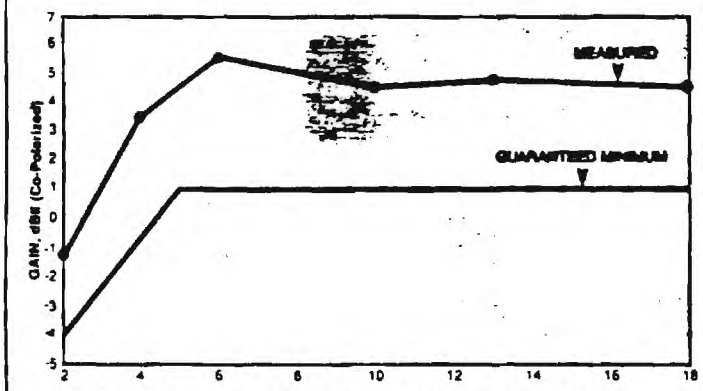

FIGURE 3: Peak boresight gain specification (V or H)

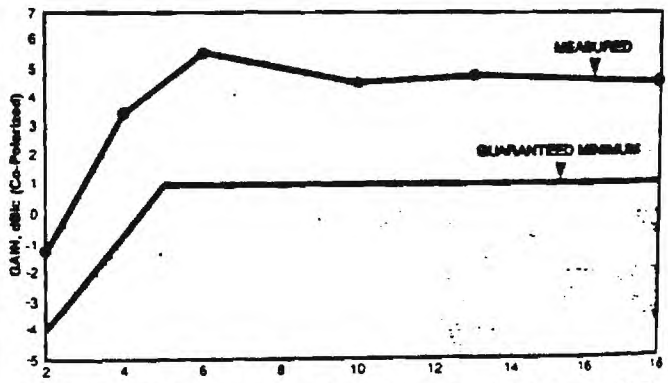

FIGURE 4: Peak boresight gain specification (RHCP or LHCP)

TECOM
9324 Topanga Canyon Blvd.
Chatsworth, CA 91311
(818) 341-4010 TLX 69-8476

(19) Europäisches Patentamt
European Patent Office
Office européen des brevets

(11) Publication number: 0 198 578 A1

(12) EUROPEAN PATENT APPLICATION

(21) Application number: 86301175.5

(22) Date of filing: 19.02.86

(51) Int. Cl.⁴: H 01 Q 11/10

(30) Priority: 19.02.85 US 703042

(43) Date of publication of application: 22.10.86 Bulletin 86/43

(84) Designated Contracting States: DE FR GB IT

(71) Applicant: Du Hamel, Raymond Horace, 707 Continental Circle Apt. No. 1627, Mountain View California 94040 (US)

(72) Inventor: Du Hamel, Raymond Horace, 707 Continental Circle Apt. No. 1627, Mountain View California 94040 (US)

(74) Representative: Cross, Rupert Edward Blount et al, BOULT, WADE & TENNANT 27 Furnival Street, London EC4A 1PQ (GB)

(54) Dual polarised sinuous antennas.

(57) A sinuous antenna is disclosed having N identically and generally sinuous arms (11) extending outwardly from a common axis (12) and arranged symmetrically on a surface at intervals of 360°/N about the central axis. Each antenna arm comprises cells of bends and curves with each cell being interleaved without contact between adjacent cells of an adjacent antenna arm.

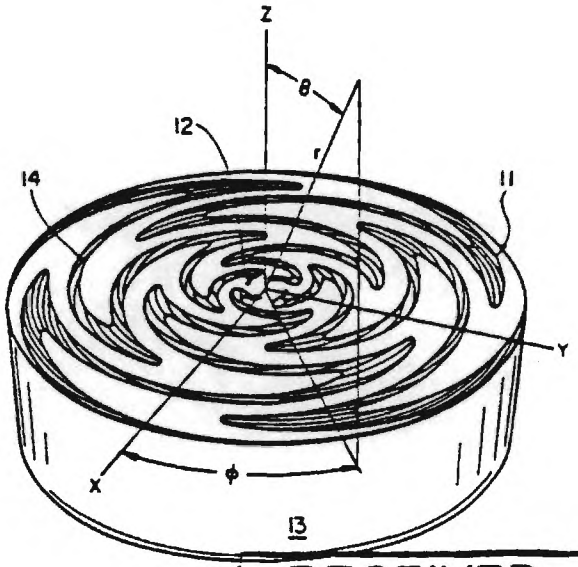

EP 0 198 578 A1

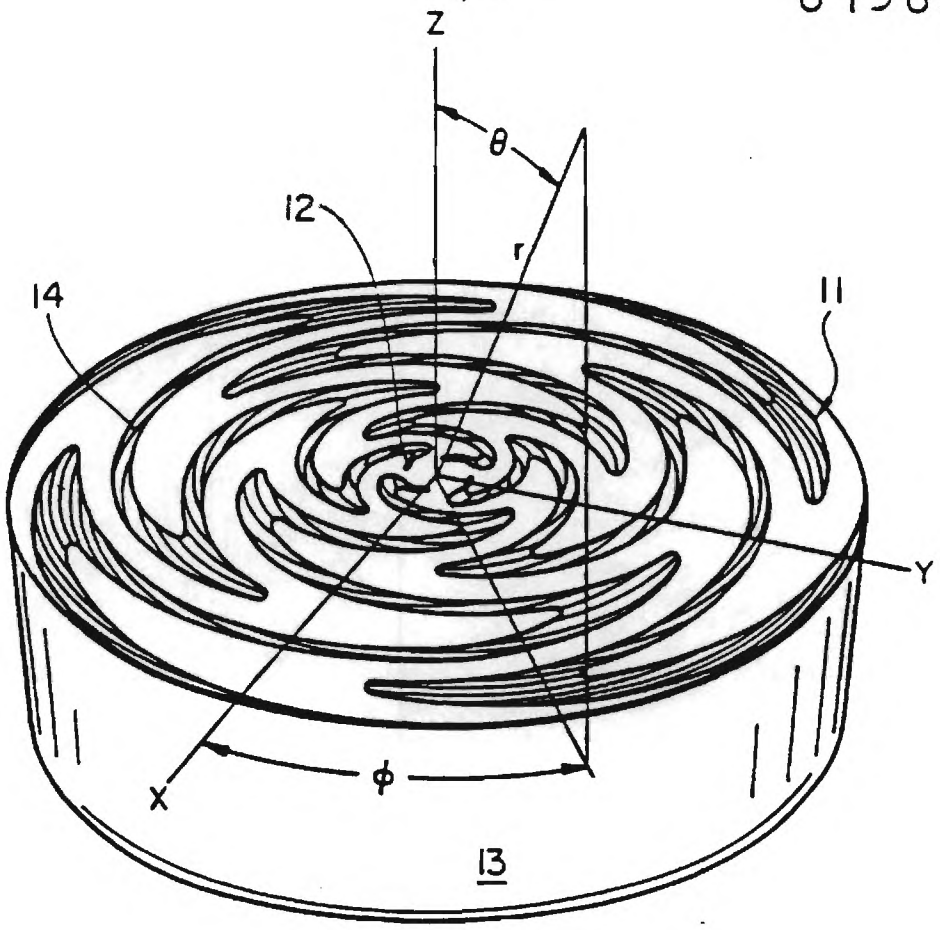
Z
θ
12
r
14
11
Y
X
φ
13

FIG_1

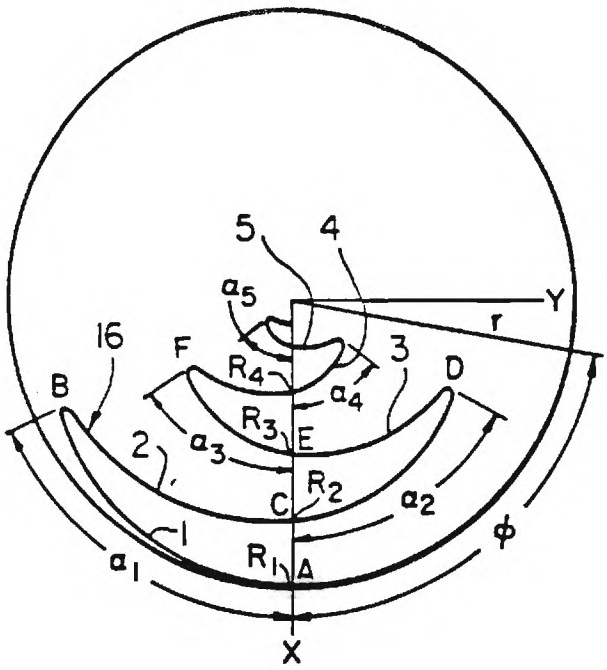
5
4
a5
Y
r
16
F
R4
3
D
B
a4
R3
E
2
a3
C
R2
a2
1
R1
A
a1
φ
X

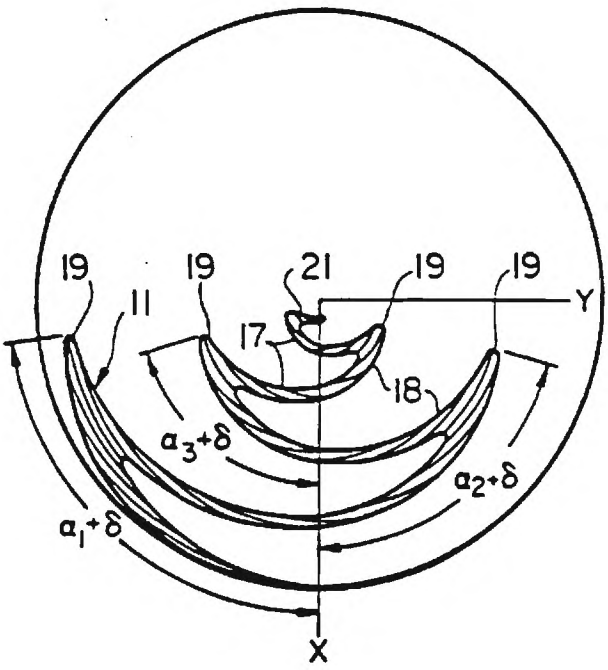
19
19
21
19
19
Y
11
17
18
a3+δ
a2+δ
a1+δ
X

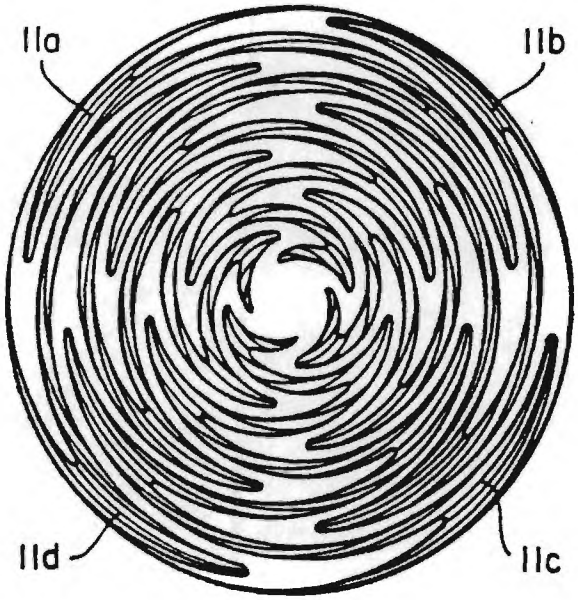

FIG_4

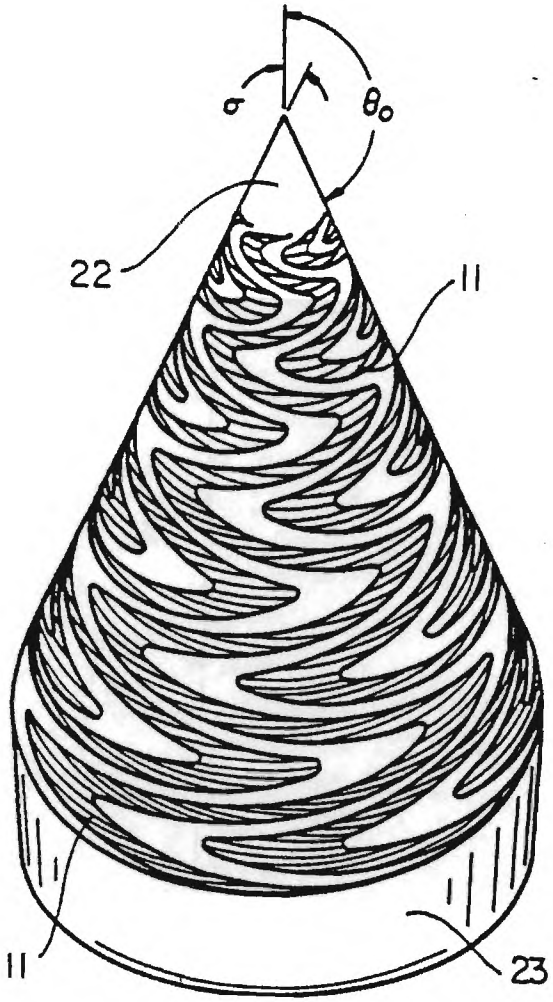

0198578

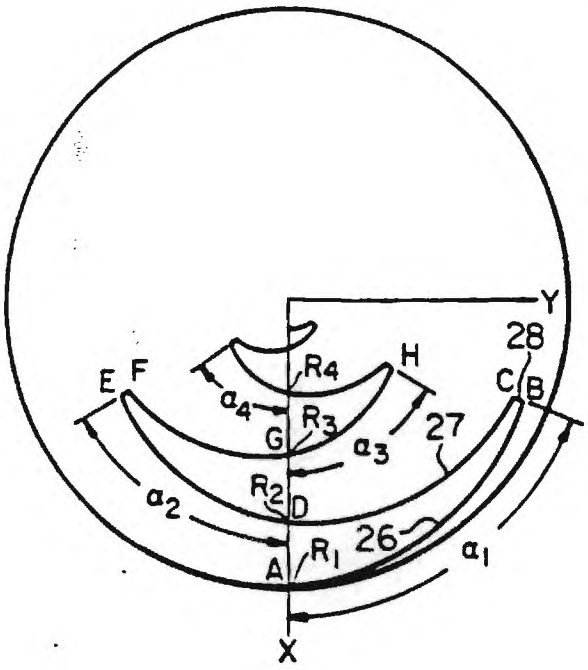

FIG_6

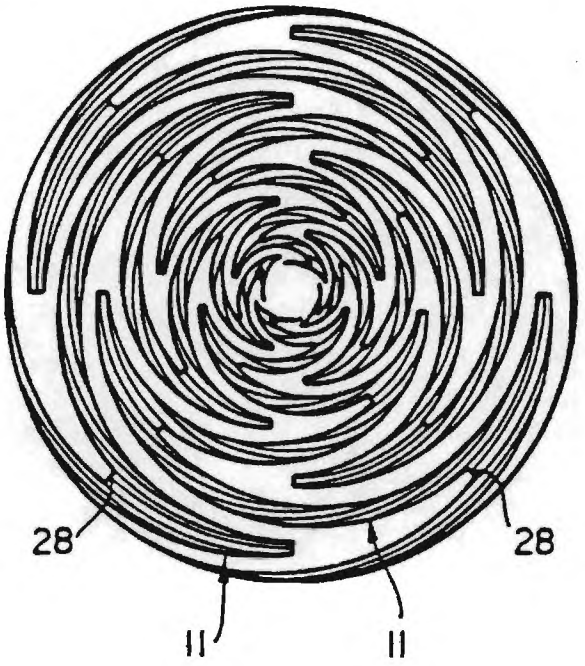

FIG_7A

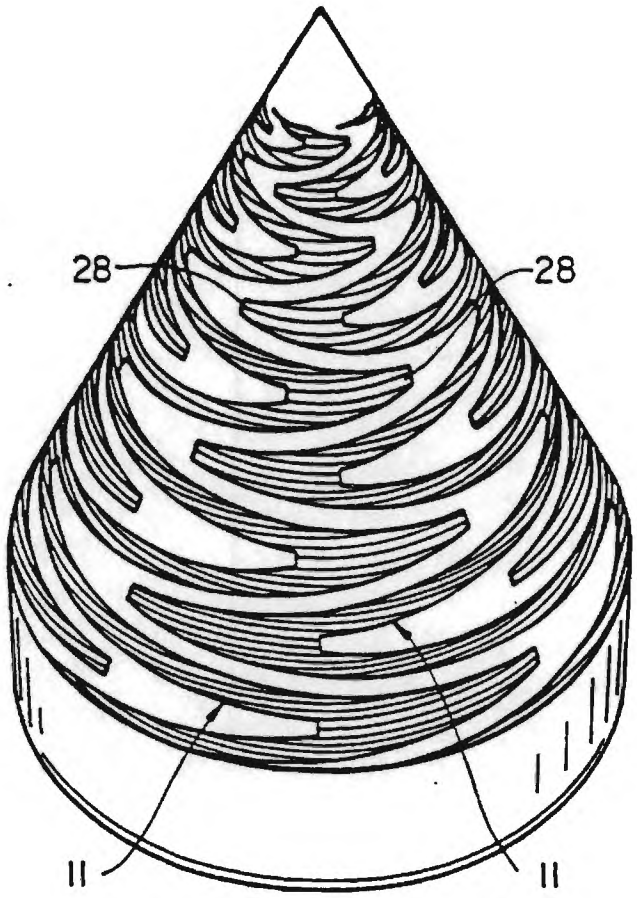

0198578

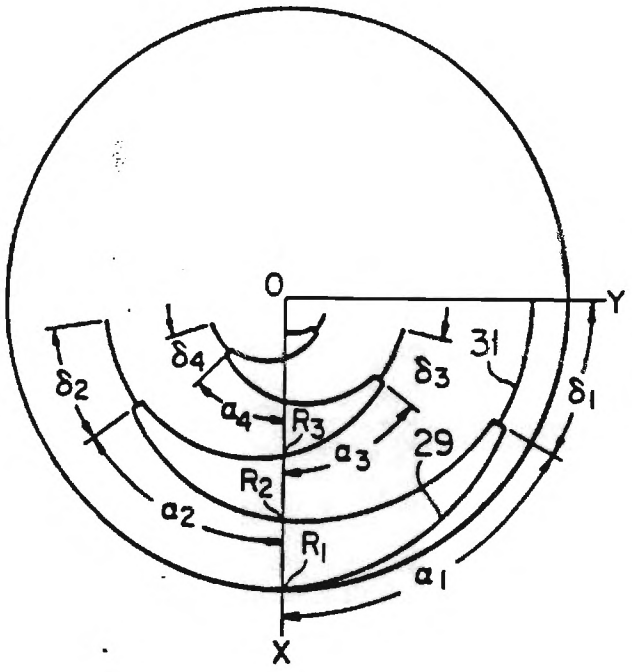

FIG_8

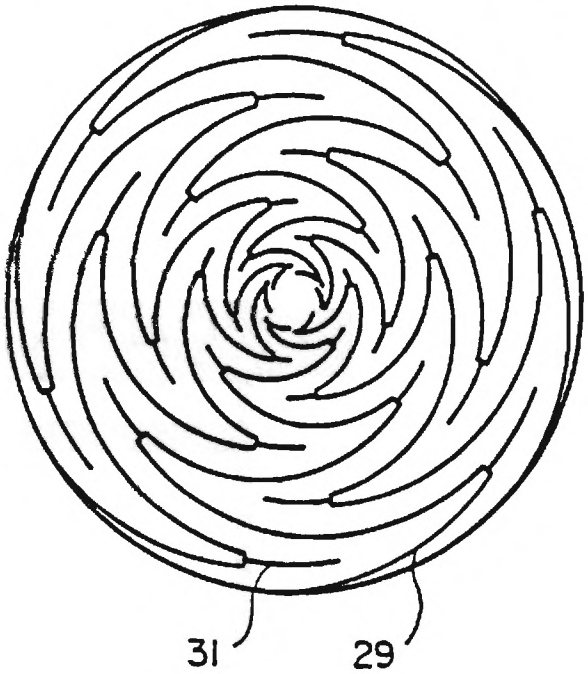

FIG_9

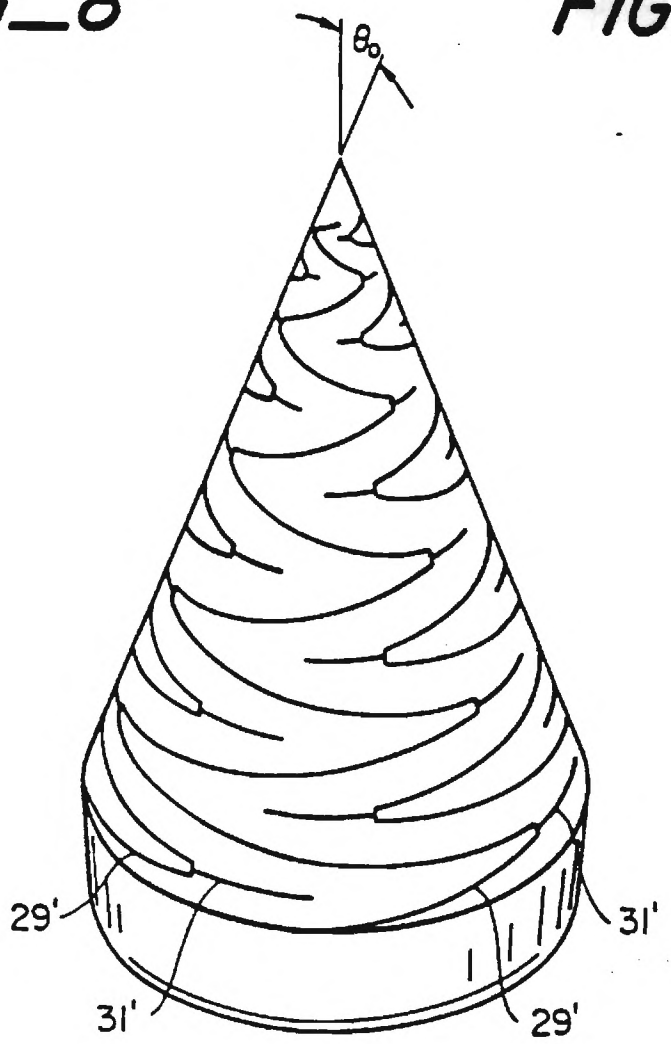

0198578

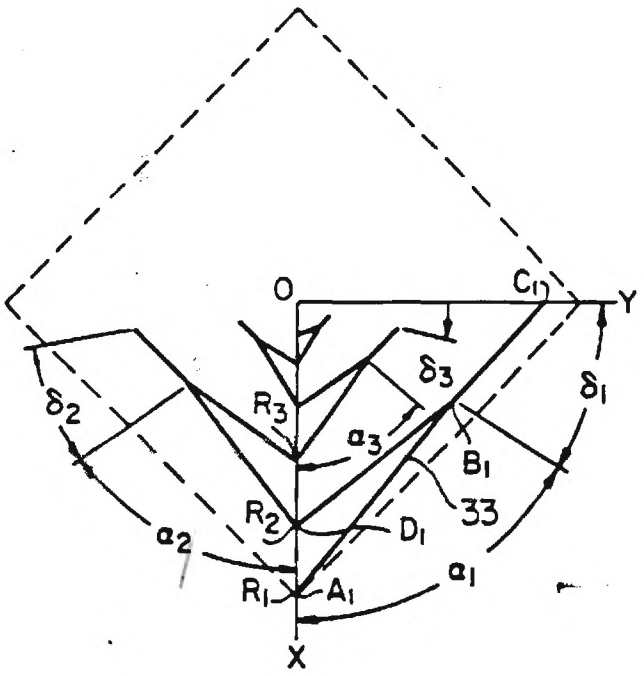

FIG_11

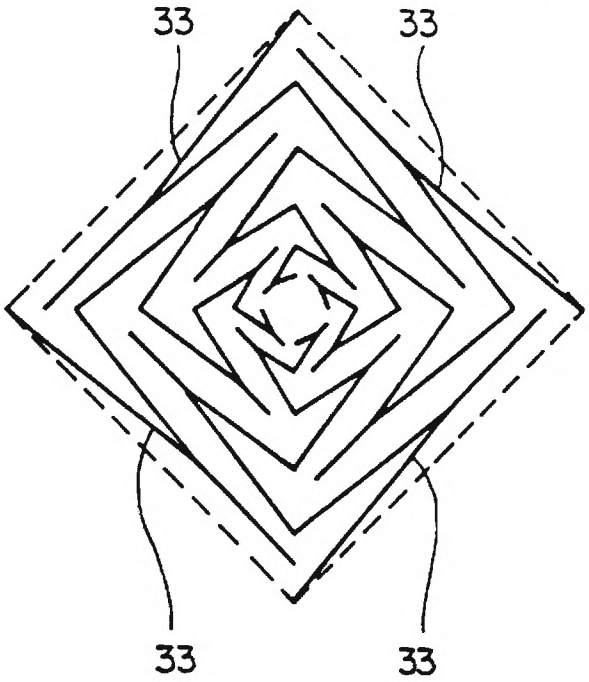

FIG_12

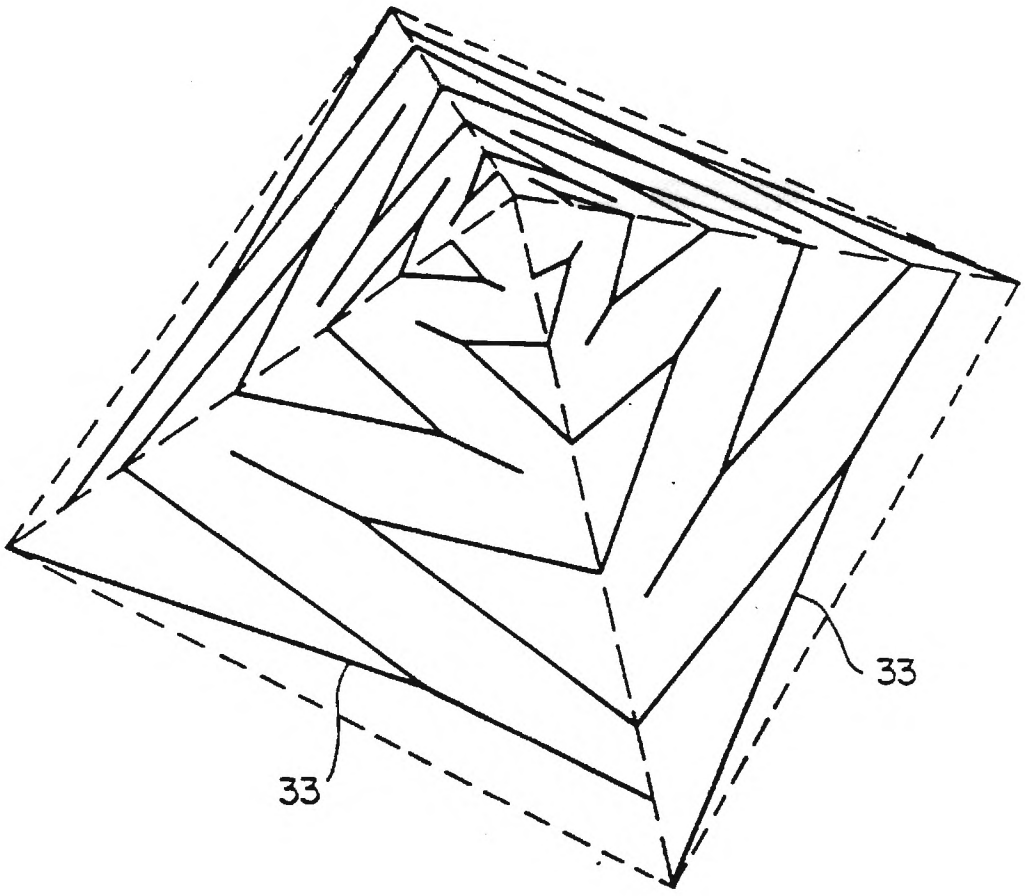

C. E. Ryan Jr.

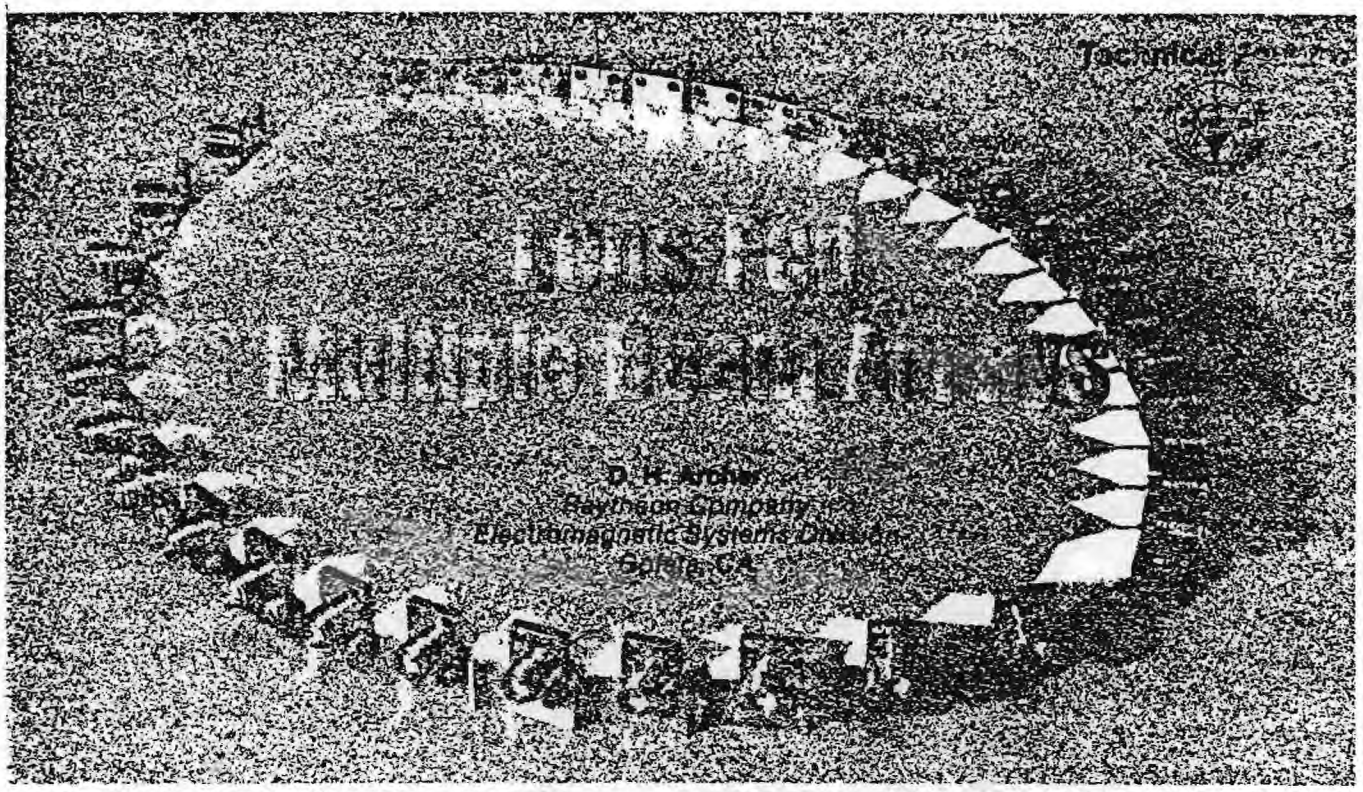

Introduction

The previous paper described the element-steered type of phased array, wherein the individual phase shifters, located behind the array radiating elements, are driven to form a focused beam that is pointed in the desired direction in space.

This paper describes the lens-fed type of phased array, wherein an entire set of contiguous beams is formed simultaneously, with each beam processing the full gain of the projected array aperture. From a single array, multiple simultaneous beams can be formed, covering a very large angular sector and an extremely wide frequency band. True time delay is used in the beam formation, so the beam-pointing directions in space remain invarient with frequency.

Lens-fed multiple beam arrays are particularly attractive for ESM receive applications, since they provide continuous spatial surveillance with high antenna gain and good angular resolution. When these arrays are used for ECM transmit applications, relatively low power amplifiers are placed in each of the array element feed lines. Such a distributed amplifier array can be sized to generate any desired level of ERP from a few kilowatts to tens of megawatts. These radiated power levels are available at 100 percent duty cycle over operating bandwidths of 3:1 and can be controlled to direct optimized ECM techniques discretely at multiple threat emitters.

Types of Multiple Beam Arrays

The optimum type of multiple beam array feed depends upon the geometry of the array aperture. The types of arrays that will be discussed are linear arrays, conformal arc arrays, semi-circular arrays, circular arrays and two-dimensional planar or conformal arrays. Only lossless types of beamformers will be considered, as opposed to the lossy types which power-divide at the elements and then power-combine to form the simultaneous multiple beams.

Linear Arrays

The simplest type of beamformer for a linear array is the parallel-plate parabolic reflector, or pillbox. Multiple beams can be formed by using multiple feeds displaced from the focal point. To eliminate the aperture blockage associated with the multiple feeds, a double-layer pillbox could be used or the reflector could be replaced by a simple plano-convex lens.

Either of these approaches would produce unacceptable beam degradation for scan angles greater than five beamwidths off axis for focal length-to-diameter ratios (f/d) in the practical range of 0.25 to 0.40. Constrained lenses such as the metal-plate type offer an additional degree of design freedom which permits the specification of two points of perfect focus. Such a lens with an f/d ratio of 0.8 or greater can provide acceptable performance for beams scanned up to fifty beamwidths off axis. However, the frequency bandwidth of the metal-plate lens is limited to approximately ten percent, which rules it out for most ESM and ECM applications.

The Butler[1] matrix is a multiple beamforming feed for a linear array which does not suffer the above limitations on beam scan or frequency bandwidth. This beamformer, which consists of a network of interconnected quadrature hybrid couplers and fixed phase shifters, forms its multiple beams by means of constant-phase ramps. Consequently, the

beams scan in angle as the operating frequency changes. This is an undesirable feature for many ESM and ECM applications.

The Blass[2] matrix uses a set of beamport lines which cross-couple into the set of array feed lines through a two-dimensional set of directional couplers located at the intersections between the beamport lines and the array lines. The Blass matrix can be designed for true-time-delay multiple beam formation so that the beam positions remain fixed with frequency. With both the Butler and the Blass beamforming networks, the hardware complexity grows exponentially with increasing array size and they are both judged to be unacceptably complex for arrays of more than 16 elements.

The most appropriate wideband, wide-angle, multiple beam feed for linear arrays is judged to be the Rotman[3] lens. In its simplest form, the lens consists of the parallel-plate region shown in Figure 1 with array port probes along the left side of the lens and beam port probes along the right side. The array port probes are connected to the array radiating elements by means of coaxial cables, whose lengths vary with position in the array.

The lengths of the cables and locations of the array port probes are designed to provide perfect focusing at three points along the circular focal arc, as indicated by beam ports 1, 4, and 7 in Figure 1. The focusing is a consequence of providing equal electrical path lengths from a given focal point out to the corresponding radiated wavefront for each element of the array. The equal-path-length, true-time-delay beam formation produces fixed beams in space that do not scan with frequency.

Although the Rotman lens design provides for only three perfect focal points, the departure from perfect focusing at intermediate beam ports is negligibly small for most practical lens designs. In fact, the maximum beam scan capability of the Rotman lens is ±400 beamwidths. Figure 2 shows a 15-element linear array, fed by a Rotman lens, that forms 13 beams covering a 120-degree azimuthal sector.

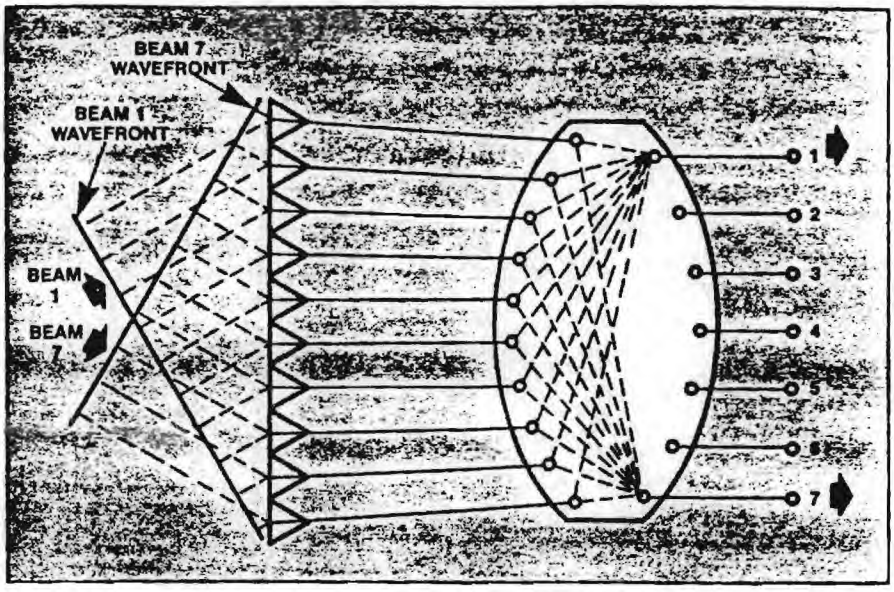

Fig. 1 Linear array fed by Rotman lens.

Conformal Arc Arrays

Generally, the Rotman lens is designed to feed straight linear arrays, but the design can accommodate array curvature up to a maximum arc length of approximately 90 degrees. This is advantageous for certain aircraft installations where it would be desirable to have the array aperture conform to the aircraft contour. The arc contour does not necessarily have to be circular. Figure 3 shows a 17-element lens-fed arc array which subtends a 45-degree arc. The array face is covered with a meanderline polarizer, which also serves as the radome.

The arc array provides more uniform antenna gain over its field of view than does the straight linear array. The different pointing directions of the elements cause a slight reduction in the on-axis gain, but the off-axis gain roll-off is decreased. In addition, the different pointing directions of the elements break up the array periodicity which effectively eliminates the possibility of having blind spots within the array field of view. Also, the curvature reduces the peak RCS of the array by spreading out the backscatter re

[Continued on page 176]

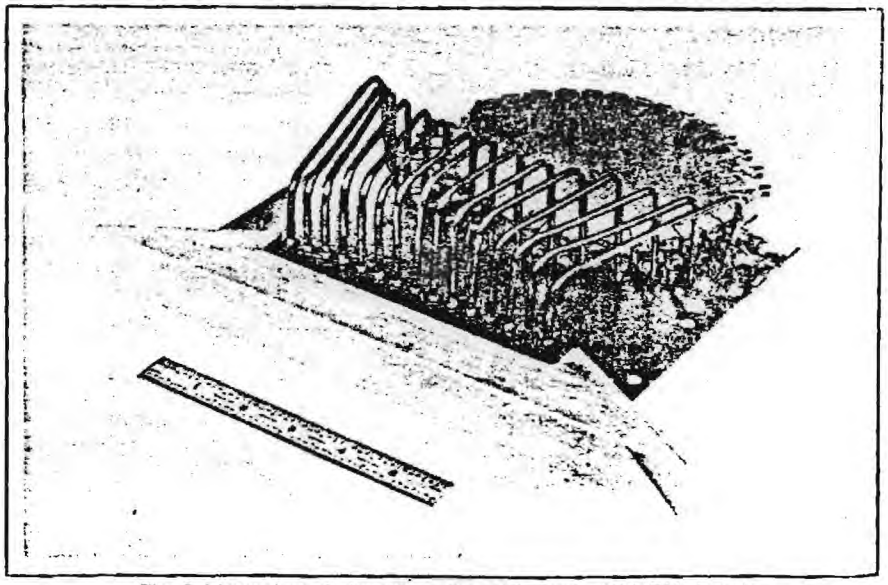

Fig. 2 Linear lens-fed array designed for 7.0 - 17.0 GHz band.

sponse caused by reflection from the radome and array elements.

Semi-Circular Arrays

Linear lens-fed arrays have been built which provide multiple beam coverage over a 180-degree sector, but the gain roll-off at the sector edges is excessively large, particularly for a polarization perpendicular to the plane of scan. If 180 degrees of coverage is required from a single array, a semi-circular array is the better choice.

The Rotman lens is not applicable as a feed for a semi-circular array. The R-2R lens[4] can feed a circular (or semi-circular) array and provide perfect focus for all beam positions in the plane of the array. The lens is circular with an electrical radius, R, when the radius of the array is 2R. Equal-length cables are used to connect the array elements to points on the lens in a 2:1 correspondence. That is, a lens feed point, located at angle θ, is connected to the array element at angle $\theta/2$. Thus, when the feed point on the lens is moved by an angle θ, the radiated beam scans by $\theta/2$.

Generally, the R-2R lens is used as a single-beam device and requires switching of the lens and array ports to accomplish wide-angle scanning. When used to form simultaneous multiple beams, the optimum configuration is to use half the R-2R lens circumference for array ports and the other half for beam ports. This will then feed a 90-degree arc array and form multiple beams over a maximum angular sector of 90 degrees.

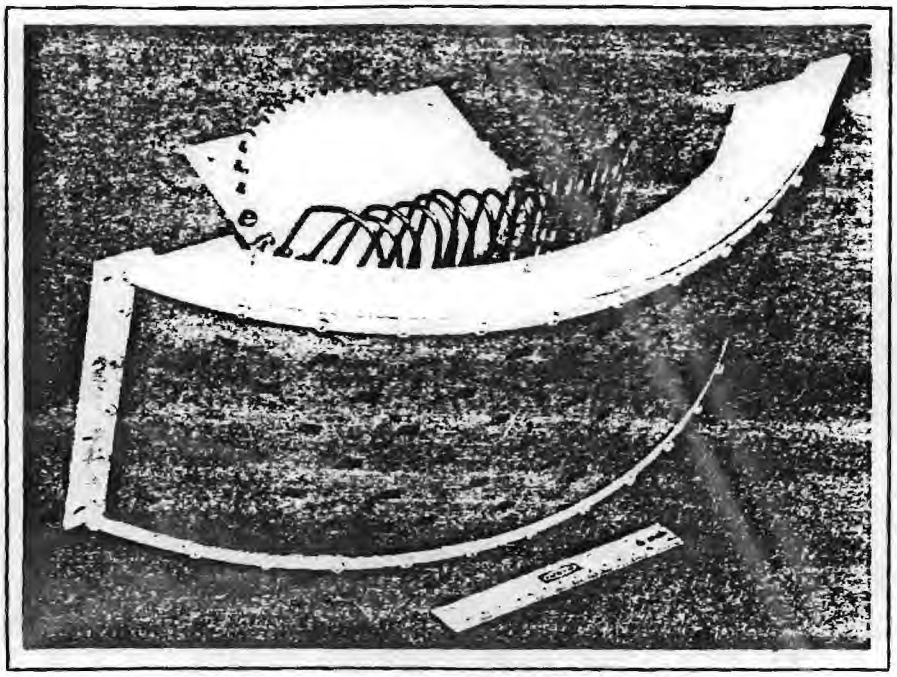

Fig. 3 Conformal arc array fed by Rotman lens.

In order to feed a semicircular array and form multiple beams over a 180-degree sector, the R-KR lens[5] is generally used. This lens also employs equal-length cables to connect lens ports to array ports, but they are connected in a 1:1 correspondence, rather than a 2:1 correspondence as with the R2R lens. For an array radius R, the electrical radius of the lens is KR, where K is chosen to optimize the focusing properties for the particular array arc length being utilized. For a semi-circular or circular array, the value of K is chosen to be approximately 1.9 for best focus. Whereas the R-2R lens radius was half the array radius, the R-KR lens radius is thus 1.9 times the array radius.

Figure 4 shows a semi-circular array of 17 elements, fed by an

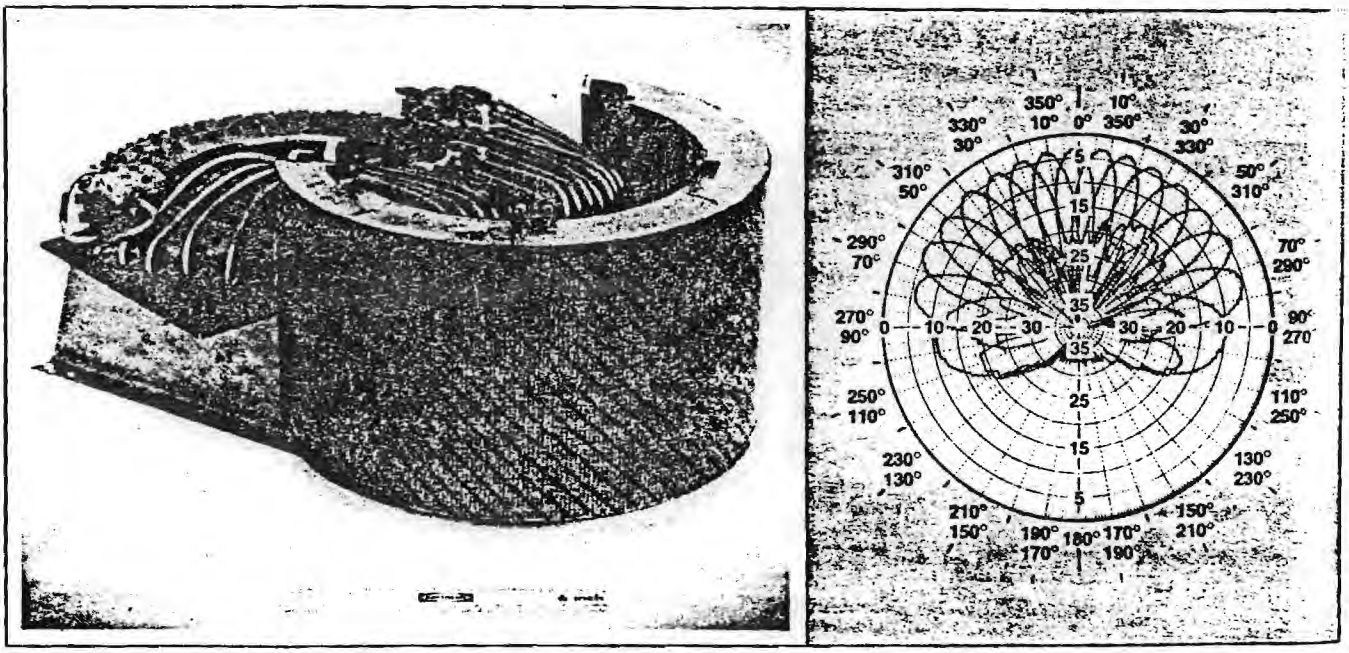

Fig. 4 Semicircular array fed by an R-KR lens.

R-KR lens which provides multiple beams over a 180-degree sector. The array operates over a 2.4:1 frequency band. The array elements are vertically polarized, so a meanderline polarizer is placed in front of the aperture to produce the desired circular polarization. The radiation patterns shown were measured with a rotating linear source, and the axial ratio is less than 1.0 dB throughout each main beam and sidelobes and throughout the entire angular sector.

Circular Arrays

A full 360 degrees of beam coverage can be obtained with an R-KR lens feeding a circular array. Figure 5 shows a 100-element array fed an R-KR lens that operates over the 4.0 to 11.0 GHz band. The radiation patterns, measured at 11.0 GHz, are presented in Figure 6. Since the array ports and the beam ports of the

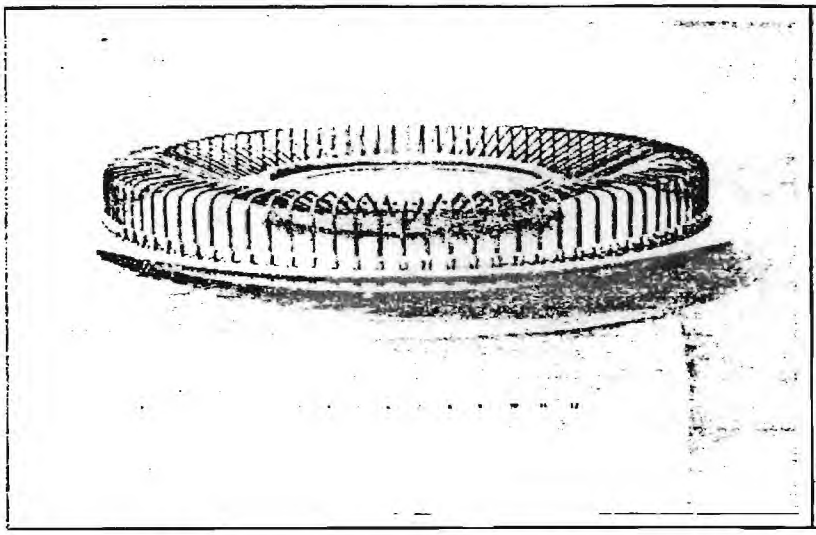

Fig. 5 100-element circular array fed by an R-KR lens.

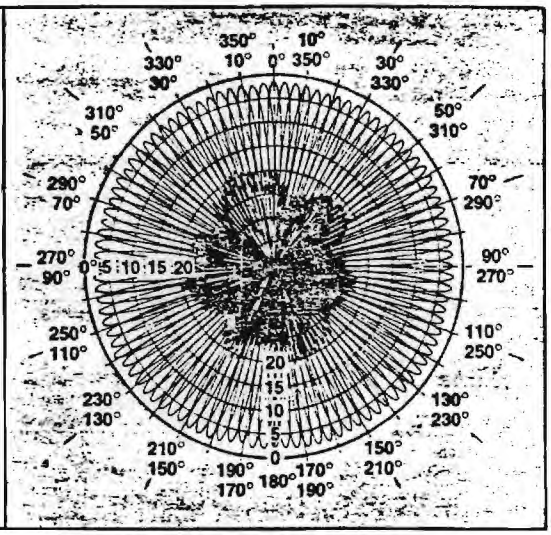

Fig. 6 Radiation patterns measured at 11.0 GHz for a 100 - element array fed by an R-KR lens.

lens are one and the same, the full connection to the circular array does not provide any output beam ports, as can be seen in Figure 5. One method of creating a set of output beam ports is to place a three-port circulator in each of the connecting lines between the lens and the array.

Generally, the bandwidth obtainable from circulators is not as great as that obtainable from the arrays and lenses. Therefore, for those cases where very wide bandwidth circular arrays are required, the approach shown in Figure 7 is recommended. Two lenses are used, and the corresponding upper and lower lens ports are fed to the input ports of a quadrature hybrid coupler. The upper output port of the hybrid feeds the associated array element while the lower output port of the hybrid forms the beam port for the diametrically opposed angle of arrival. This method of circular beam formation is extremely broadband.

An advantage of the circular array is that all beams have the same gain and the same beamwidth, and the beam intersections lie in planes perpendicular to the plane of the array. This is to be contrasted to the linear array in which the beamwidth broadens in proportion to the secant of the scan angle, the gain rolls off approximately as the cosine of the scan angle, and the beam intersections lie on the surfaces of cones, whose axes coincide with the line connecting the phase centers of the array elements.

There are two features of the circular array geometry which could rule out its use of particular applications: Proper focusing is provided only in the plane connecting the array (or in a pair of conjugate cones if the value of K is decreased); and the beamwidth in the vertical plane (perpendicular to the plane of the circular array) is inversely proportional to the square root of the array diameter. The halfpower beamwidths in the horizontal and vertical planes are given by:

$$BW_{Horizontal} = \frac{59\lambda}{D} \qquad (1)$$

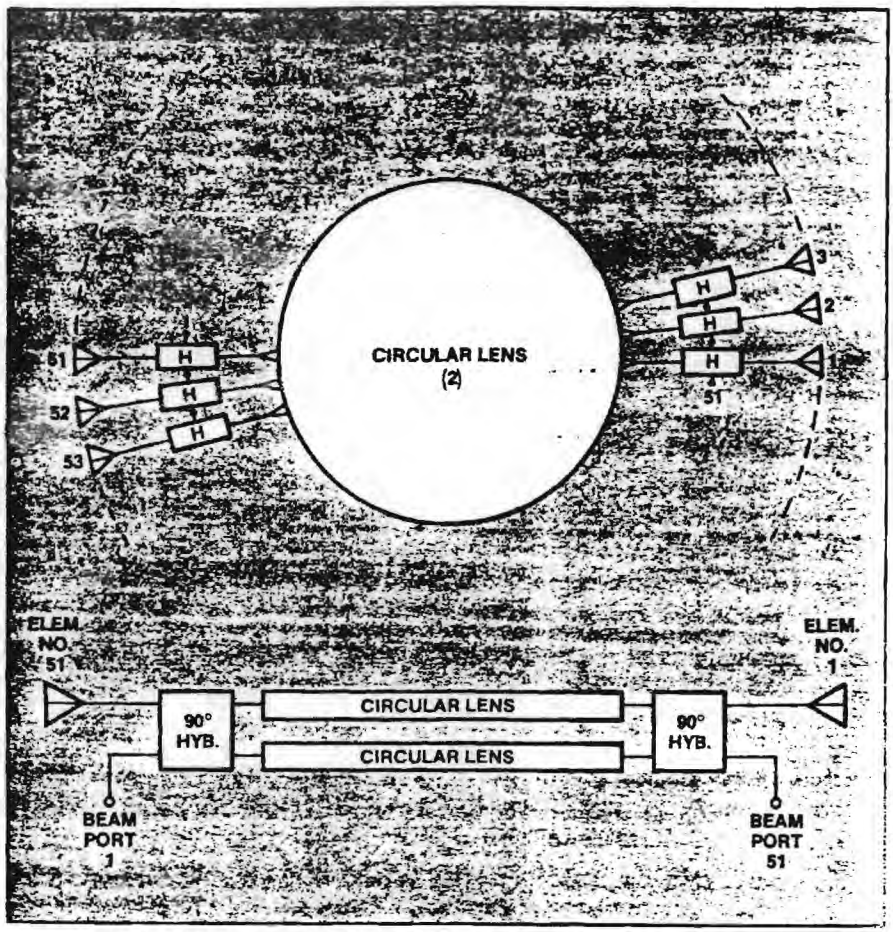

Fig. 7 Hybrid coupling of two circular lenses to create output beam ports.

$$BW_{Vertical} = 202\sqrt{\frac{\lambda}{D}} \qquad (2)$$

where D/λ is the array diameter in wavelengths.

For example, Equation 2 states that a horizontal circular array that is 25 wavelengths in diameter can provide no more than 40 degrees of elevation coverage, no matter how small the vertical array aperture is made. Thus, large diameter circular arrays are limited in the elevation coverage that they can provide.

Two-Dimensional Arrays

The linear, arc, semicircular and circular lens-fed arrays described above focused only in a single plane and formed a one-dimensional cluster of fan-shaped beams. It is frequently required to focus a two-dimensional array to form pencil beams. Actually, the Rotman lens is a parallel-plate slice of the two-dimensional bootlace aerial described by Gent.[6] Rather than use the large volumetric bootlace type of two-dimensional beamformer, cascaded stacks of one-dimensional Rotman lenses can be used to form a two-dimensional set of pencil beams from a planar array. For example, a vertical stack of lenses can be connected to the rows of array elements to provide focusing in the horizontal plane. The columns of output beam ports from the first stack of lenses can then be connected to an orthogonal stack of lenses to provide focusing in the vertical plane. The output beam ports of the second lens stack provide the desired two-dimensional cluster of pencil beams.

Printed Circuit Lenses

Early models of the Rotman lens were fabricated as parallel-plate structures. Coaxial probes were inserted along the periphery to form the array ports and beam ports. The major design problems associated with this method of construction were the broadband-

[Continued on page 183]

ing of the coaxial probe and the control of its radiation pattern. Current lenses are fabricated in printed-circuit format, either as stripline or as microstrip devices.

Figure 8 shows a 20-element, 16-beam Rotman lens constructed in microstrip format on a ceramic substrate. The input signal to the lens is fed through a standard SMA connector, which launches the signal onto a short length of 50-ohm microstrip line. Horn-like tapers are used as impedance transformers between the 50-ohm feed lines and the low impedance of the parallel-plate region. Satisfactory impedance match can be obtained over bandwidth ratios of 4:1 or greater.

Relative to the air wavelength, the wavelength within the parallel-plate region is reduced by a factor of $\sqrt{K}$, where K is the relative dielectric constant of the substrate material. Accordingly, all lens dimensions decrease by the factor $\sqrt{K}$; this provides a means for making the lens smaller. The lens substrate shown in Figure 8 is the ceramic barium tetratitanate with $K = 38$. Other ceramics that have been used as lens substrates are: alumina (K = 9.7), magnesium titanate (K = 16), titanium dioxide (K = 97), and cadmium titanate (K = 233). Thus, ceramics are available to achieve a wide range of lens size reduction factors.

The smallest port-to-port spacing on the lens is approximately a half wavelength at the high end of the band, which corresponds to the array element spacing. Consequently, for high fequency lenses, care must be taken not to shrink the lens size so much that there is no room for the connectors. Thus, lenses designed to operate in the 10 to 40 GHz region generally utilize substrate materials having very low dielectric constants; e.g., Teflon-fiberglass (K = 2.5) and Duroid (K = 2.35 or 2.2). Whenever the latter two plastic types of substrate materials are used, the lenses are generally constructed in stripline format. All ceramic lenses constructed by Raytheon have been in microstrip.

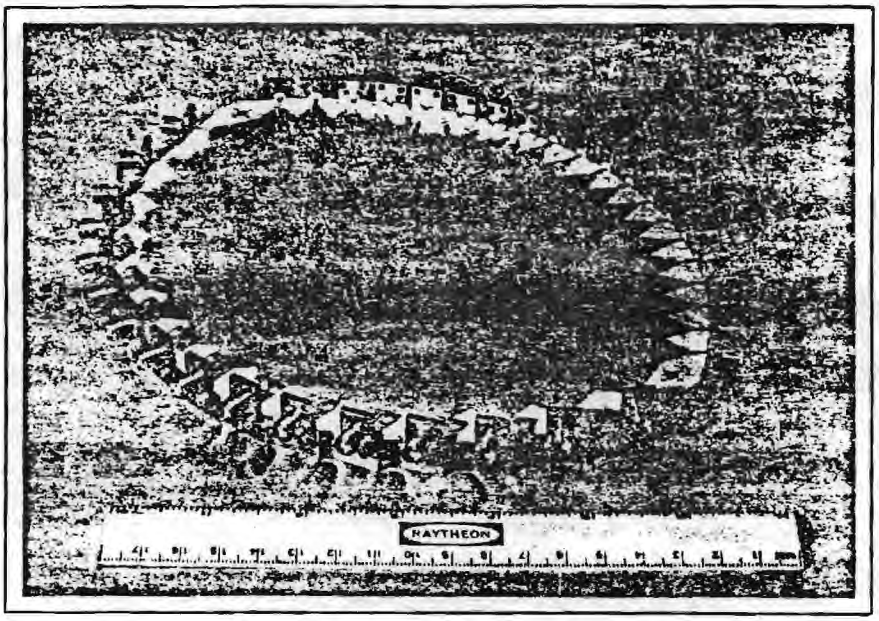

Fig. 8 Microstrip lens fabricated on a K = 38 ceramic substrate.

Broadband Array Elements

To be compatible with the bandwidth obtainable from the multiple beam lenses, the array elements should be capable of operating over frequency bandwidths of 4:1 or greater. Angular coverage sectors up to 120 degrees are desirable. For ESM and ECM applications, circular polarization is generally desired in order to be responsive to a wide range of threat polarizations. In order to prevent grating lobes from forming when the array is scanned to wide angles, the element spacing should not exceed a value of approximately 0.5 λ_{high}, where λ_{high} is the wavelength at the high end of the operating band.

The simplest broadband, circularly polarized element is the Archimedean spiral. If grating lobes are to be avoided, the maximum allowable spiral diameter is 0.25 λ at the low end of a 2:1 bandwidth array and only 0.125 λ at the low end of a 4:1 bandwidth array. The efficiency of such small spirals is unacceptably low, particularly for ECM transmit applications. Conical helices or log spirals with a small cone angle and small base diameter can be built to have better efficiency than the Archimedean spiral. However, the long taper causes unacceptable element-to-element shadowing when operating in a wide-scan array environment.

The most popular method for obtaining circular polarization from a broadband array is the use of linearly polarized radiating elements with a meanderline polarizer placed in front of the aperture (as shown in Figures 3 and 4). Multi-sheet polarizers have been built to operate over a frequency bandwidth of 4:1.

There are many types of linearly-polarized array elements that can provide high aperture efficiency when tightly packed in a broadband array environment. The radiating elements which have found the widest acceptance at Raytheon are the double-ridge horn, the double-ridge trough, the printed-circuit notch, and the printed-circuit horn.

Thirty-eight horizontally-polarized double-ridge horns arrayed in the E-plane are shown in Figure 9. This linear array provides an elevation coverage of 20 degrees and an azimuth scan coverage of 90 degrees. The array operates over a 2.6:1 frequency band. An in-line SMA connector transition is used to launch the input wave onto the ridges.

Seven vertically-polarized double-ridge elements arrayed in the H-plane in a trough are shown in Figure 10. This linear array provides an elevation coverage of 60 degrees and an azimuth coverage of 120 degrees. The operating frequency bandwidth of the array is in excess of 4:1. The center conductor of the SMA input tran-

[Continued on page 184]

sition passes through the upper ridge and press-fits directly into the lower ridge.

Eight printed-circuit tapered notch elements arrayed in the E-plane are shown in Figure 11. Both stripline boards making up the assembly have the tapered notch copper pattern etched on the outside. The inner sides of each board contain open-circuited printed transmission line feeds that pass under the narrowest part of the tapered notches. The radiated field is polarized horizontally (parallel to the plane of the stripline board). The array shown in Figure 11 is driven by a fixed power divider to form a single beam. When the array is driven by a Rotman lens, the coverage sector is approximately 120 degrees in azimuth by 120 de-

[Continued on page 186]

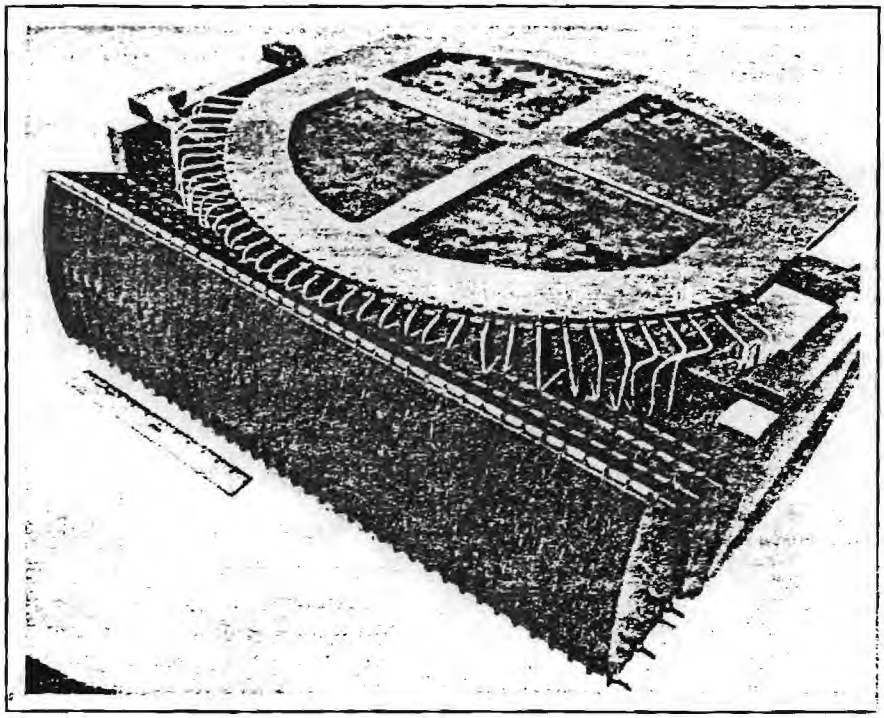

Fig. 9 E-plane array of double-ridge horns.

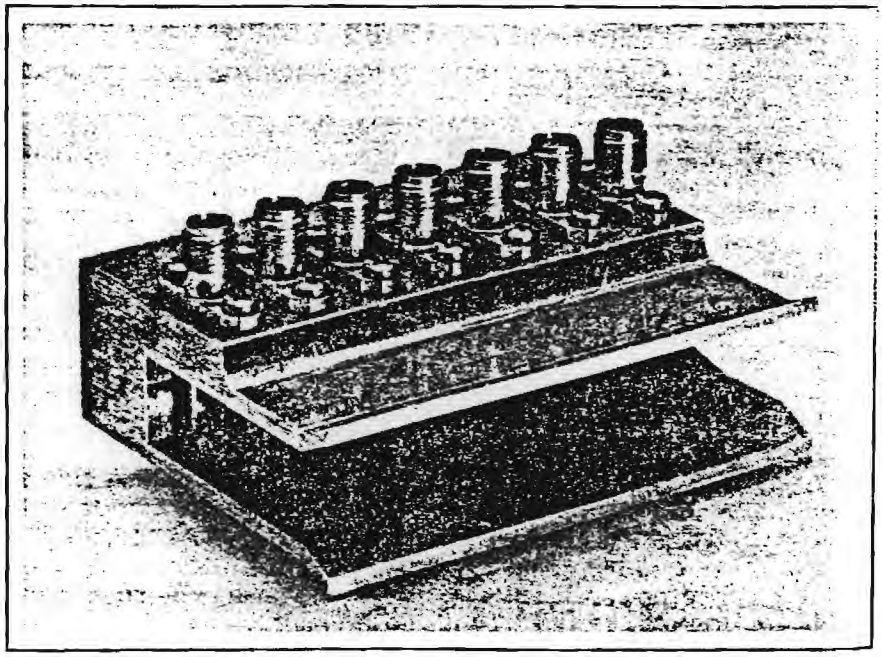

Fig. 10 H-plane array of double-ridge elements in trough.

[From page 184] ARCHER

grees in elevation. Frequency bandwidths of 4:1 have been achieved.

Eight printed-circuit horn elements arrayed in the H-plane are shown in Figure 12. This array is fed by a stripline eight-way power divider etched on the inner surface of the board. Immediately following the power divider circuit is a transition to microstrip which is followed by a tapering of the center conductor to form a horn. Radiation occurs directly from the microstrip, and tapered conducting plates are placed on the upper and lower surfaces of the microstrip assembly to increase the E-plane radiating aperture. Dielectric is placed within the tapered region for matching purposes. When the array is driven by a Rotman lens, the coverage sector is approximately 120 degrees in azimuth by 120 degrees in elevation.

ECM system requirements are increasingly calling for adaptive polarization on transmit. This is generally accomplished by implementing two orthogonally-polarized transmitters and driving them with the appropriate relative

[Continued on page 188]

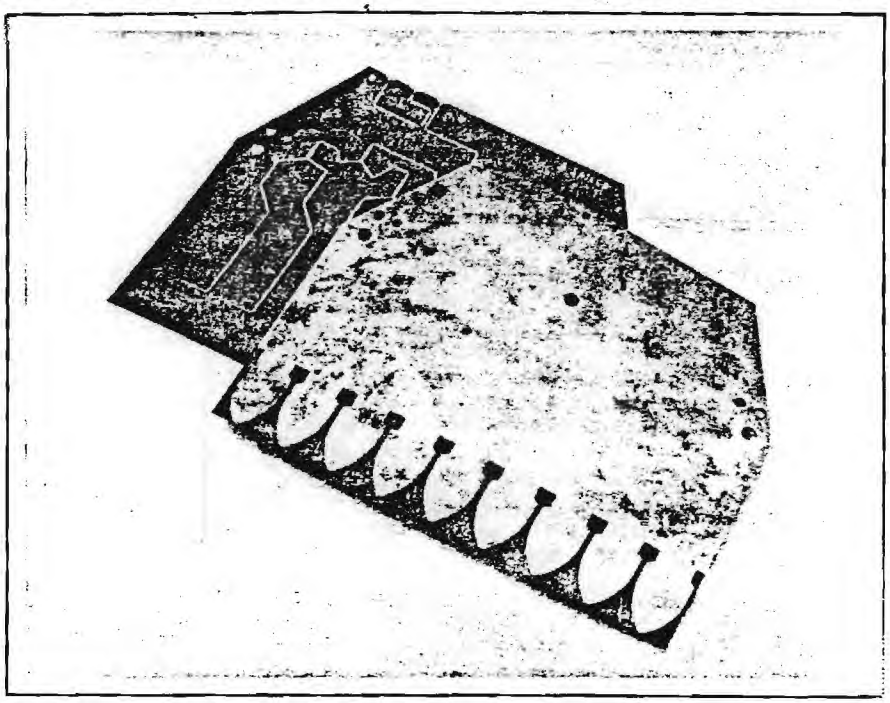

Fig. 11 E-plane array of eight printed-circuit notch elements.

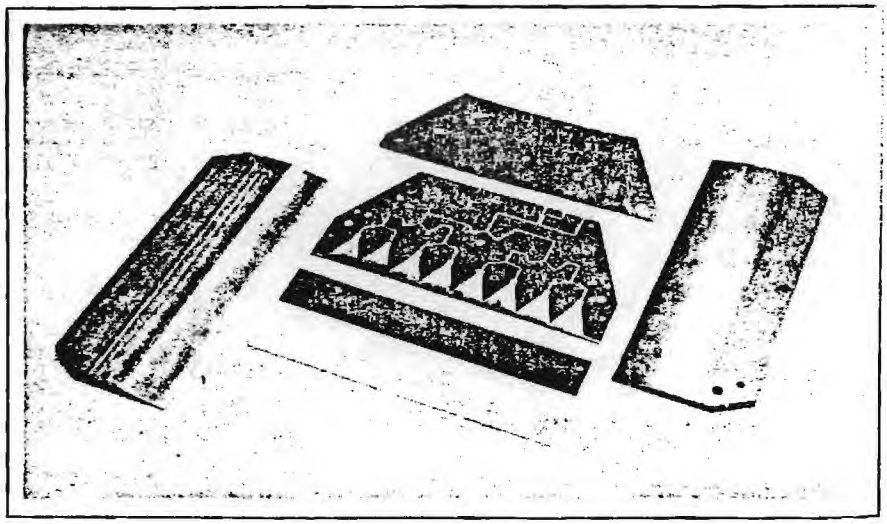

Fig. 12 H-plane array of eight printed-horn elements.

amplitude and phase relationship to generate the required transmit polarization. It is desirable that the phase centers of the orthogonally-polarized antennas be coincident so that the radiated polarization will be stationary (i.e., not vary with aspect angle).

The classic, broadband dual-polarized radiating element is the quadri-ridge horn. For operation in a broadband array that must be free from grating lobes, the horn aperture must be reduced in size to such an extent that extremely heavy ridging is required to prevent waveguide cutoff at the low end of the band. Such a heavily ridged horn has problems handling high input power levels, and the matching of the horn to free space is difficult.

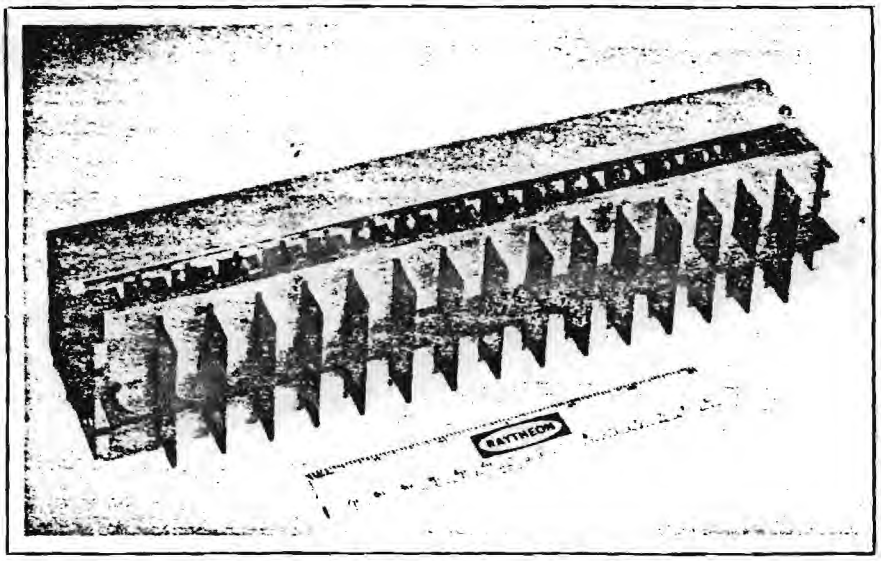

Fig. 13 Dual-polarized crossed notch array.

Types of dual-polarized arrays that have been used at Raytheon are shown in Figures 13, 14 and 15. Figure 13 shows a 15-element array of printed-circuit, tapered notch elements which have been crossed in "egg-crate" fashion to provide dual linear polarization with coincident phase center. The array provides a coverage sector of 120 degrees by 120 degrees and was designed to operate over a 2:1 frequency band. With this type of array, care must be taken to avoid surface wave resonances which can cause blind spots.

Figure 14 shows an eight-element array of double-ridge horns in which each horn sidewall has been replaced by a stripline circuit containing a four-way power divider feeding four stepped-notch elements etched at the front edge of the aperture. The alternating vertically-polarized notch sub-arrays and horizontally-polarized double-ridge horns individually have phase centers that are offset by half an element spacing. However, coincidence of the phase centers of the entire array is obtained by using an odd number of vertically-polarized elements and an even number of horizontally-polarized array elements. The coverage sector for the array of Figure 14 is 120 degrees in azimuth by 30 degrees in elevation. The frequency bandwidth is 4:1.

Figure 15 shows a third type of dual-polarized array that alternates the vertically-polarized notch sub-arrays of Figure 11 with the horizontally-polarized printed-horn sub-arrays of Figure 12. Coincidence for the phase centers of the interspersed arrays is maintained by using 33 vertically-polarized sub-arrays and 32 horizontally-polarized sub-arrays. The operating bandwidth for this array is 2:1, and the coverage sector is 120 degrees in azimuth by 10 degrees in elevation.

Lens-Fed Arrays for ECM

Electronic countermeasures systems' requirements continue

[Continued on page 190]

to demand higher and higher levels of ERP to enable the systems to cope with increasing numbers of threats of a more sophisticated nature. These increased demands can be met readily with the distributed-amplifier lens-fed array, without requiring any breakthroughs in either RF power sources or in the power-handling capability of the transmit antennas. For example, a doubling of the number of transmit array elements will double the transmit power and will also double the antenna gain, thus quadrupling the ERP. Yet, the maximum RF power levels of tens of megawatts are obtainable, if desired, merely by selecting the appropriate number of array elements.

Generally, lens-fed array transmitters use mini-TWTs as the power amplifiers. This is a small, lightweight, high-gain tube that

[Continued on page 192]

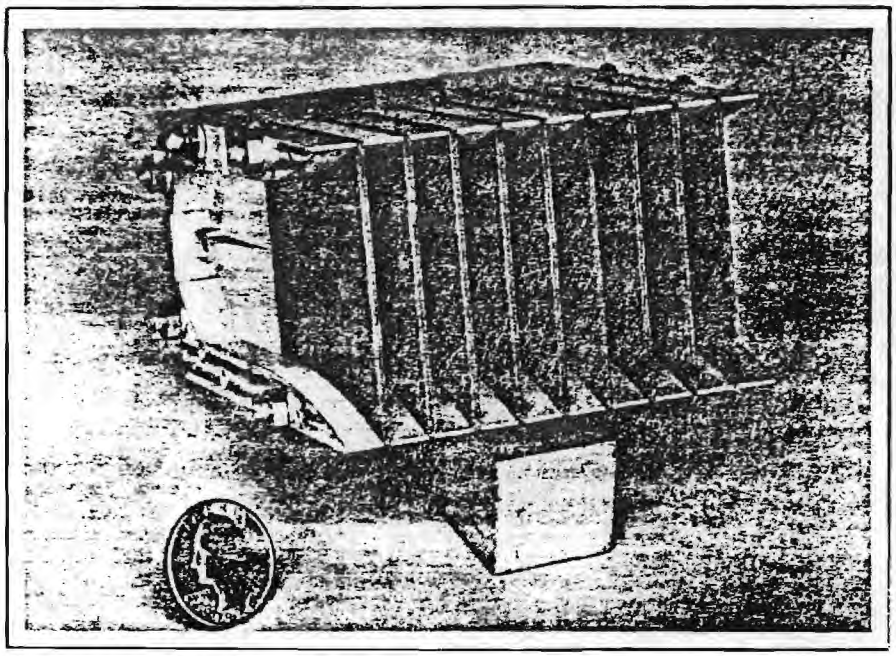

Fig. 14 Dual-polarized array of double-ridge horns and printed-circuit stepped notches.

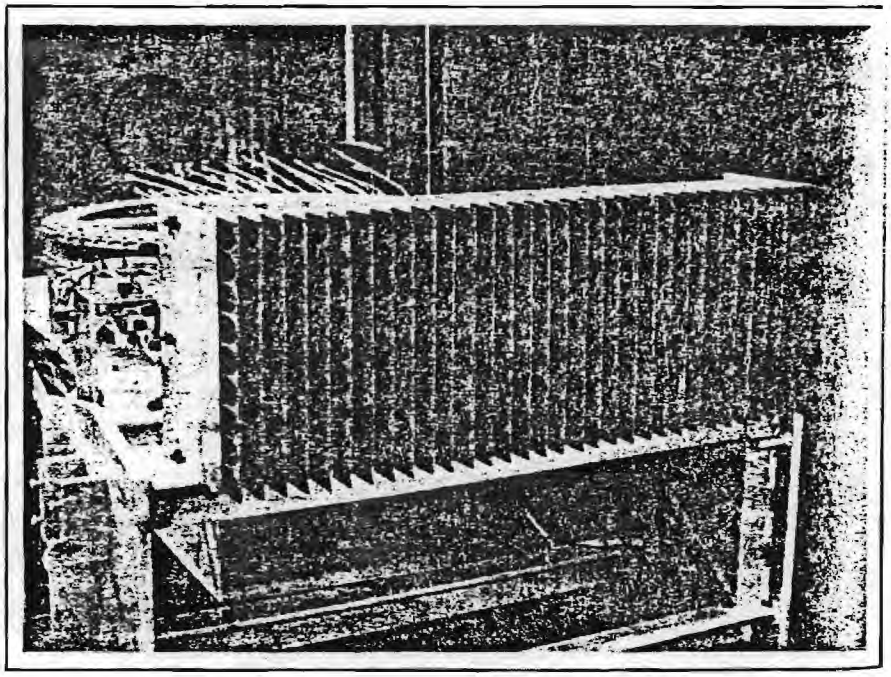

Fig. 15 Dual-polarized array of printed-circuit notches and printed circuit horns.

operates over the 4.5 to 18.0 GHz band and provides 50 watts of CW output power in the central part of the band, while requiring approximately 230 watts of DC input power. Relatively low electrode voltages are used, so the tubes are highly reliable. Because the tubes are distributed across the array elements, when they do fail, they fail gracefully. That is, the transmitter ERP falls off gradually, while the transmit beam remains well-focused and pointed in the right direction.

An important feature of the lens-fed array transmitter is its capability for efficiency forming multiple simultaneous transmit beams either at the same or at different frequencies. For example, if two input drive signals are simultaneously fed to the lens, each of the distributed TWTs will see two input drive signals. The output power of the tube will then divide between the two signals, and the power split ratio can be controlled by appropriately controlling the relative amplitudes of the drive signals. When the tubes are in hard saturation, the presence of two input drive signals causes spurious signals to appear at the output, and these intermodulation products reduce the total desired output power by approximately 1.0 dB.

Thus, when the array is driven to obtain an equal power-split between two frequencies at saturation, the ERP at each of the two frequencies is reduced by approximately 4.0 dB. That is, each beam still has the full array gain, since only the *power* is divided between the two frequencies. To form four simultaneous transmit beams at saturation, the ERP for each beam will decrease by 7.0 dB from the single-beam level (6.0 dB for the 4-way power division and 1.0 dB for intermodulation loss).

Lens-Fed Arrays for ESM

The lens-fed ECM transmit array achieves its high ERP by concentrating its transmit power into a narrow antenna beam. This places a requirement on the ESM system for measuring the angular location of the threat in order to properly direct the ECM response. Figure 16 shows a lens-fed multibeam receive array that determines the threat signal angle of arrival. There are half as many receive beams as there are transmit beam positions in the associated transmitter. Therefore, the angle of arrival must be determined to an accuracy of one-half the receive beamwidth, i.e., two-to-one beamsplitting is required.

The angle measurement is performed by placing crystal video receivers on each beam port and then measuring the ratio between the signal levels as received on the pair of adjacent beam ports containing the two greatest signal levels. For 3-dB adjacent-beam crossover levels, equal-width, half-beamwidth cells can be defined, which correspond to amplitude ratios less than 6.0 dB (near a beam peak) or ratios greater than 6.0 dB (near a beam crossover). The beamwidth of an array normally varies with frequency, and this would change the relative widths of the beam-split cells.

Therefore, the receive array of Figure 16 employs a constant beamwidth technique within the lens which maintains the beamwidth essentially constant over greater than an octave frequency band. This technique automatically provides increasing attenua-tion of the outer array elements as the frequency increases, thus keeping the array size constant in terms of wavelength. At the same time, the attenuation provides an amplitude taper across the array, which serves to reduce sidelobes.

The placement of crystal video receivers on every beamport of a lens-fed array yields an ESM receiver that is wide open in both frequency and angle and thus provides 100 percent probability of detection for all signals above the receiver threshold. If greater sensitivity is required on a wide-open basis, low-noise preamplifiers can be placed behind the array elements. Having detected a particular emitter in its main lobe, if it should be desired to follow the signal down into its back lobes, a narrowband superheterodyne receiver can be switched to the par-

[Continued on page 194]

ticular receive beam port for more detailed analysis.

The lens-fed receive array offers significant advantages when operating in highly dense signal environments. The antenna divides the coverage sector into narrow angle cells that remain fixed in space with respect to frequency. Only those signals falling within the boundaries of a given angular cell need be processed by the receiver associated with that cell. Thus the antenna provides an angle-sorting function that greatly thins the signal environment as seen by any given receiver.

Future Trends

The rapid advances currently being made in the state-of-the-art of solid-state FET amplifiers may have a profound effect upon future designs of lens-fed multiple beam arrays. However, for the FET to be competitive with the TWT, the cost for a one-watt amplifier will have to be reduced to the vicinity of $200 to $400. In order to replace each 50-watt

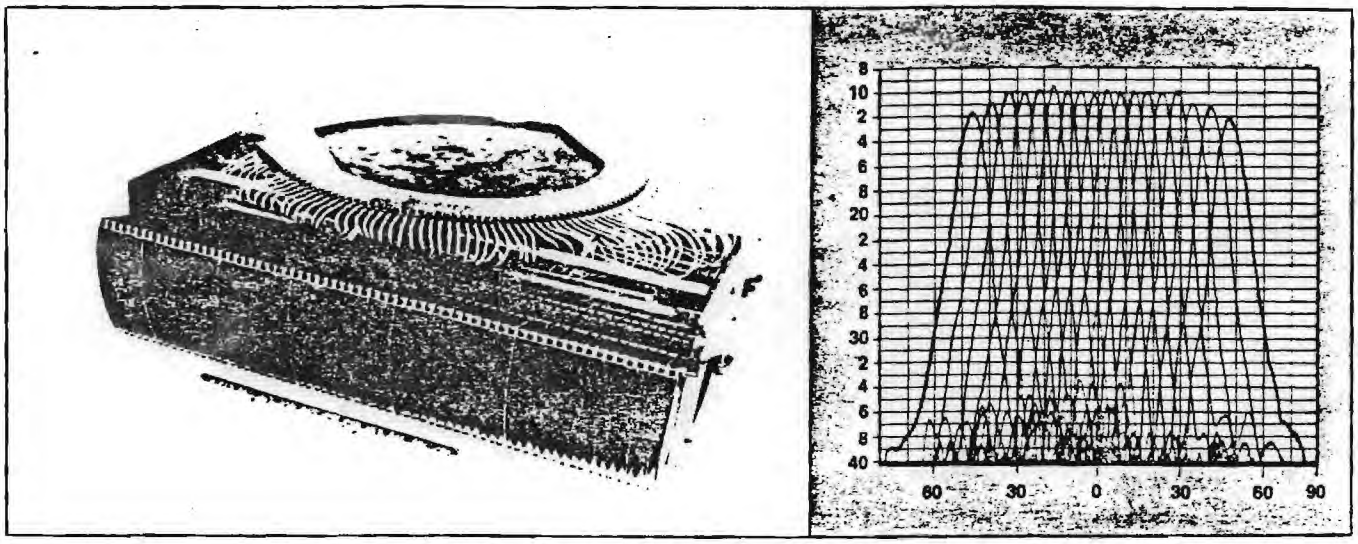

Fig. 16 Lens-fed, constant-beamwidth, receive array used in SLQ-32 system.

mini-TWT and its associated transmit element, a seven-element sub-array driven by seven one-watt FETs would have to be used. The seven watts of total transmit power coupled with the sevenfold increase in antenna gain is required to compensate for the 50-fold decrease in the amplifier power output.

Also, each seven-element, solid-state sub-array would have to be driven by a multibeam lens, a beamport switch (single-pole-seven-throw for single-beam operation), and a driver amplifier. It is the cost of this full seven-element distributed-amplifier, lens-fed array and driver circuitry that must be competitive with one mini-TWT and its associated radiating element.

The large numbers of array elements, amplifiers, lenses and switches required for a solid-state transmitter of moderate ERP would create an excessively complex package if they were to be interconnected in the customary manner, using semi-rigid coaxial cables. Therefore, the future trend must be towards the employment of a high level of RF component integration in MIC subassemblies in order to reduce the size, complexity and cost of the solid-state transmitter package and to make it maintainable.

The seven-fold increase in the number of solid-state array elements that are needed to match the ERP of its mini-TWT equivalent will increase the radar cross section (RCS) of the solid-state array by a factor of 49:1. Therefore, another future trend must be towards the reduction of the RCS contributions from antenna arrays. These reduction techniques ae expected to include aperture shaping, improved array element match for all polarizations, improved impedance match for internal antenna components, and a decrease in reflections from antenna structural components.

Another future trend in lens-fed arrays is expected to be a move towards extremely wide frequency bandwidths. Wider and wider bandwidths are being obtained from TWTs and solid-state amplifiers these days. In fact, a traveling wave type of FET amplifier is being developed by Raytheon with a power output approaching one watt over the 2.0 to 20.0 GHz decade. Therefore, it is expected that the lens-fed array bandwidth will need to be expanded accordingly.

Concerning the performance of wideband arrays, the antenna gain varies as the square of the frequency if the elements are tightly packed, as they would be when the array is designed to be free from grating lobes. Thus, for constant amplifier output over a decade bandwidth, the array ERP will fall off 20 dB from the high end to the low end of the band. This ERP rolloff can be greatly decreased by increasing the element spacing, with no sacrifice in ERP at the high end of the band. Wide element spacings increasingly will be used in future wideband lens-fed arrays, but attention will need to be devoted to dealing with the numerous grating lobes that will be introduced by the wide element spacing.

Future lens-fed arrays are expected to be polarization-diverse. The ESM arrays will measure the polarization on each received pulse and use this discriminant as a signal-sorting parameter. The ECM arrays will adapt their transmitted polarization to the threat in order to optimize the effectiveness of the jamming. ■

REFERENCES

1. Butler, J. and R. Lowe,: "Beamforming Matrix Simplifies Design of Electronically Scanned Antennas," *Electronic Design* Vol. 9, 1961, pp. 170-173.
2. Blass, J.: "Multi-Directional Antenna -A New Approach to Stacked Beams," IRE Natl. Conv. Record, 1960, Pt. 1, pp. 48-50.
3. Rotman, W. and R.F. Turner,: "Wide-Angle Lens for Line-Source Applications," IEEE Trans. on Antennas and Propagation, 1963, Vol. AP-11, pp. 623-632.
4. Boyns, J.E., A.D. Munger, J.H. Provencher, J. Reindel and B.I. Small: "A Lens Feed for a Ring Array," IEEE Trans. on Antennas and Propagation (Communications), Vol. AP-16, pp. 264-267, March 1968.
5. U.S. Patent No. 3,754,270 for "Omnidirectional Multibeam Antenna," Inventor: Wilbur H. Thies, Jr.
6. Gent, H.: "The Bootlace Aerial," *Royal Radar Establishment Journal*, Malvern, Worcester, October 1957.

A Survey of Circular Symmetric Arrays

J. H. PROVENCHER

Naval Electronics Laboratory Center
San Diego, California

Introduction

Considerable interest in circular, cylindrical and conical array antennas in recent years has prompted development of feed systems and components to provide rapid and highly agile beam positioning. Many of the problems associated with planar array design also exist in non-planar array design and a natural outcome is to apply solutions of the planar array design problems to circular arrays with appropriate changes. Beam steering generally requires a method to commute the amplitude and phase distribution around the array and this is usually accomplished by one of the following means:

1. Mechanical or electronic switch
2. Lens-switch combination
3. Hybrid-matrix phase shifter combination

The theory of the circular or ring array has been covered in the literature and some of the earlier arrays, primarily of the mechanically scanned type, will not be discussed here. It is only necessary to say that these arrays employed many of the concepts to be discussed and more recent applications will be presented.

Switched Arrays

A necessary requirement to steer the beam is that the amplitude and phase distribution be varied in such a manner that the excited portion or active sector of the array have the same distributions at each beam position. Several techniques make use of diode switches and phase shifters to effect the permutation. Figure 1 gives a schematic diagram of an array of this type developed by Wheeler Laboratories of Smithtown, New York.

The array has 32 elements with 8 elements activated at a time. In this case, the sector selection is provided by eight single-pole four-throw switches. The proper amplitude-and-phase ordering of the elements is maintained by the inter-connection of transfer switches, permitting cyclic permutation of the outputs from the distribution network. Phase shifters are included for fine steering; their location in the network requires as many phase shifters as there are excited elements. Eight phase tilt steerings are provided in the demonstration model to obtain steering to 0.1 beamwidth. The distribution network is used to obtain desired sum and difference pattern illuminations. The excitations are then carried through the equal path-length switching network without distortion.

The switching network activates a contiguous set (usually $\frac{1}{4}$ the total number) of the elements on the cylinder. The network consists of two parts; one part chooses the desired sector, and the other maintains the desired ordering of the elements. The switching network effects a "coarse" steering, moving the beam in angular increments corresponding to the element spacing (approximately 0.8 beamwidth steps). For any setting of the switches phase tilt can be introduced by the phase shifters to provide "fine" steering. A distribution network is used to derive the aperture illumination as in the case of a linear array; fixed line lengths are used to correct for the curvature of the aperture. Sum and difference excitations are provided. For a 32 element array, 56 PIN diodes are required for the switches and 64 diodes for 4-bit phase shifters. If the modal approach, which is described elsewhere (Reference 1, 2), were to be implemented for the same size array, 256 diodes would be required with

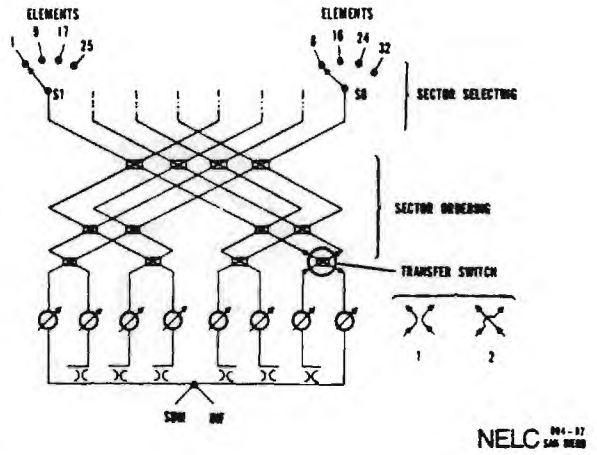

Fig. 1 Schematic Diagram of Diode Switched Array Developed by Wheeler Laboratories.

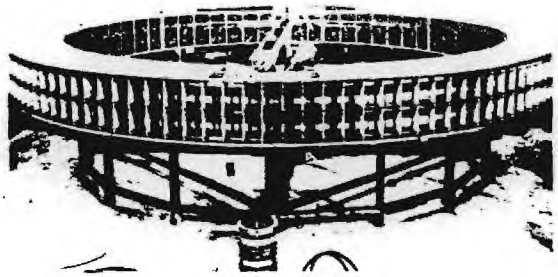

Fig. 5 Circular Array Developed by Scanwell Laboratories.

side of the antenna ring. Each box contains two (2) RF switches, SPDT, in which the switching elements consist of magnetically energized, mercury-wetted reed capsules.

The heart of the feed network is a device termed a "Pass-Around", which is contained in the RF scanner unit. It has 31 input ports, 31 output ports, and consists of 155 interconnected SPDT switches. Its function is to switch the input distribution of 30 element signals into the proper sequence at its output ports so that they will be transferred by the feed network to correctly illuminate the particular group of 30 elements required in forming a given radiated beam. The amplitude illumination tapers required for selectable azimuth beamwidths are set up by a dual directional coupler power divider.

Beam steering is accomplished by feeding a seven-bit digital signal into the electronics cabinet from the remote beam controllers. They permit automatic beam command control from external digital or synchro inputs, and they can also be switched into a manual stepping or slewing of the beams via a binary analogue-to-digital encoder. The antenna was designed for the IFF frequencies and has a beam-to-beam switching speed of 3 milliseconds. The azimuth beamwidth is variable; 4.5° or 8.8°, and has sidelobes on the order of -26 dB.

By virtue of its symmetry, a cylindrical array has obvious appeal when an antenna is needed for high-speed scanning of a pencil beam 360 degrees in azimuth and over some range of elevation angles. With such an array, the radiation pattern is formed by establishing the proper currents on the elements (ordinarily on just a sector of the cylinder), and is then scanned in aximuth by moving the excitation around the cylinder, and in elevation by varying the frequency or phases of the currents. Recent work at the Naval Research Laboratory on circular arrays resulted in the development of a matrix and diode switches capable of performing the first function, permitting switching from beam to beam in azimuth in less than a microsecond. A schematic is shown in Figure 6. To demonstrate 3-D scanning with a

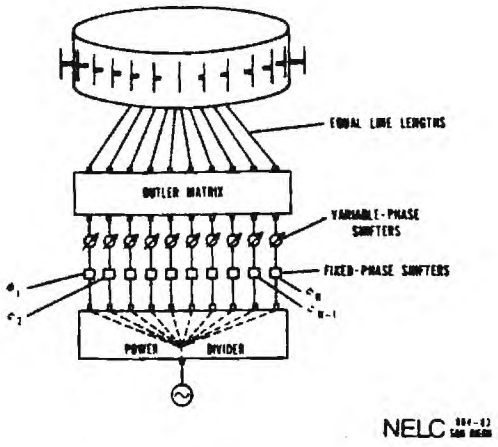

Fig. 6 Schematic Diagram of Cylindrical Array Developed by Naval Research Laboratory.

cylindrical array, a 256-element, S-band array consisting of 32 8-element linear arrays has been built and tested.

The 32 arrays making up the cylinder each consist of 8 vertically polarized dipoles series fed by a serpentine transmission line by means of directional couplers. The radiating elements are sandwich dipoles fed directly from the transmission line and occupying a single surface. Eight of the 32 linear arrays are excited at a time. The currents to be applied are first established by a corporate structure having 8 outputs equal in phase and having a 25 dB Tchebyscheff amplitude distribution. The switch system has a total of 44 transfer switches. An array of 32 elements around the ring would have 5 switches in series in each path. A 64 element array would require 6 switches in series. A pass-around network is made up of eight 4 x 4 matrices with 4 transfer switches per matrix.

The array is scanned in elevation from -20 to +40 degrees by varying the frequency from 3.07 to 3.37 GHz, a larger frequency excursion than the switch matrix was originally designed to cover

and diode switch combination array (4). This method of feeding and scanning the circular array uses the well-known R-2R parallel-plate lens feed system. The lens is a parallel plate region of radius R, with the spacing between parallel plates less than $\frac{1}{2}$ free-space wavelength in order to restrict propagation to the electric field component perpendicular to the plates. Energy is launched and extracted from the lens by means of monopoles mounted $\frac{1}{4}$ wavelength in front of the circumferential ground plane enclosing the parallel plate region. From Figure 9, it can be seen that energy introduced at point A travels a distance $2R \cos \gamma/2$ when received by a pickoff probe at γ. For a beam cophasal distribution on a ring array of radius ρ the energy must be delayed a distance $\rho \cos \alpha$ for an antenna element located at α measured from the beam direction. Thus, the distribution will be provided by the lens if

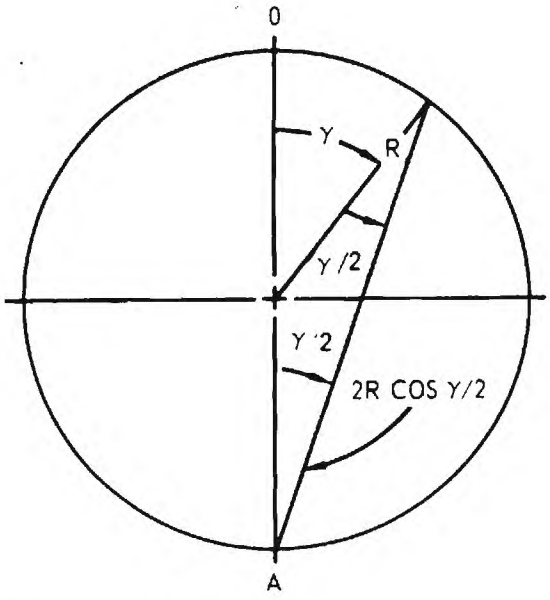

Fig. 9 R-2R Lens Coordinates.

$$R = \frac{1}{2}\rho$$

and

$$\gamma = \frac{1}{2}\alpha \ .$$

The lens must be one half the radius of the ring array. The lens angle will be twice the array angle if all of the lens ports are used to illuminate one half of the array aperture (180°). The illumination of the ring is accomplished using 64 equispaced probes on the lens, each switchable to one of two diametrically opposite elements on the array. Figure 10 shows typical amplitude and phase distributions obtained from the R-2R lens, where R=4'. Four lens input probes are excited simultaneously to achieve aperture amplitude taper as shown in Figure 11. Three-hundred-sixty-

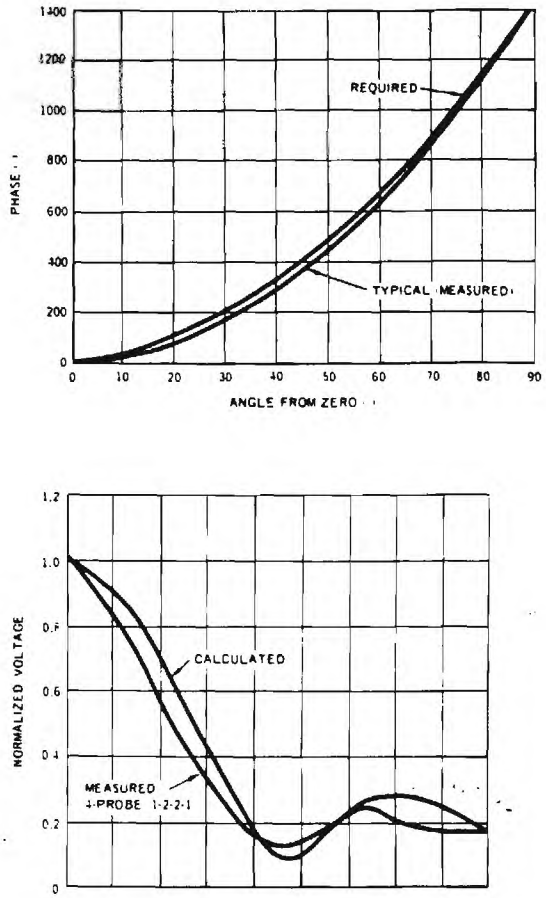

Fig. 10 R-2R Lens Amplitude and Phase Distributions.

degree azimuth beam steering is implemented by means of a SP4T switch at each input-output port of the lens. This switch selects one of the two radiating elements to which it is connected, or a matched load when the terminal is inactive, or the input-output probe.

The radiating array shown in Figure 4 was used with the lens feed and had an azimuth beamwidth of 5° at 3.2 GHz. Figure 12 shows a typical radiation pattern from the array.

siderable interest in the past. Radiation Systems, Inc., McLean, Virginia has recently conducted a development program to demonstrate some of the performance advantages which are possible with this type of TACAN antenna. The benefits which accrue through the combination of circular phased array techniques and the unique biconical radiator developed by RSi are:

a. Pattern rotation with a fixed antenna

b. Continuous full band coverage from 960 to 1220 MHz without adjustment

c. Improved elevation plane patterns wherein the modulation remains unchanged for elevation angles up to 60°

d. Improved cross polarization

e. Around the mast installation if required.

It should be recalled that the TACAN pattern consists of a limacoid with nine lobes superimposed upon it which rotates at 900 rpm. This pattern is shown in

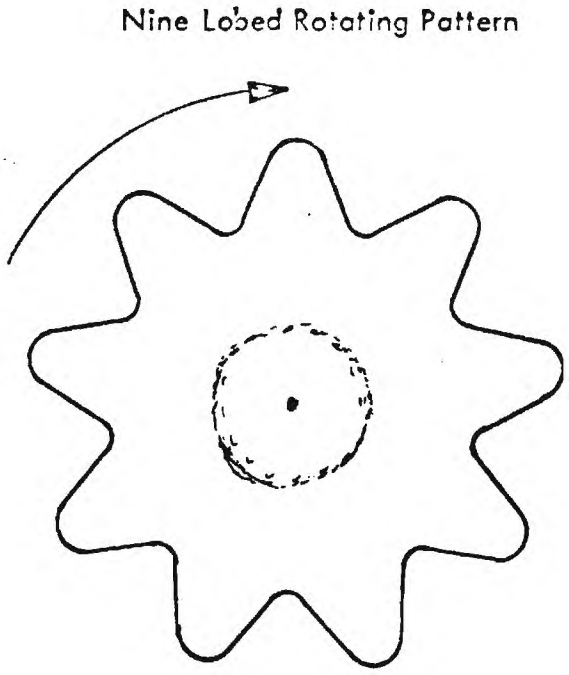

Fig. 14 TACAN Rotating Pattern.

Figure 14 and has the mathematical form:

$$E(\theta) = A_0 + B_1 \sin\theta + B_9 \sin 9\theta$$

where θ = azimuth angle
A_0 = omni pattern content and
B_1 and B_9 represent the ripple content of the fundamental and 9 lobed patterns respectively.

The trigonometric functions can be formed by combining symmetric modes of the proper mode number as done for fan beam antennas. In this case, the onmi term is provided with the 0 order mode. the θ term is provided by combining the +1 and -1 modes and the 9θ term is supplied by combining the +9 and -9 modes. This pattern is rotated about the fixed array by inserting variable phase shifters in the lines feeding the first and ninth order modes.

A $\frac{1}{2}$ scale model, shown in Figure 15, was con-

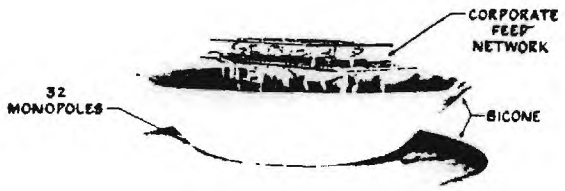

Fig. 15 Experimental TACAN Antenna Developed by Radiation Systems, Inc.

structed of both the antenna array and the RF processing networks. The radiator consists of thirty-two probes positioned in a circle at the throat of a biconical horn. The RF processing networks are fabricated in strip-transmission-line. A composite of measured azimuth patterns of this experimental TACAN antenna for frequencies of 1.9 to 2.5 GHz is shown in Figure 16. Developmental work to optimize the array antenna and the feed networks across the full band are incomplete. However, these pattern traces demonstrate the full TACAN bandwidth capability at the scaled frequencies. The amplitude modulation of the pattern is virtually unchanged over a 60° range of elevation angles.

The use of these types of arrays for wide band systems has been established by experimental models. A matrix fed array has been developed by RSi to cover a 5 to 1 band; Naval Electronics Laboratory Center has tested a circular array for the lens-fed type to cover an octave bandwidth and the arrays discussed of the switched-type have been operated over a 20% band. A major problem area appears to be in the choice of feeding and switching devices to minimize the losses of the switch and phasor components. Considerable losses occur in the element connectors and cabling required to commute the amplitude and phase distributions. Many of the arrays described suffer from this condition and serious consideration should be given to other types of techniques to simplify the design. The utility of the asymmetric arrays has been demonstrated and as in planar phased arrays, the cost is a most important factor. The feeding techniques are, in general, more complicated than those for the planar phased array. However, the inherent advantages of the beam symmetry, wide band capability and physical stability offer attractive trade-offs for some types of systems.

System Application and Performance

The electronically scanned antenna array is utilized in an airborne microwave radiometer imaging system. As shown in the block diagram of Fig. 8, this system consists of four basic parts: 1) the antenna with its associated drive and control network, 2) the Dicke switching network, including the calibration and control subsystem, 3) the receiver, and 4) the data processing and display system.

Electromagnetic energy emitted from the surface of the earth is received by the array antenna. The magnitude of this energy is proportional to the radiometric temperature observed. By comparing this energy with that emitted by a known calibration standard, normally a hot and/or cold reference load, it is possible to determine the radiometric temperature of the body seen by the antenna. A two-dimensional map of the radiometric temperature of the earth is therefore generated when the antenna beam is scanned as the vehicle moves.

The radiometer receiver is a solid-state superheterodyne double sideband receiver. Included in this receiver are a balanced mixer, solid-state local oscillator and multiplier, synchronously tuned IF amplifier, square law detector, preamplifier, and synchronous detector. The overall noise figure of the receiver ranges between 6.0 and 7.0 dB. The measurement accuracy and sensitivity of the receiver are 2.0°K and 0.7°K, respectively.

Data processing is performed by a digital data acquistion system which produces a computer-compatible tape output. A real-time grey level display, an analog readout, and a digital printout are also generated simultaneously. The tape output can be processed to give either a grey level display or a color presentation, the latter offering almost a sixfold increase in display resolution.

Scanning of the antenna beam is accomplished in an incremental manner. A total of 39 steps are required to move the beam through the 100° angular range. Each step corresponds to a half-power beamwidth interval. The time required for a complete scan is adjustable to one or two seconds. This includes the time required to reposition the beam to each of the 39 positions and the dwell, or integration, time at each position.

Typical of the data that have been obtained with this system by the NASA Goddard Space Flight Center are those shown in Fig. 9. This radiometric map of the Southern California coastal area was obtained from an altitude of 37 000 feet. The black to white span on the grey level scale represents a temperature range of 228°K to 290°K.

Conclusions

A 19.35-GHz electronically scanned two-dimensional phased array has been described in detail. It has been shown that this configuration is compatible with the overall airborne microwave radiometer system requirements. The phased array described here has a high beam efficiency, can be scanned rapidly, is volumetrically compact and light in weight, consumes little power, and can be flush-mounted. The performance of the array, as well as that of the radiometer system in which it is used, has also been discussed.

Acknowledgment

Appreciation is extended to R. Bowers who assisted in the collection of a large portion of the data presented herein. Acknowledgment is also made of the efforts of the many others who have designed and assembled the overall radiometer system.

A Matrix-Fed Circular Array for Continuous Scanning

BORIS SHELEG

***Abstract*—The Butler-matrix-fed circular array will form a focussed radiation pattern when the proper current distribution is established on the inputs to the matrix. Further, this beam can be scanned through 360° by changing only the phases of the matrix input currents, just as with a linear array scanning is accomplished by varying the phases of the element currents. This operation was experimentally demonstrated with a 32-dipole circular array and reasonable agreement was obtained between the measured and calculated patterns. Finally, a synthesis procedure is described for determining the matrix input currents required to attain a prescribed current distribution on the array.**

Manuscript received April 1, 1968; revised July 31, 1968.

The author is with the Microwave Antennas and Components Branch, Electronics Division, Naval Research Laboratory, Washington, D. C. 20390

Introduction

ANTENNAS consisting of radiating elements arrayed on a circle have been studied and have been used for many years, but recent developments in switching and phase shifting have led to a renewed interest in them. The appeal of the circular array is that, because of its

symmetry, it can be used to scan a beam in discrete steps through a full 360° without the variations in gain and pattern shape that occur when four linear arrays are used, each scanning through a single quadrant. The purpose of this study was to determine some of the possibilities and also the limitations of scanning with circular arrays and, in particular, to demonstrate the use of the Butler matrix in feeding the elements of the array. The idea of using a Butler matrix for this purpose is due to Shelton [1], who showed that it permitted the formation of a narrow radiated beam that could then be scanned essentially like the beam from a linear array, by the operation of phase shifters alone.

The operation of a Butler-matrix-fed circular array (multimode array) is first described heuristically in terms of "modes" and then, more satisfactorily, by considering the distribution of currents impressed on the radiating elements by the matrix. In addition, calculations were made to show how the radiation pattern of the multimode array varies as it is scanned continuously, rather than in discrete steps.

The experimental portion of this program was performed at L-band with a circular array of 32 dipoles around a conducting cylinder. Sidelobe level control was shown by using different amplitude tapers over the illuminated portion of the array.

Theory of Operation

The principles involved in scanning a multimode array are most easily seen by considering not an array, but a continuous distribution of current. When this distribution is expressed as a Fourier series, in general infinite, each term represents a current mode uniform in amplitude but having a phase varying linearly with angle. The radiation pattern of each mode has the same form as the current mode itself, and these pattern modes are the Fourier components of the radiation pattern of the original distribution. The expression of the radiation pattern as the sum of modes of this form is then seen to be analogous to the summation of the contribution made to the pattern of a linear array by its elements, so the operation of a multimode array can be explained by referring to an equivalent linear array.

Referring to Fig. 1, consider a current distribution $I(\alpha)$ to be the sum of a finite number of continuous current modes $I_n e^{jn\alpha}$ with $-N \le n \le N$. The radiation pattern for $\theta = \pi/2$, is then given by

$$E(\phi) = \sum_{n=-N}^{N} C_n e^{jn\phi} \tag{1}$$

where the C_n are complex constants given by

$$C_n = 2\pi K j^n I_n J_n\left(\frac{2\pi a}{\lambda}\right) \tag{2}$$

with K a constant [2]. There is a one-to-one correspondence between the current modes $e^{jn\alpha}$ and the far-field pattern modes $e^{jn\phi}$, but note that their relative phases are not necessarily the same. Another property peculiar to circular arrays with isotropic radiators is that some modes can be made to give zero contribution in the plane of the circle by the selection of a proper diameter. However, for practical

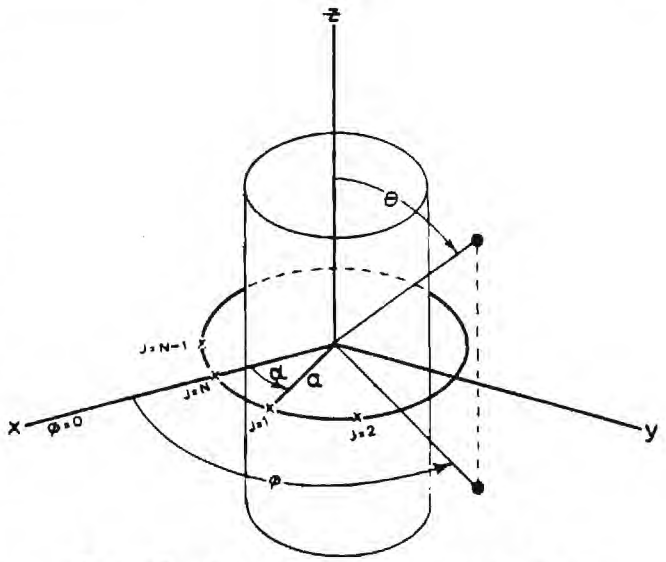

Fig. 1. Coordinates for a continuous cylindrical sheet of vertical current elements.

antennas of interest (e.g., dipoles approximately one-quarter wavelength over a reflecting cylinder) all the modes make contributions in the plane of the array.

Equations (1) and (2) demonstrate that a change in relative amplitude and phase of each current mode results in a corresponding change in the corresponding pattern mode (this can be done by controlling I_n). This is nearly identical to the formulation for linear arrays. A linear array of $2N+1$ isotropic elements with interelement spacing a has a radiation pattern given by

$$E(u) = \sum_{n=-N}^{N} A_n e^{jnu} \tag{3}$$

where $u = ka \sin \phi$, ϕ is the angle off-broadside, and A_n is the current on the nth element. Equations (1) and (3) show the similarity of the patterns of the circular current sheet and the linear array, with the role of the current mode in the circular array taken by the element in the linear array. One difference is that for the circular array the argument is ϕ, and for the linear array it is $ka \sin \phi$. A second difference is that equally excited elements in a linear array make contributions of equal magnitude to the radiation pattern, but equally excited current modes do not contribute equally, because their elevation patterns are not identical. This results in differences in their strength of contribution in the plane of the antenna. For example, if in the antenna being considered (Fig. 1) it is desired that the pattern modes be equal in magnitude and be in phase at $\phi = 0$, the excitations of the current modes must be [from (2)]

$$I_n = \frac{1}{2\pi K j^n J_n\left(\frac{2\pi a}{\lambda}\right)}. \tag{4}$$

Its radiation pattern is then given by

$$E(\phi) = \sum_{n=-N}^{N} e^{jn\phi}, \tag{5}$$

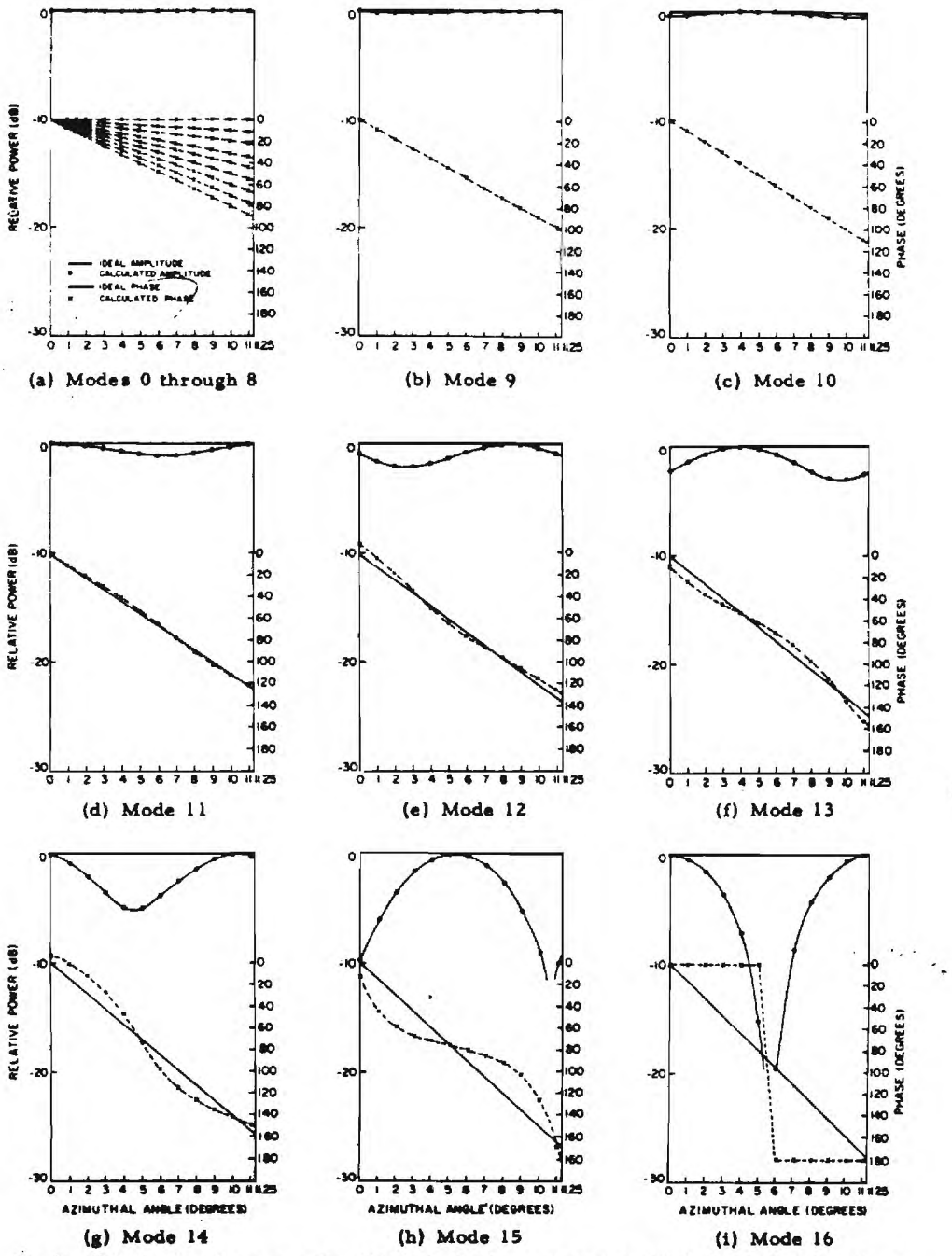

(a) Modes 0 through 8 (b) Mode 9 (c) Mode 10

(d) Mode 11 (e) Mode 12 (f) Mode 13

(g) Mode 14 (h) Mode 15 (i) Mode 16

Fig. 3. Calculated mode patterns for a 32-dipole circular array compared with the ideal mode patterns.

The approximate pattern of the dipole in front of a cylinder is given by

$$A(\phi) = \tfrac{1}{2}(1 + \cos \phi), \tag{8}$$

where the phase was assumed constant in azimuth when referred to a point one-third the distance from the cylinder to the dipole. This assumption is reasonably good, at least in the unshadowed region. Mode patterns and pencil beam patterns computed using (8) were in good agreement with those obtained using the exact pattern of the vertical current element, and no results for the latter have been included.

Consider, as in Fig. 1, a circular array of radius R with N elements equally spaced at $\alpha_J = J2\pi/N$, where $J = 1, 2, \cdots, N$. Referred to the center of the circle, the relative space phase of the Jth element is $(2\pi R/\lambda) \cos(\phi - \alpha_J)$, where only the plane of the array is considered. If the element pattern is $A(\phi - \alpha_J)$ and the current on the element is $A_J e^{j\psi_J}$, the radiation pattern of the array is given by

$$E(\phi) = \sum_{J=1}^{N} A_J e^{j\psi_J} A(\phi - \alpha_J) e^{j(2\pi R/\lambda)\cos(\phi - \alpha_J)}. \tag{9}$$

Mode patterns were calculated from this equation with the element pattern given by (8) and, for the Kth mode, a current distribution given by $A_J = 1$, $\psi_J = 2\pi KJ/N$. Results are shown for a 32-element array, for which the modes correspond to $K = 0, \pm 1, \pm 2, \cdots, \pm 15, 16$. The phase and amplitude of computed mode patterns for a 32-element circular array (0.5λ spacing) are compared with ideal modes in Fig. 3. It is seen that all modes up to ± 10 are in sub-

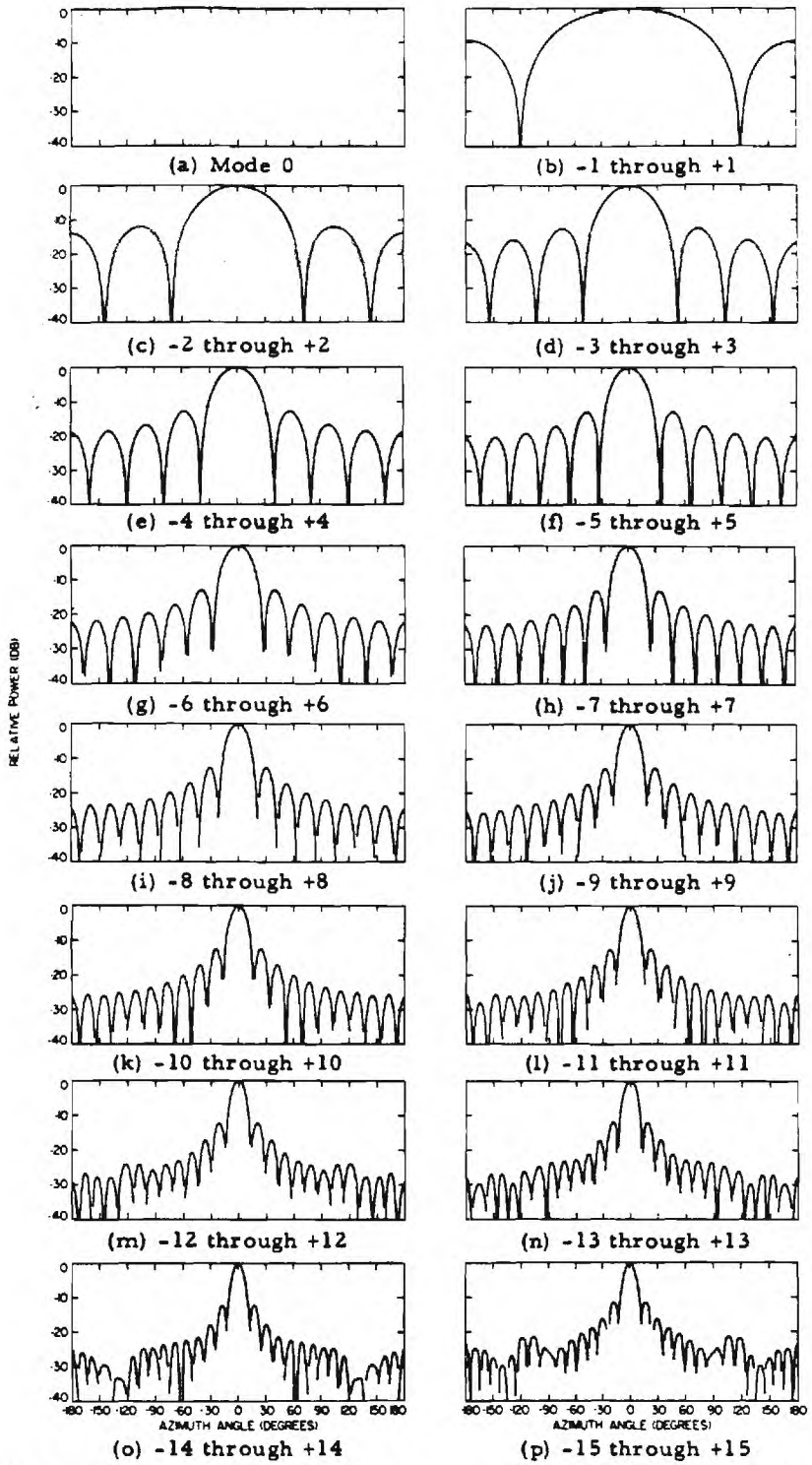

Fig. 4. Mode-by-mode buildup of the pattern of a 32-element array with uniform excitation of the modes.

case more than 95 percent of the total power is radiated from the 9 elements closest to the beam and on these elements the currents differ from cophasal by at most 5°.

One of the distributions used in the experimental program was $B_K = \cos^2(\pi K/40)$, which provided a 17-dB taper over the 31-mode inputs. To indicate how much the pattern shape could be expected to change as the beam was scanned, patterns were computed for various beam positions. Fig. 7 shows three patterns, one phased so that its peak is in the direction of element 32 ($\phi = 0$), the other two having the same amplitude distribution over the modes but phased to scan the beam one quarter and one half, respectively, of the angle between elements. It may be seen that, at least for this distribution, the pattern changes only slightly as the beam is scanned.

Patterns were also calculated for different element spacings, element patterns, and amplitude distributions, but those shown satisfactorily illustrate the beam formation

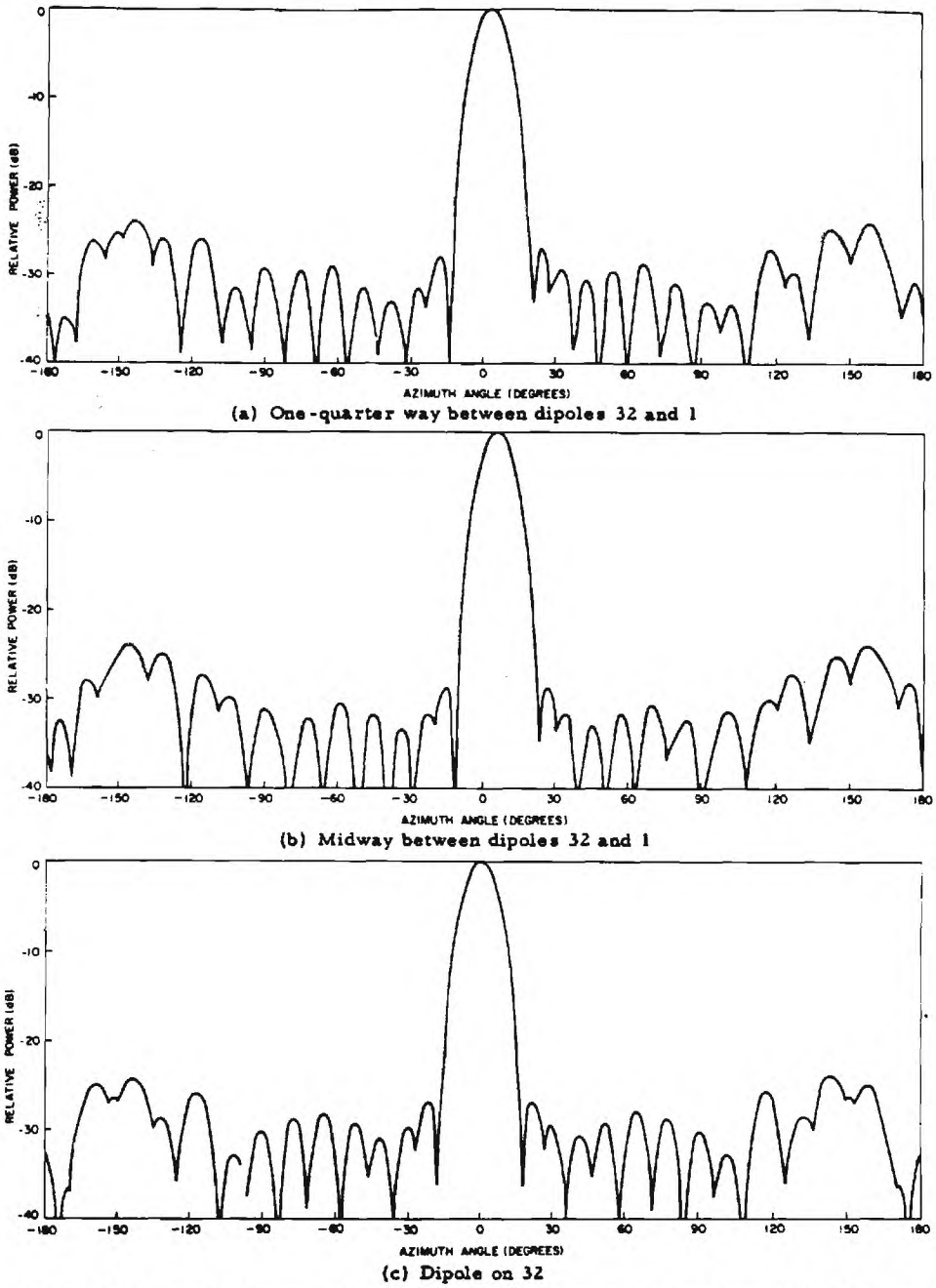

Fig. 7. Patterns and the corresponding current distributions on a 32-element array for beams at 0°, 5.625°, and 2.813°. The amplitude taper on the modes is $B_K = \cos^2(\pi K/40)$ with $K = 0, +1, \pm 2, \cdots, \pm 15$.

and scanning and also indicate how the pattern differs from one based on the existence of perfect pattern modes.

Synthesis of Aperture Distributions

It should now be evident that the radiation pattern of a circular array computed on the assumption that the pattern modes are perfect is not the same as that computed from the actual current distribution, and that a certain amount of cut-and-try is involved in determining the number of modes to use and in adjusting the phases of the modes to form a beam in a particular direction. Instead of picking the mode excitations, only to find that the corresponding current distribution results in a poor radiation pattern, it would be preferable first to pick a current distribution having an acceptable pattern and then to find the mode excitations which will give these currents. That this is always possible was discovered by Davies [8], who showed that any prescribed output currents can be achieved with a Butler matrix by properly exciting the matrix inputs.

Consider an $N \times N$ Butler matrix with input and output ports labeled K and J, respectively. If the prescribed currents $A_J e^{j\psi_J}$, where $J = 1, 2, \cdots, N$ are to be set up on the array, the N currents that must be applied to the inputs of the matrix are

is then applied to the inputs, the excitation is switched to element 1. If, however, the linear phase progression were only half this (i.e., $e^{-jK\pi/N}$), two elements, N and 1, would be strongly excited, but there would be currents on all the elements of the array. As a practical example, consider a 32-element array with a cophasal distribution on the 14-element sector which includes elements 26–7. The desired amplitude distribution is cos $[(K-1/2)\pi/16]$, which is symmetrical about a point midway between elements 32 and 1, and the elements are to be phased to form a beam in this direction. All other elements are to be inert. To show how the current distribution varies as the beam is scanned in small steps, the input currents required to achieve this distribution are first determined from (14), then their phases are changed to scan the pattern and the new distribution on the array is computed from (11). Table II gives the original distribution, phased for a peak at $\phi=5.625°$, and the corresponding input currents to the Butler matrix. Also in Table II is the distribution on the array when the beam is scanned to 11.25° (the direction of element 1) and the distribution when the beam is scanned to the angle midway between the first two. It is seen that, for the scanned beams, the currents are no longer confined to a sector; all elements are illuminated, with those on the rear of the array about 30 dB down. The stronger currents are on 15 or 16 elements, and over this sector there are only minor amplitude ripples with the currents differing from the cophasal condition by about 20°. The two scanned patterns (Fig. 8) do not differ significantly from the original one. Their beamwidths, near-in sidelobes, and the general level of their far-out lobes are comparable. If this distribution had been designed for very low sidelobes, it is likely that the pattern changes would have been more significant.

Experimental Program

The circular array used in the experimental program had 32 elements and was operated at 900 MHz. Various radiating elements were used: dipoles, short back-fire elements, and Yagis (the latter two to reduce the elevation beamwidth without increasing the height of the antenna), but the only array that will be described is a 32-element array of slot-fed dipoles, vertically polarized, spaced 0.5λ apart and 0.25λ from a conducting cylinder. This antenna is shown in Fig. 9 and the associated beamforming and scanning network is shown in Fig. 10. Since 3-dB quadrature couplers were used in the matrix, it had no zero mode; therefore, the coaxial cables connecting the matrix to the dipoles had to be cut to the proper lengths to correct for this. Corporate structures made in triplate line were used to establish the various amplitude distributions over the inputs to the Butler matrix.

The measured mode patterns for this array (Fig. 11) do not compare favorably with the computed patterns in Fig. 3. The deviations are attributable primarily to phase and amplitude errors in the matrix. All the current modes were fed so as to have the same phase at element 32, and the relative phases of the pattern modes were determined by comparing

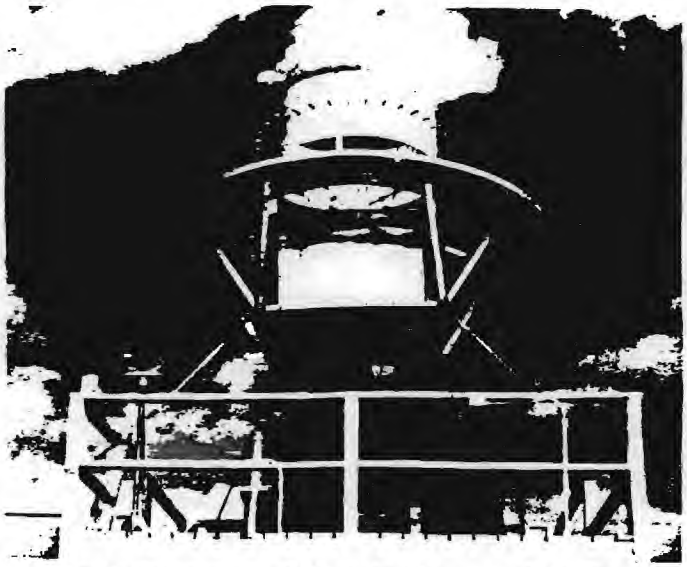

Fig. 9. Circular array of 32 dipoles ($\lambda/2$ spacing, 900 MHz).

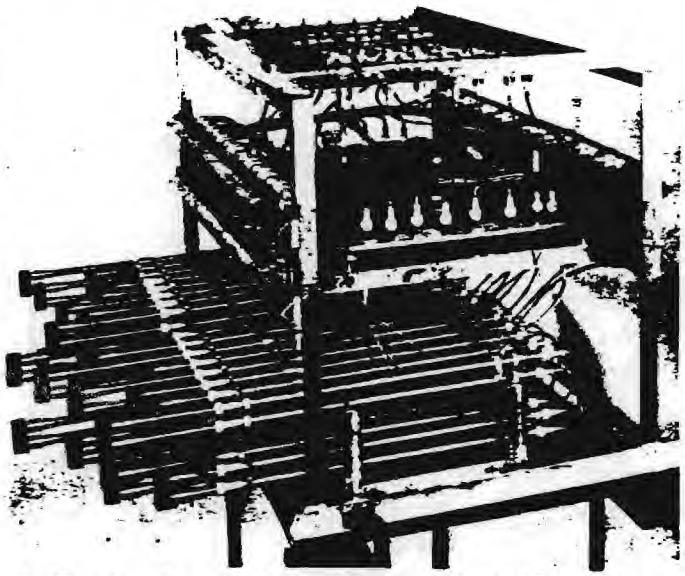

Fig. 10. Beam-forming and scanning network for the 32-dipole array.

the phase of each mode with that of the zero mode in the far field at $\phi=0$.

Fig. 12 shows the pattern of the array when a corporate structure was used providing currents of equal amplitude to all the mode inputs but number 16. For comparison, the corresponding calculated pattern (from Fig. 5) is shown solid. The two patterns agree reasonably well; both have beamwidths of about 10°, the measured first sidelobes are 1.5 dB higher than those calculated, and the general level of the far-out sidelobes is about 21 dB down for both.

The next series of patterns was taken with a tapered amplitude distribution over the modes. By dividing the outputs with tees, 31 modes were fed from a 16-element corporate structure. This resulted in a stepped distribution (since pairs of adjacent modes had equal amplitudes) with a 17-dB taper. The measured beamwidth (11.5°) and the first side-

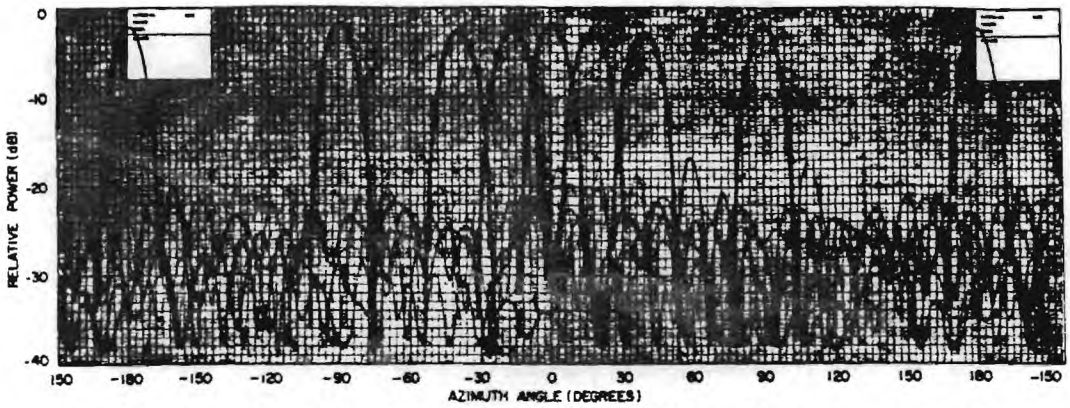

Fig. 13. Scanned patterns for the 32-element array with a tapered stepped distribution on the modes.

lobe (19 dB down) agree well with those calculated, but the level of the far-out lobes was somewhat worse than for the calculated pattern. The beam was then scanned by operating the phase shifters, and some of the patterns are shown in Fig. 13. It was found that the beamwidth and sidelobe level changed only slightly, and the gain varied by about 1 dB as the beam was scanned.

Conclusions

It has been shown that a Butler matrix can be used to feed a circular array to form a narrow pattern that can be scanned through 360° in azimuth by the operation of phase shifters alone. One explanation of this, based on the assumption that the radiation pattern could be written as the sum of a finite number of uniform pattern modes, was found to work only qualitatively in that it could not be used to predict the structure of the sidelobes. A 32-element array of dipoles was used to demonstrate experimentally how a beam was formed by superposition of the pattern modes (even though imperfect) and how the scanning was performed. Finally, the synthesis procedure of Davies was described, and as an example, the inputs to the Butler matrix required to achieve a prescribed cophasal sector distribution on the array were determined and the change in the current distribution for other beam positions were shown.

Acknowledgment

The author acknowledges the help given by R. M. Brown through numerous discussions and consultations, the contributions of F. W. Lashway, who was responsible for the mechanical design, and of R. J. Wiegand, who helped with the measurement program. In addition, the author expresses his gratitude to J. Tyszkiewicz of the Naval Air Systems Command, who sponsored and supported this work.

References

[1] G. C. Chadwick and J. C. Glass, "Investigation of a multiple beam scanning circular array," Scientific Rept. 1 to USAF Cambridge Research Lab., Cambridge, Mass., Contract AF19(628)367, December 31, 1962.

[2] W. R. LePage, C. S. Roys, and S. Seely, "Radiation from circular current sheets," *Proc. IRE*, vol. 38, pp. 1069–1072, September 1950.

[3] R. C. Honey and E. M. T. Jones, "A versatile multiport biconical antenna," *Proc. IRE*, vol. 45, pp. 1374–1383, October 1957.

[4] A. C. Schell and E. L. Bouché, "A concentric loop array," *IRE WESCON Conv. Rec.*, vol. 2, pt. 1, pp. 212–215, August 1958.

[5] C. P. Clasen, J. B. Rankin, and O. M. Woodward, Jr., "A radial-waveguide antenna and multiple amplifier system for electronic scanning," *RCA Rev.*, vol. 22, no. 3, pp. 543–554, 1961.

[6] J. L. Butler, "Digital, matrix, and intermediate-frequency scanning," in *Microwave Scanning Antennas*, vol. 3, R. C. Hansen, Ed. New York: Academic Press, 1966, ch. 3.

[7] P. S. Carter, "Antenna arrays around cylinders," *Proc. IRE*, vol. 31, pp. 671–693, December 1943.

[8] D. E. N. Davies, "A transformation between the phasing techniques required for linear and circular aerial arrays," *Proc. IEE* (London), vol. 112, pp. 2041–2045, November 1965.

LOGARITHMICALLY PERIODIC ANTENNA ARRAYS

R. H. DuHamel & D. G. Berry

Collins Radio Company
Cedar Rapids, Iowa

Summary

Previous research on logarithmically periodic structures has provided frequency independent antennas with gains comparable to that of an aperture of one square wavelength. The purpose of this research has been to study frequency independent methods of arraying logarithmically periodic antennas so as to achieve higher gain. The theory and design procedure for an array of endfire log periodic elements is described. Design data for the element unit patterns and phase centers is presented. Experimental as well as theoretical array patterns are given. Gains of the order of 15 db over an isotropic radiator have been achieved and it is felt that up to 20 db gain is feasible. An element which will be useful for an array of broadside elements is also described.

Introduction

Previous research on logarithmically periodic antenna structures has led to structures for which the pattern and impedance are essentially independent of frequency over theoretically unlimited bandwidths. Structures have been devised,[1, 2, 3] which give omni-directional, bi-directional, and uni-directional patterns with linear or circular polarization and with beamwidths ranging from approximately 50 to 100°. All of these antennas have consisted of two structures fed against each other with gains comparable to that of an aperture of one square wavelength. Although there are many important applications for the structures described previously, there are other applications which demand narrower beamwidths and higher gains. It does not appear possible to obtain a significant increase in gain with the previous structures by merely changing their design parameters. An obvious way of increasing the gain is to array more than two of these structures, such as 4, 6, 8, etc., in order to obtain narrower beamwidths and higher gains. The purpose of this research has been to study frequency independent methods of arraying logarithmically periodic antenna structures and to obtain data which will allow the design of arrays to give specified patterns. As will be described later, experimental results have demonstrated gains of 15 db and indicate that gains of 20 db may be obtained.

The geometry of logarithmically periodic structures is defined so that the pattern and impedance repeat periodically with the logarithm of frequency. A period of frequency is defined in terms of the design parameter τ by $f \pm \tau f$. Thus for an infinite structure the operation is the same for any two frequencies related by an integral power of τ. If the shape of the structure and the factor τ are such that the variation of pattern and impedance over one period is small, then this will hold true for all periods, the result being essentially a frequency independent antenna. Fortunately, it has been found that since the "end effect" is negligible, a variety of finite logarithmically periodic antennas provide extremely broadband operation.

For the trapezoidal tooth wire structure of figure 1a, which has been reported on previously,[3] τ is the ratio of the lengths of two similar adjacent teeth and the angle α defines the extremities of the teeth. This structure produces a horizontally polarized beam along the positive Y axis. The principal plane beamwidths are on the order of 60 to 70° and the side lobe level is on the order of 15 db down. For ψ equal to 60° the characteristic impedance is approximately 200 ohms. Over bandwidths of more than 10 to 1 the beamwidth does not change more than 20% and the VSWR referred to the characteristic impedance is less than 2 to 1. Figure 1b shows a sketch of a trapezoidal tooth structure in which the two halves are coplanar with an angle ζ between the center lines of the two halves. As will be described, excellent frequency independent operation has been obtained with this type of structure which is considered as a basic element of several of the arrays. The two halves of either of the structures shown in figure 1 are fed against each other at the vertices either with a balanced two wired line or with a coaxial line running up the center line of one structure. The lower and higher frequency limits are obtained when the longest and shortest transverse wires respectively are approximately 1/2 wavelength long.

In the sections to follow the general theory of arrays of logarithmically periodic antennas will be presented along with experimental results. A new type of broadside element which should prove useful in arrays is also described. Only wire structures are considered in this paper, since the research has been directed toward applications for frequencies below 500 mc. Triangular tooth structures have not been considered because their low frequency limit is approximately 20% higher than that of a trapezoidal tooth structure of the same size.

The frequency independent nature of the logarithmically periodic antennas has been adequately

1. R. H. DuHamel and D.E. Isbell, "Broadband Logarithmically Periodic Antenna Structures," 1957 I.R.E. National Convention Record, Part I, pp. 119-128.

2. D. E. Isbell, "Non-Planar Logarithmically Periodic Antenna Structures," University of Illinois, Antenna Laboratory TR #30, February 20, 1958, Contract AF 33(616)-3220.

3. R. H. DuHamel and F. R. Ore, "Logarithmically Periodic Antenna Designs," 1958 I.R.E. Convention Record, Part I, pp. 139-151

demonstrated previously. Therefore the experimental results presented in this paper usually cover frequencies over only a period of operation. Results for much larger frequency ranges are not presented because of space limitations.

Endfire Element Arrays

2.1 Theory

It would be a simple matter to form a linear array of structures similar to those of figure 1a. However the electrical spacing between the elements of the array would change with frequency which would cause the radiation pattern of the array to vary with frequency. In order to obtain frequency independent operation with an array it is necessary that the locations of the elements with respect to each other be defined by angles rather than distances. This implies that all of the elements of the array have their vertices or feed points at a common point such as illustrated in the photograph of figure 2. Shown there are six elements of the trapezoidal tooth type which form what is termed an endfire element array, since the basic elements themselves are endfire. The three elements on the left may be fed against the three elements on the right. The center line of the elements lie in a common plane.

A schematic representation of an array of N elements as viewed from the top is illustrated in figure 3. The radial lines defined by δ_n represent the elements of the array. The direction to a distant field point is given by ϕ. The α and τ parameters for the N elements are made identical so as to assure identical element patterns. Typical element patterns are shown in the schematic. The distance from the feed point to the phase center of an element is given by d. The xy plane radiation pattern of the array is given by

$$E(\phi) = \sum_{n=1}^{N} A_n f(\phi - \delta_n) e^{j\left[\beta d \cos(\phi - \delta_n) - \gamma_n\right]} \qquad (1)$$

where $f(\phi)$ is the element pattern and $\beta d \cos(\phi - \delta_n)$ represents the phase advance of the phase center relative to the origin. The value of the feed point voltage for the n^{th} element is given by A_n. The parameter γ_n is the relative phase of the field radiated from the n^{th} element. It may be controlled by expanding or contracting the element according to the phase rotation principle to be described later.

The assumptions made in equation (1) are that the element patterns and input impedances are identical. Although mutual effects can make these assumptions invalid, good correlation between theory and experiment has been obtained. "Cut and try" synthesis procedures may be used with equation (1) but it is not ideally suited for synthesis problems because it is not in the form of an orthogonal series.

2.2 Element Characteristics

A primary objective of this investigation has been to determine the dependence of the radiation characteristics of a single element upon the design parameters α and τ so that the above theory may be used to predict the performance of general arrays. Since it is necessary to feed two logarithmically periodic elements against each other in order to obtain frequency independent operation, it would appear very difficult to determine the radiation characteristics of a single element. A trick which circumvents this apparent difficulty is illustrated in figure 4. Here the logarithmically periodic element is fed against a vertical wire by connecting the center conductor of the coax (which forms the center line of the element) to the wire. Although the input impedance of the element is no longer frequency independent, the patterns are and are very similar to the patterns of the element when placed in an array. Since the wire radiates vertical polarization, it is possible to measure the principal plane horizontal polarization patterns of the periodic element alone. This technique is also used to measure the phase center of an element.

Figure 5 shows several of the elements investigated with $\alpha = 14.24°$ and $\tau = 0.75$, 0.83, 0.915 and 0.95 from right to left. Since these structures were investigated only over a period of frequency, it was not necessary to extend the teeth down to the feed point. For the endfire elements referred to in figures 6, 7, 8, 9 and 13, .08" diameter wire was used to construct the teeth and a 1/8" O.D. tube was used for the boom. A microdot RG-196/U coaxial feed cable was inserted in this tube. The longest transverse wire (the last wire) was six inches long. Measurements were made between 1.0 and 2.2 kmc.

Sample patterns for various values of the parameters α and τ are shown in figure 6. These, as well as the rest of the patterns presented here, are relative field intensity patterns. The endfire characteristics of a single element are quite apparent. The graph and table of figure 7 summarizes the pattern data taken on the various types of elements. It is noticed that the E-plane beamwidths are relatively insensitive to changes in τ but that the H-plane beamwidths generally decrease with increasing τ.

The phase centers of the elements were determined by mounting the elements on a vertical rotating mast and measuring the phase of the received signal at a distant antenna. The center of rotation of the element was adjusted so that the phase variation over a 60° sector in the direction of the element beam was minimum. It was relatively easy to find fairly well defined phase centers for all the elements tested. Figure 8 gives the distance, d, in wavelengths from the vertex to the phase center for the various values of α and τ. It will be noticed that d is essentially independent of τ and, as would be expected, quite dependent upon α. Before these measurements were performed it was estimated that the phase center would fall at a point on the structure near a half wavelength long transverse wire. If we let g represent the distance to the vertex from a half wavelength wire, then the ratio $\kappa = d/g$ is a measure of the proximity of the phase center to the halfwave wire. From the values given on figure 8 it is seen that κ increases as α increases, but that the phase center falls considerably short of the halfwave wire. On the other hand it was found that for a structure with α equal to 74° that κ was greater than 1.

For one of the structures the phase center position was measured over a period of frequency as shown in figure 9. Since d is proportional to the wavelength within the accuracy of the measuring equipment, this implies that the phase center does not shift when a logarithmically periodic element is expanded or contracted.

A basic characteristic of logarithmically periodic antennas is the phase rotation phenomenon. It has been verified experimentally that if the phase of the electric field received at a distant dipole (see figure 10a) is measured relative to the phase of the current at the feed point of the structure, the phase of the received signal will be delayed 360° as the structure is expanded through a period. In figure 10a the distance to an element is given by KR_n. The expansion of the structure through a period is accomplished by letting K increase from one to $1/\tau$. During this expansion all lengths involved in the structure are multiplied by K. In figure 10b the phase delay in radians is plotted versus the logarithm of K. The ideal phase variation is given by the solid straight line. Measurements have indicated that the actual phase variation is something like the dashed line. The approximate measurements made to date indicate that the deviation of the dashed line from the straight line is not more than 20°. The relation between γ_n and K_n is given by

$$K_n = \tau^{\frac{\gamma_n}{2\pi}} \tag{2}$$

Fortunately the phase center and the patterns are independent of the expansion or contraction of a logarithmically periodic element provided that α and τ are not changed.

The information given above is sufficient for predicting the pattern of an array of similar endfire elements. The only difference between the elements is the scale factor K. The method could be generalized to include arrays of elements with different α's and possibly τ's. (In order for the array to maintain its periodicity using different τ's, $\tau_1 = \tau^{\pm n}$, n an integer.) However, if different α's are used it would be necessary to obtain more information on the phase of the radiation from an individual element. The phase center gives only the center of the phase front. It would also be necessary to determine the relative phase of the radiated field compared to the feed point current.

[redacted]

In designing an array, a judicious choice of the parameters N, α, τ, and δ_n should be made so as to achieve a minimum amount of space and material and number of elements. Although the design method is "cut and try" a rough approximation to an optimum design may be obtained by the following procedure. [redacted] aperture D, may be calculated from

$$\frac{D}{\lambda} = \frac{40}{B.W.} \tag{3}$$

where B.W. is the half-power beamwidth in degrees. The number 40 instead of 50 (which is for a uniform aperture) is used because the endfire directivity of the elements tends to enhance the effective aperture. The distance between the phase centers of the two outer elements must be approximately D. Results indicate that a reasonable maximum spacing between the phase centers of adjacent elements is 0.7 wavelengths. Thus the number of elements may be determined approximately from

$$N - 1 \approx \frac{D}{0.7\lambda} = \frac{57.1}{B.W.} \tag{4}$$

The maximum value of the angle $\delta_N - \delta_1$, which defines the sector occupied by the array depends on the beamwidth of the element pattern. If $\delta_N - \delta_1$ is greater than the element beamwidth, then elements 1 and N will contribute little to the formation of the main beam. An examination of figure 7 indicates that reasonable maximum values of $\delta_N - \delta_1$ are 60° for an E-plane and 80° for an H-plane array. If low first side lobes are desired values somewhat smaller than the maximum should be chosen. The distance d to the phase center is equal to

$$\frac{d}{\lambda} = \frac{D}{2\lambda \sin\left(\frac{\delta_N - \delta_1}{2}\right)} = \frac{20}{(B.W.)\sin\left(\frac{\delta_N - \delta_1}{2}\right)} \tag{5}$$

The angle α is determined from

$$\tan\frac{\alpha}{2} = \frac{\kappa\lambda}{4d} \tag{6}$$

In this expression $\kappa\lambda/4$ is the half length of a transverse wire placed a distance d from the origin. Substituting from (3) and (5) the final result is

$$\alpha = 2\tan^{-1}\left[\frac{(B.W.)\ \kappa \sin\left(\frac{\delta_N - \delta_1}{2}\right)}{80}\right] \tag{7}$$

Unfortunately, κ is an unknown (at this time) function of α so that an explicit solution for α is not possible. However, the values given in figure 8 serve as a guide in choosing κ.

The parameter τ should be made as small as possible without causing element pattern breakup so as to conserve material. An approximate lower limit on τ can be set as follows. Let ρ be the ratio of the spacing between adjacent wires to the length of the longer wire. Simple trigonometry may be used to establish that

$$\rho = \frac{1 - \sqrt{\tau}}{2\tan\frac{\alpha}{2}} \tag{8}$$

Experimental results indicate that ρ should not be greater than approximately 0.4 in order to prevent element pattern breakup. However the maximum value does change somewhat with α. Thus, roughly, τ

should be set equal to

$$\tau = \left[1 - 0.8 \tan \frac{\alpha}{2}\right]^2 = \left[1 - \frac{(B.W.)\ \kappa \sin\left(\frac{\delta_N - \delta_1}{2}\right)}{100}\right]^2 \qquad (9)$$

Since A_n and $(\delta_n - \delta_{n-1})$ are usually made independent of n, the remaining parameter to determine is K_n. If high gain and a beam direction of ϕ_0 are desired, then K_n is chosen so that $[\beta d \cos(\phi_0 - \delta_n) - \gamma_n]$ has the same value for all n. Equation (2) gives the relation between K_n and γ_n. For shaped beams γ_n and hence K_n would be determined on a "cut and try" basis.

After the approximate synthesis given above the array pattern may be calculated by the method of section 2.1 using the results given in section 2.2. If the pattern is considerably different than desired, appropriate changes must be made.

2.4 Experimental Results

2.4.1 Array Patterns

Experimental results have been obtained for arrays with 2, 4, and 6 elements. All except one array used identical elements, i.e. γ_n was the same for each element of the array.

Good correlation has been obtained between predicted and measured patterns for the 6 element phased array shown in figure 2. Table one lists the design parameters of this array and the values of $f(\phi)$ used in the calculation. The predicted and measured patterns are shown in figure 11. It will be noticed that the beam width of the measured pattern is approximately 10% greater than that predicted. In addition a somewhat higher side lobe level and null filling is apparent in the measured patterns. It is felt that the difference in beam width is caused by the mutual effects between elements of the array which was neglected in the calculation and by an error in the position of the phase center which was not measured for this particular antenna. The side lobe level and null filling can be attributed to inaccuracies in construction which have been found to materially effect the behavior of the minor characteristics of the pattern. The beam width variation over a period was 18° - 21° in the H plane and 45° - 53° in the E plane. The directivity, as estimated from the beam widths, ranged between 15.8 and 17 db over that of an isotropic radiator.

Figure 12 illustrates the measured and predicted beam widths for two element coplanar arrays as a function of ζ for three values of α. The vertical dashed lines indicate the variation of beam width over a period of frequency. In all cases the measured beam width was less than that predicted from single element pattern and phase center data and the difference is generally less as ζ increases. This leads one to suspect that these differences are again caused by the mutual effects between elements. At that the measured beam widths were always within 14% of that predicted. The elements from which this data was taken were made of .08" diameter wire with the boom consisting of 1/8" o.d. rigid brass tubing.

TABLE I
DESIGN PARAMETERS FOR SIX ELEMENT PHASED ARRAY

ARRAY PARAMETERS

τ = .885	d = 1.95 λ (assumed)
κ = .65 (assumed)	N = 6
α = 9.5°	R_{max} = 36"

ELEMENT PARAMETERS

ELEMENT #	ELEMENT POSITION δ_n	ELEMENT PHASING γ_n
1	48.1°	-184°
2	66.4°	- 80°
3	82.3°	0°
4	97.7°	0°
5	113.6°	- 80°
6	131.9°	-184°

ELEMENT PATTERN

ϕ	$f(\phi)$
90°	1
85°	.999
80°	.995
75°	.980
70°	.955
65°	.910
60°	.840
55°	.745
50°	.635

The patterns of figure 13 are an example of to what degree true frequency-independent operation can be approached. The E-plane beam widths of this two-element coplanar array are between 39° and 40° over a period of frequency while the H-plane beam widths are between 66° and 78°. The directivity as estimated from the beam widths is between 11 and 12 db over isotropic.

It will be noticed from figures 6 and 13 that the single-element patterns exhibited rather large side lobes whereas the coplanar arrangement has very small side lobes. The side lobes for the individual element are caused by radiation from the front portion of the boom or center element. When the two elements are placed together the currents on the two booms are out of phase which tends to cancel this radiation.

Figure 14 gives data on the beam width and spread of beam widths over a period as a function of α, τ and ζ for all two-element coplanar arrays measured. The general behavior is as would be expected. As ζ is increased the E plane beam width decreases and the side lobes become larger and as ζ becomes small the variation of E plane beam width over a period increases indicating mutual effects.

Two element arrays of the above type can be used as basic elements in H plane arrays. Figures 15, 16 and 17 illustrate such arrays of identical coplanar elements. Figure 15 shows typical E and H plane patterns of a four element array. The E and H plane beam widths were between 33° - 37° and 41° - 47° respectively and the estimated directivity was 13.7 db - 14.8 db over an isotropic radiator.

The H plane beam widths of a six element array of identical elements are shown in figure 16. These widths varied between 31° and 34° over a period. The difference in the phase of the field emanating from the center two elements and the outside elements in the direction of the main beam is, in this case, less than 30°. Consequently, very little is lost by not phasing the outside elements with respect to the center element. It is apparent, however, that for arrays that have quite a few long elements the resultant pattern will be degraded if phased elements are not employed.

Figure 17 illustrates a multi-element array whose pattern is electrically steerable over an azimuthal angle of about 140°. In this scheme identical elements are equally spaced and cover close to 180°. Two, four, six, etc. adjacent elements are fed at a time in the manner of figures 13, 15 or 16 and the rest of the elements are terminated in their characteristic impedance. The elements that are chosen to be fed determine the beam direction and by switching feeds and terminations the beam can be steered in azimuth. The patterns shown are the result of feeding six elements. The H plane beam width of this particular arrangement varied between 29.5° - 34° over a period of frequency. It was found that the manner in which the parasitic elements were terminated had a marked effect on the degree of change in the patterns over a period. Only when terminated in their characteristic impedance was the influence of the parasites limited enough to give satisfactory patterns. The antennas of figures 11, 13, 15 & 16 were constructed from .05" diameter wire and their booms consisted of RG-196/U miniature coaxial cable.

2.4.2 Array Impedance

The impedance behavior of log periodic antennas can be described by a characteristic impedance and a maximum standing wave ratio with respect to that characteristic impedance. This characteristic impedance is a function of the element parameters and the number and orientation of elements in the array. The maximum standing wave ratio is primarily a function of the angles between elements and in arrays of more than two elements, the manner of feed and the orientation of elements within the array.

The two antennas of figure 1 will serve to illustrate the effect of element orientation on characteristic impedance. If all elements of figure 1 are identical, the coplanar structure of figure 1b will have the higher characteristic impedance. In both cases as the angle between elements decreases the characteristic impedance decreases. Because of mutual effects the SWR increases as ψ and ζ decrease. Typical figures for the two element type array are $Z_o = 150\ \Omega$ SWR = 1.5:1 for the type of 1a and $Z_o = 180\ \Omega$, SWR = 1.7:1 for the type of 1b. Because element pairs of a multielement array are fed in parallel, adding elements reduces the characteristic impedance.

In arrays of more than two elements, if half the elements are rotated about their (the element) axis by 180° and are fed out of phase from the previous arrangement the currents on the transverse elements and hence the radiation patterns, remain unchanged. When this is done the wires running radially at the ends of the transverse wires are reoriented with respect to the same wires on the adjacent element. This reorientation effects a reduction of mutual effects and hence a reduction of SWR. For example, in figure 1b when one of the elements is rotated about its axis the radial wires are no longer adjacent to the identical radial wires of the other element.

In the case of one four element array the SWR was reduced from 3:1 to less than 1.5:1. Generally it can be said that for all arrays of endfire elements the standing wave ratio with respect to the Z_o of the array will be under 2:1 provided that phase centers are not too close and the elements are properly oriented.

Broadside Element Arrays

It is apparent from the previous sections that small α and relatively large τ values are required for high gain endfire element arrays. This is undesirable since it means that the array occupies a large area and requires considerable material. For example, with $\alpha = 14\%$ and $\tau = .83$, the element is approximately two wavelengths long at the low frequency limit and thirty transverse wires are required to cover a ten to one frequency range. It would be much more economical if a planar array of broadside logarithmically periodic elements such as pictured in figure 18 could be used to achieve high gain. Again, the relative element positions are described by angles rather than distances. The direction of the beam is normal to the plane of the array.

It would be relatively simple to design a broadside array with a bidirectional beam. However, since most applications call for a unidirectional beam, there exists the need for unidirectional broadside elements. A reflecting sheet or wire screen could possibly be used. Regardless of whether a reflecting screen could be made to work satisfactorily, a more feasible solution has been obtained by arraying four log periodic elements as shown in figure 19. Even though the four individual elements are endfire in nature, they can be arranged to produce a unidirectional broadside beam. A side view of the four elements is shown schematically in figure 20. The two left and right elements form arrays 1 and 2 respectively. The angle between the two top elements is ψ. Now, for small ψ angles, the radiation patterns in the plane of the paper for arrays 1 and 2 will be bidirectional and nearly identical. The effective centers of the arrays are shown in the sketch. If the phase of the radiation from array 2 can be delayed an amount equal to 180° minus the electrical separation between the effective centers, then the fields will cancel to the left but add to the right. Thus a unidirectional beam, as illustrated by the pattern multiplication in figure 20, will be formed.

The proper phasing can be accomplished by scaling either array 1 or 2 by the factor K as described previously. The distance between the effective centers is controlled by the angle ψ. The optimum values of ψ and K for the structure shown in figure 19 were arrived at experimentally. These values and the corresponding E-plane radiation patterns are shown in figure 21. The beamwidths are on the order of 65° and the side lobe

level is approximately 10 db. Recent results for a similar structure but with $\tau = .707$ have demonstrated even better side lobe and frequency independent characteristics. Time has not permitted the investigation of arrays of broadside elements similar to that shown in figure 18. However, no major problems in accomplishing this are foreseen.

Conclusion

The foregoing has demonstrated the feasibility of constructing high gain arrays whose properties are essentially independent of frequency. Such arrays should prove useful in communication, direction finding, search, and countermeasures systems, or any application that requires pattern control over a wide range of frequencies. When an array like that of figure 2 is placed above ground with its vertex on the ground the distance from ground to the array phase center measured in wavelengths will be independent of frequency. Consequently the radiation pattern, including the vertical plane pattern, will be essentially independent of frequency provided that the ground reflection coefficient changes little with frequency. The elevation angle of the main lobe may be controlled by the angle with which the array is oriented with respect to ground. This type of antenna would be ideal for point to point h-f communication nets where the operating frequency is determined by varying propagation conditions.

Since broadside arrays appear to hold promise of providing a more economical method of producing directivity, further efforts in this direction are warranted.

Acknowledgement

It is a pleasure to acknowledge the assistance of F. R. Ore who performed the phase center investigation and R. D. Gorman who fabricated and tested many of the antennas.

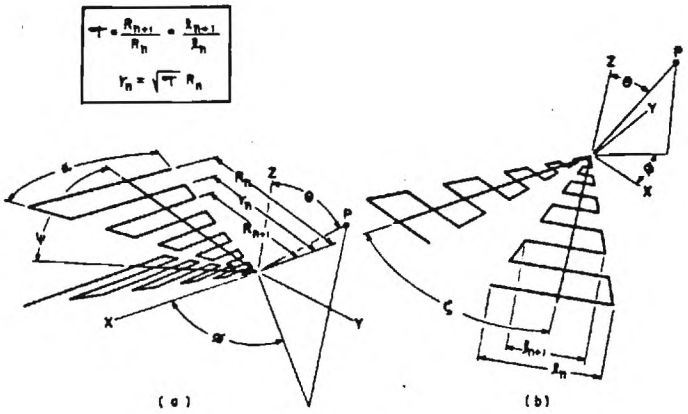

PARAMETER & COORDINATE SYSTEM FOR TRAPEZOIDAL TOOTH STRUCTURES

Fig. 1.

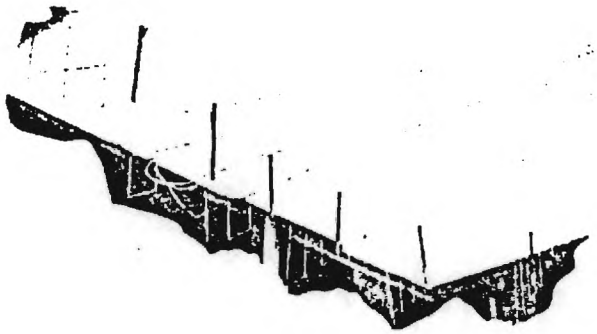

Fig. 2. Six-element phased array.

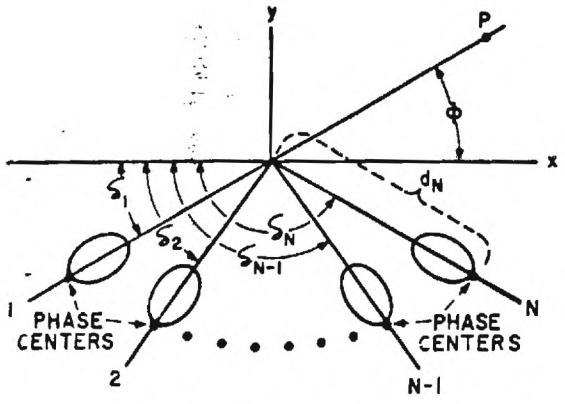

$$E(\phi)=\sum_{n=1}^{N} A_n f(\phi-\zeta_n)\, e^{-j[\beta d \cos.(\phi-\zeta_n)-\gamma_n]}$$

GEOMETRY FOR ARRAY OF END-FIRE ELEMENTS

Fig. 3.

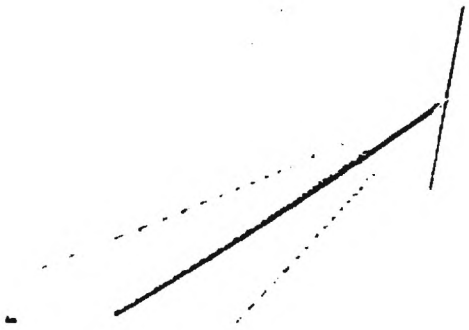

Fig. 4. Single element fed against a short rod.

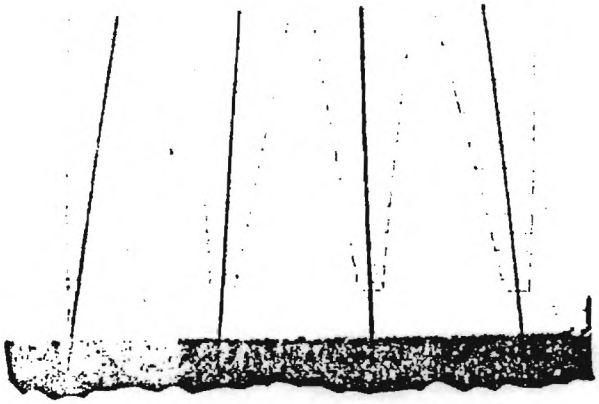

Fig. 5. Single elements showing variation in T.
From left: T = .95, .915, .83, .75.

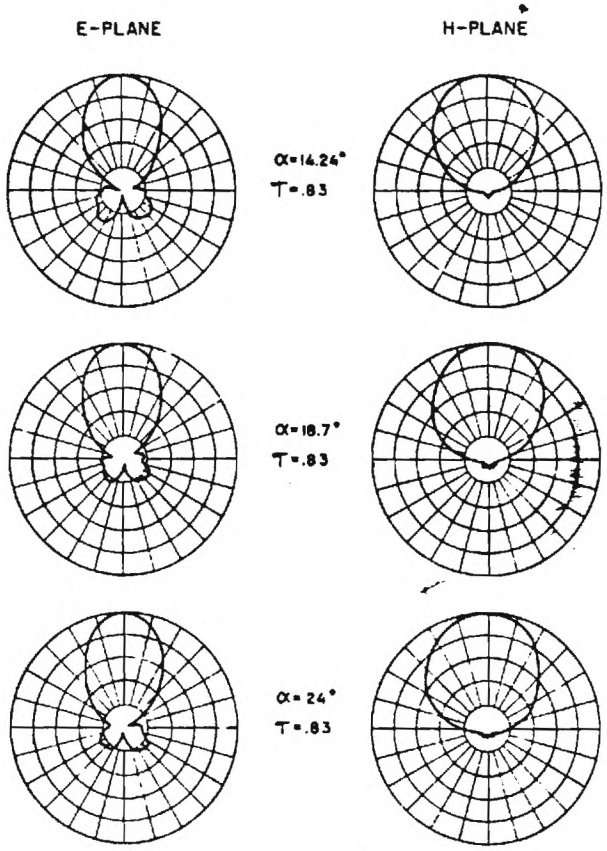

RADIATION PATTERNS OF SINGLE ELEMENTS

Fig. 6.

BEAM WIDTH

	α = 14.24°		α = 18.7°		α = 24°	
τ	E PL.	H PL.	E PL.	H PL.	E PL.	H PL.
.75	63°-72°	96-125	63-66	111-114	61-64	93-113
.83	55-62	73-87	54-59	73-88	56-60	88-96
.915	48-54	60-70	52-59	69-75	54-56	76-80
.95	47-54	58-67	47-52	66-69	53-62	67-79

VARIATION OF BEAM WIDTH OF SINGLE ELEMENTS OVER A PERIOD

(a)

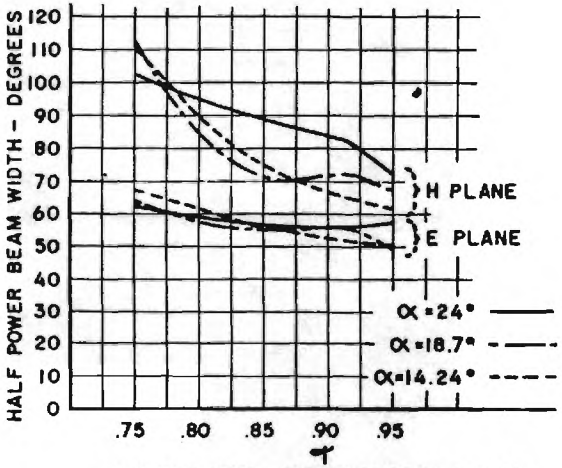

HALF POWER BEAM WIDTH VS. τ OF SINGLE ELEMENTS

(b)

Fig. 7.

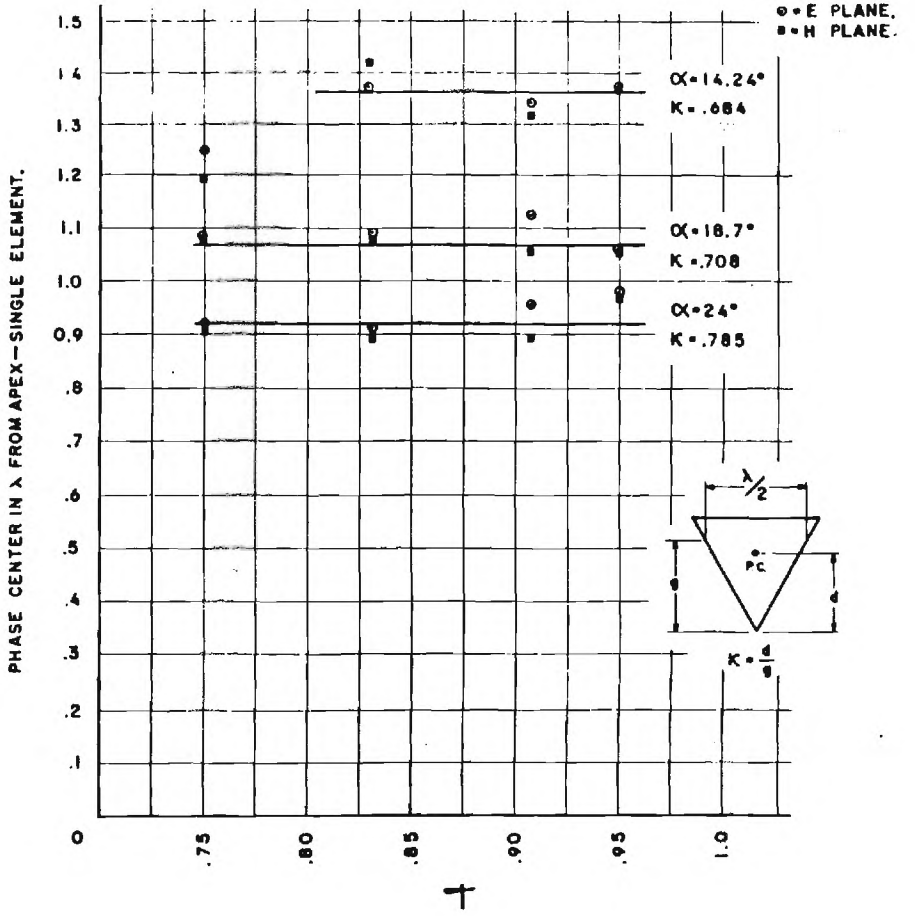

GRAPH OF DISTANCE FROM APEX TO PHASE CENTER IN WAVE LENGTHS VS. τ FOR VARIOUS α's.

Fig. 8.

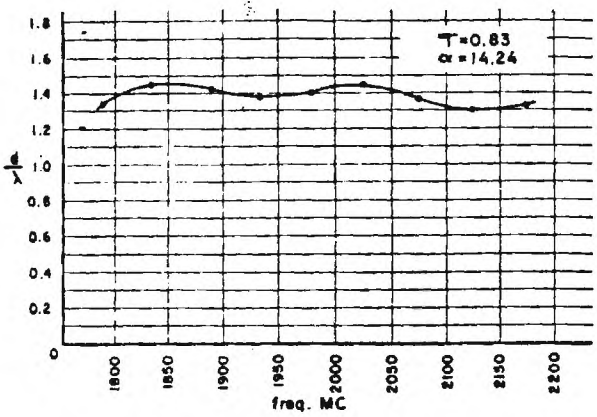

GRAPH OF DISTANCE FROM APEX TO PHASE CENTER IN WAVE LENGHTS vs. FREQUENCY FOR A SINGLE STRUCTURE.

Fig. 9.

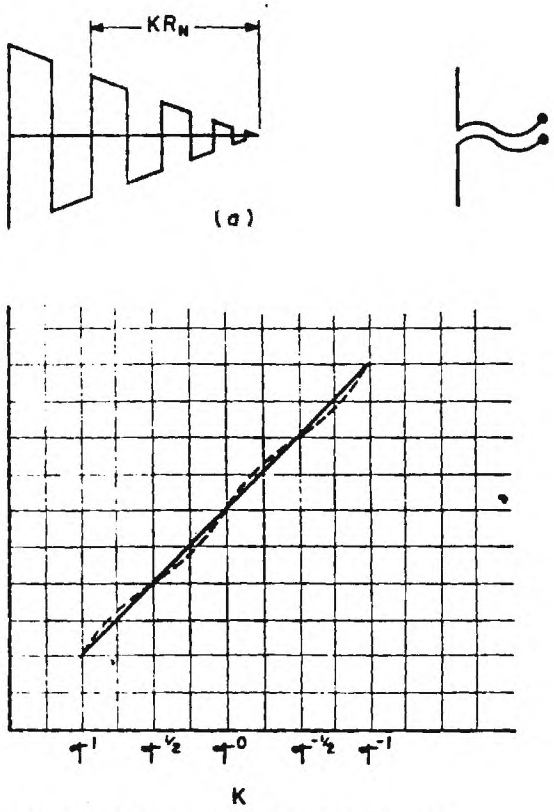

PHASE OF RADIATED FIELD VS. SCALE FACTOR (K)
(b)

Fig. 10.

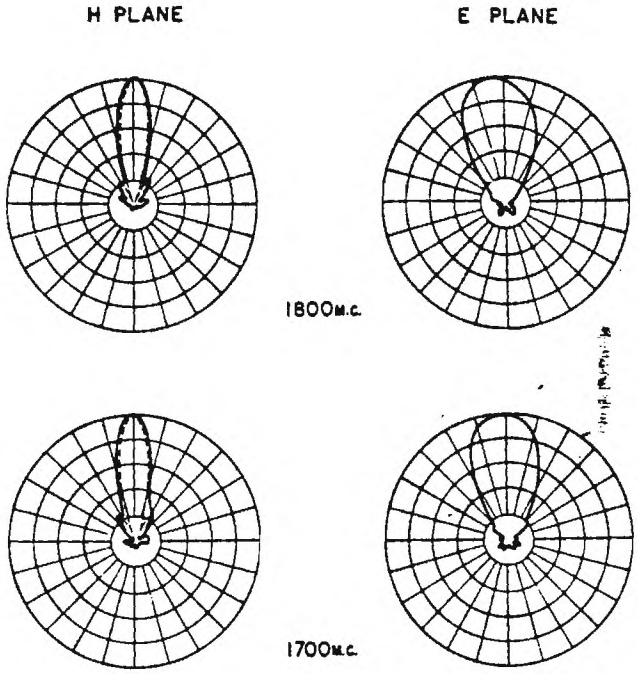

PREDICTED (----) & MEASURED (——) PATTERNS OF SIX ELEMENT PHASED ARRAY

Fig. 11.

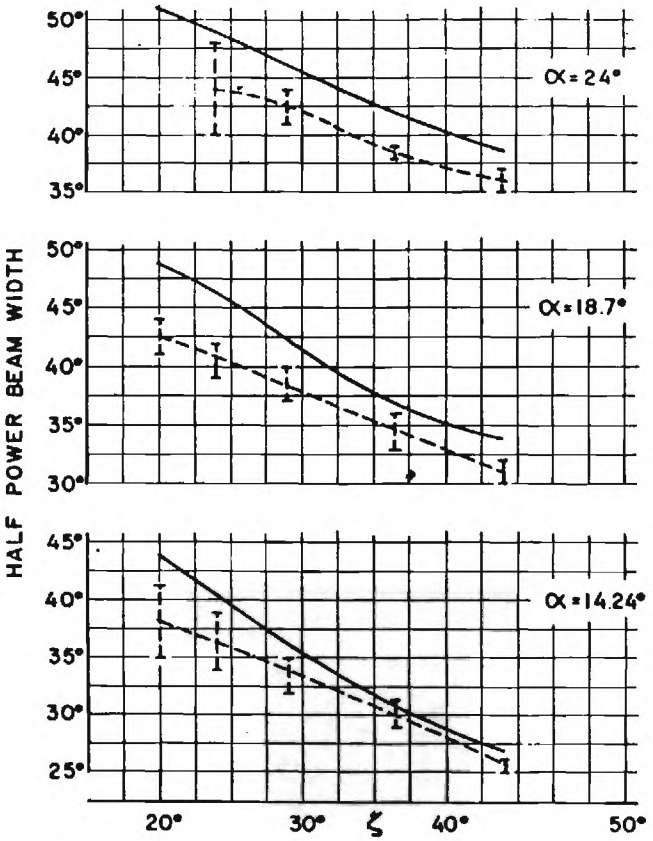

PREDICTED (——) & MEASURED (----) E PLANE HALF POWER BEAM WIDTHS VS. ζ FOR VARIOUS α's.

Fig. 12.

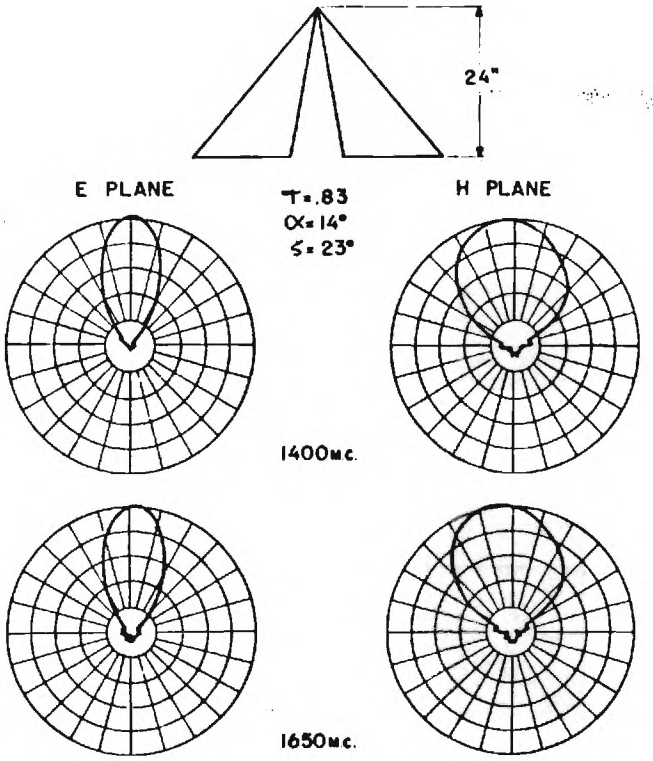

RADIATION PATTERNS OF A TWO ELEMENT COPLANER ARRAY

Fig. 13.

— α = 14.24° —

ζ IN DEGREES →	20°		24°		29°		36.4°		44°	
τ	E PL.	H PL.	E PL.	H PL.	E PL.	H PL.	E PL.	H PL.	E PL.	H PL.
.75	41°-48°	99-135	38-43	92-139	34-40	81-116	28-33	101-146	24-29	100-147
.83	35°-41°	68-81	34-39	69-82	32-38	78-94	29-31	88-106	25-26	85-108
.915	30°-43°	56-62	33-37	57-64	31-34	59-72	28-33	62-91	26-29	68-86
.95	33°-38°	46-70	31-38	54-95	28-33	49-86	24-33	59-86	23-30	50-100

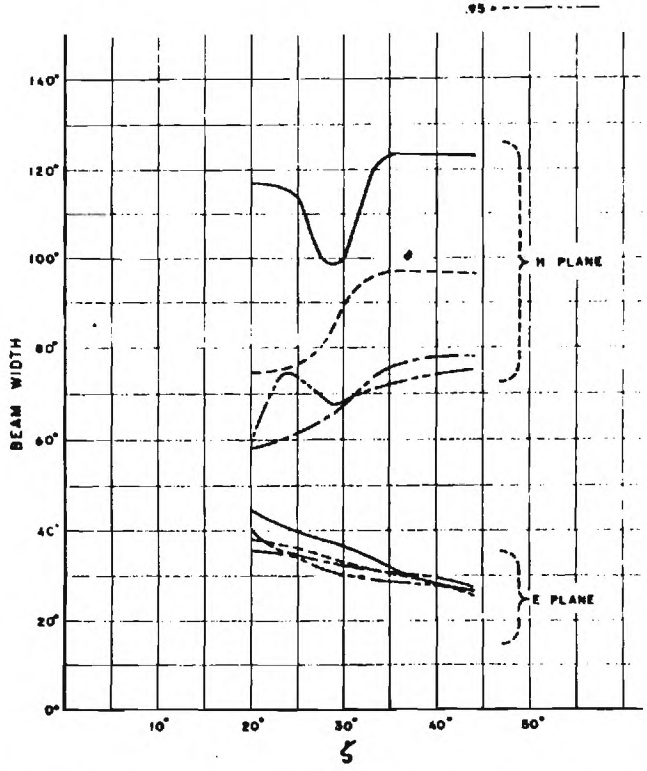

Fig. 14 a . Half-power beam width vs. ζ for two-element coplanar arrays: α = 14.24 degrees.

— α = 18.7° —

ζ IN DEGREES →	20°		24°		29°		36.4°		44°	
τ	E PL.	H PL.	E PL.	H PL.	E PL.	H PL.	E PL.	H PL.	E PL.	H PL.
.75	43°-45°	91-100	41-44	97-111	39-41	105-117	34-36	107-131	30-33	105-133
.83	41°-44°	87-95	39-42	70-79	37-40	71-81	33-36	76-95	30-32	84-103
.915	40°-47°	62-80	38-44	64-70	39-43	66-78	39-37	68-77	32-35	73-86
.95	40°-46°	68-77	42-53	64-73	38-41	64-73	33-36	64-72	31-34	65-86

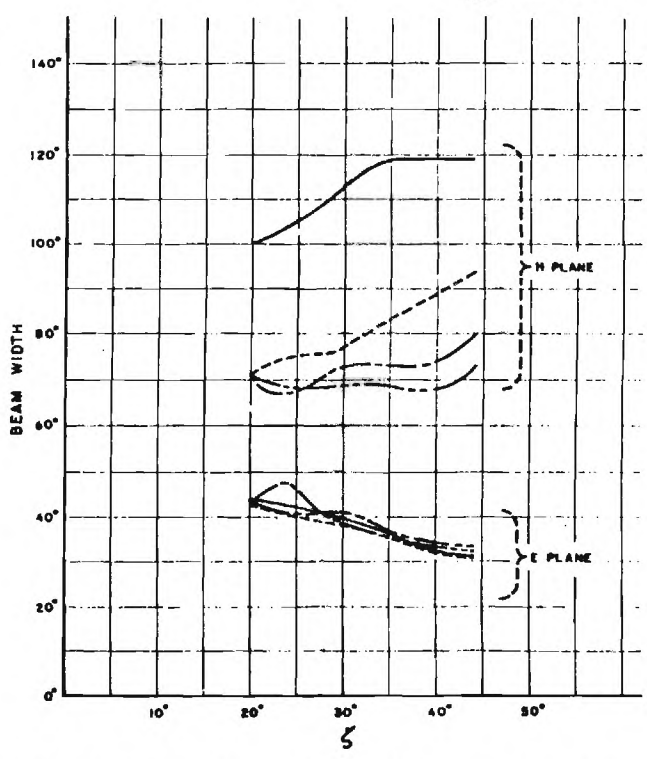

Fig. 14 b . Half-power beam width vs. ζ for two-element coplanar arrays: α = 18.7 degrees.

$\alpha = 24°$

ζ IN DEGREES →	20°		24°		29°		36.4°		44°	
Υ	E PL.	H PL.	E PL.	H PL.	E PL.	H PL.	E PL.	H PL.	E PL.	H PL.
.78			40-46	103-116	40-44	100-115	37-40	100-122	33-37	112-137
.83			40-48	69-78	41-44	78-85	38-39	77-99	35-37	96-113
.915			43-58	60-72	42-43	70-76	39-41	72-80	34-38	74-85
.98					39-43	68-77	38-44	80-93		

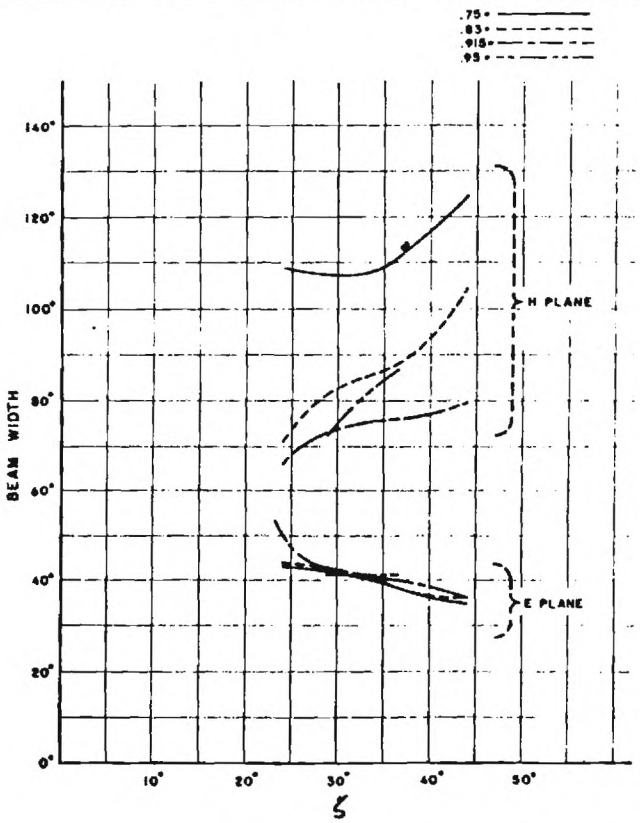

Fig. 14 c . Half-power beam width vs. ζ for two-element coplanar arrays: α = 24 degrees.

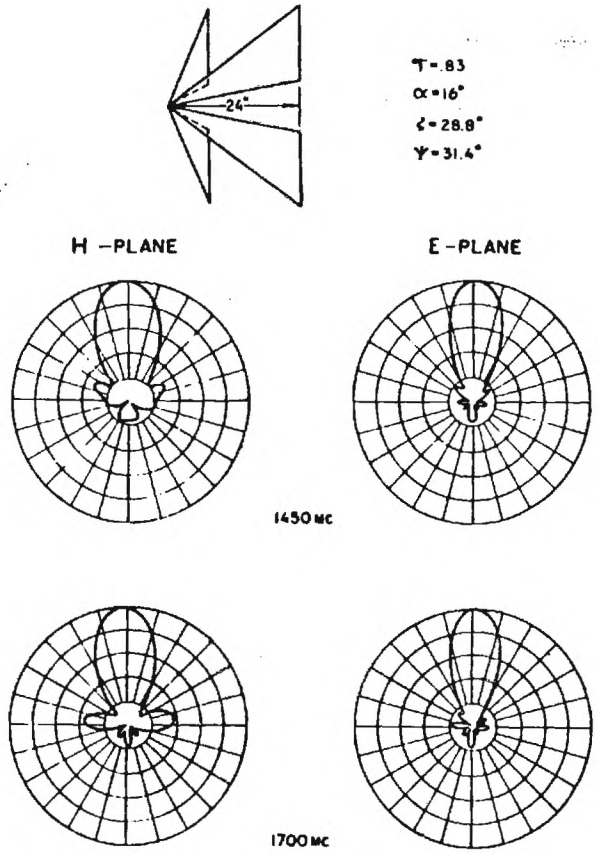

RADIATION PATTERNS OF A FOUR ELEMENT ARRAY OF IDENTICAL ELEMENTS

Fig. 15.

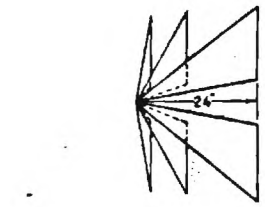

RADIATION PATTERNS OF A SIX ELEMENT ARRAY OF IDENTICAL ELEMENTS

Fig. 16.

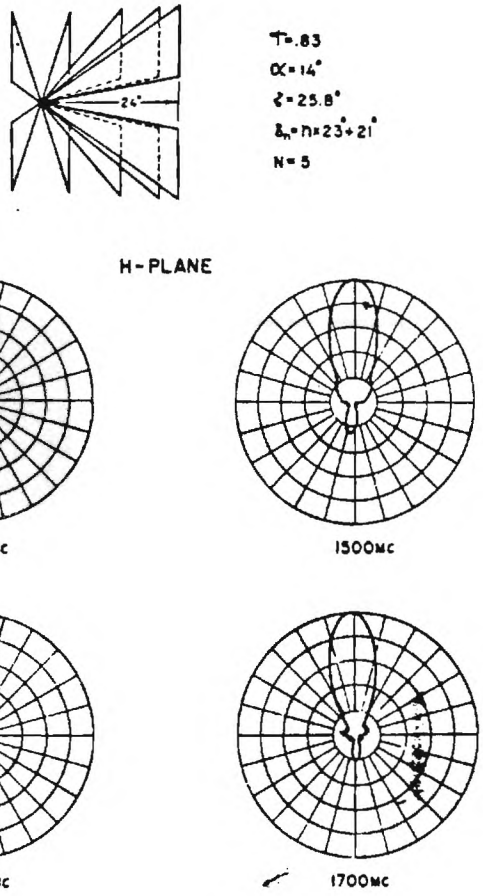

RADIATION PATTERNS OF AN ELECTRICALLY STEERABLE ARRAY

Fig. 17.

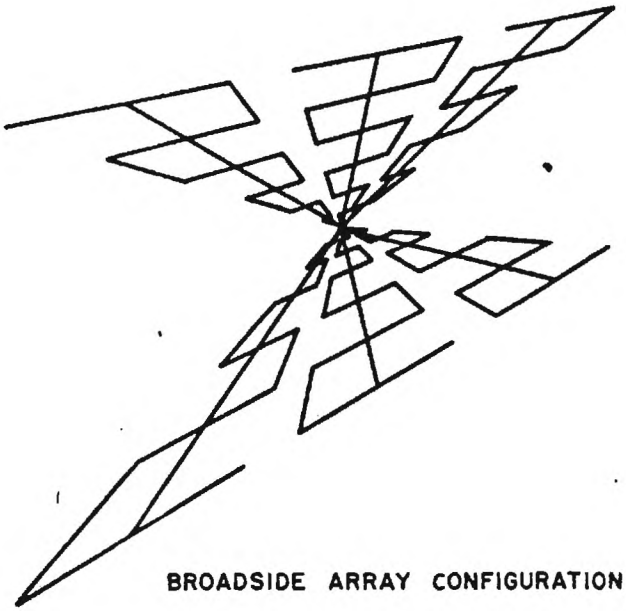

BROADSIDE ARRAY CONFIGURATION

Fig. 18.

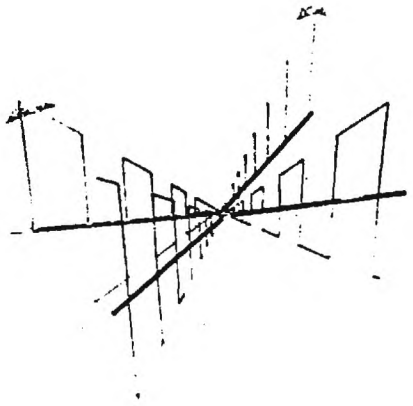

Fig. 19. Unidirectional broadside array.

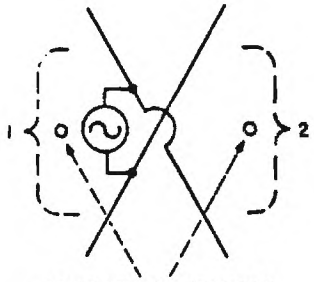

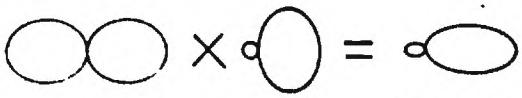

APPROXIMATE SCHEMATIC REPRESENTATION FOR UNIDIRECTIONAL BROADSIDE ARRAY

Fig. 20.

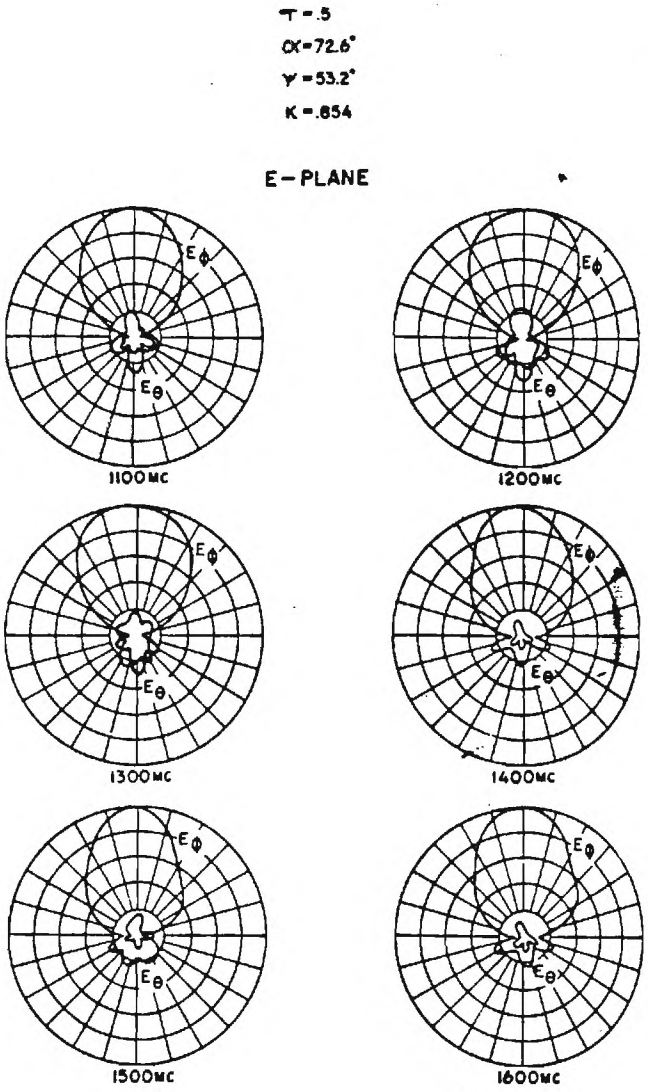

PATTERNS OF UNIDIRECTIONAL BROADSIDE ARRAY

Fig. 21.

Arleigh Burke (DDG 51) class

Origin: USA
Type: Destroyer (DDG)
Built: 1984-
Class: 1 building; 28 to be ordered
Displacement: 8,400 tons full load
Dimensions: Length 466ft (142.1m) oa; beam 60ft (18.3m); draught 30ft (9.1m) over sonar dome
Propulsion: 2-shaft gas turbine (4 General Electric LM2500), 80,000shp
Performance: Speed 30+ knots; range 5,000nm at 20 knots
Weapons: SSM: 2 x 4 Harpoon launchers; 56 Tomahawk
SAM: Vertically-launched Standard SM-2 (MR)
Guns: 1 5in/54 Mk 45; 2 20mm Phalanx Mk 15 CIWS
ASW weapons: Asroc; 2 x 3 Mk 32 torpedo tubes
Vertical Launch System: 2 Mk 41
Sensors: Radar: SPY-1D (Aegis) multi-purpose phased array; SPS-67(V) surface search; Mk 99 (3 SPG-62 radar) missile fire control system
Sonar: SQS-53C; SQR-19 (TACTAS) towed array
Complement: 303

Background: The Arleigh Burke (DDG 51) class is intended to replace the Adams and Coontz class guided-missile destroyers, which have been in service since the early 1960s. The primary mission of the DDG 51 class will be anti-air warfare, for which they will be fitted with the SPY-1D version of the Aegis system, and they will also have significant anti-surface and anti-submarine capabilities.

The first of class is already under construction at the Bath Iron Works, in Maine, and is due to be commissioned in October 1989. Another two ships will be requested from Congress in FY87, followed by five ships annually in FY88, FY89, and FY90, with a further 11 to follow.

Following the disastrous fire on the USS Belknap (CV 26), the only aluminium to be used will be on the funnels, the rest of the ships being constructed of steel. In addition, in consequence of the Royal Navy's experience in the South Atlantic War of 1982, armoured protection is to be reintroduced, with some 70 tons (71,000kg) of Kevlar armour being incorporated in the structure to protect vital spaces.

The early ships of the class will be powered by the proven General Electric LM 2500 gas turbines, but experiments are continuing with the Rankin Closed Cycle Energy Recovery (RACER) system, in which heat from the exhaust gases is used to create steam which drives another turbine. This is estimated to add another 1,000nm to the ship's range. The system is to be tested in a Military Sealift Command vessel (the *Admiral William Callaghan*), and if successful could be installed in the ninth ship of the Arleigh Burke class (DDG 59).

One of the more controversial aspects of the ships' design is that they will not have hanger facilities,

Below: The *Arleigh Burke* as constructed. The greater beam incorporated into this design in comparison with destroyers and frigates constructed in the 1960s and 1970s is obvious from this drawing. Another feature clearly shown is the uncluttered foredeck, which leads uninformed critics to conclude that US ships are poorly armed in comparison with Soviet ships such as those of the Krivak class, whose foredecks bristle with weaponry. In fact, the automatic 5in/54 Mk 45 gun is highly capable and has a large magazine below decks, while the forward Mk 41 Vertical Launch System has no less 29 missiles.

and be able to refuel and rearm helicopters. This decision was greeted with some incredulity at first. It will certainly impose limitations on single ship deployments, and is obviously now regretted, as it has already been announced that the improved Arleigh Burke class will have hanger facilities.

There has been much study in various Western naval design bureaux of the possible advantages of a shorter, beamier hull. The US Navy appears to be following this trend with the Arleigh Burkes, which have a beam-to-length ratio of 1:7.9 compared to 1:10.2 for the Spruance class. These shorter, beamier designs are claimed to confer better sea-keeping qualities as well as improved manouvrability and more usable space.

Future: It has already been decided that only 29 ships will be built to the original DDG 51 design. There will then be a follow-on class of 31 ships to be built to an improved design, with better machinery and electronics. In addition, proper helicopter facilities will be installed, indicating that the decision not to fit a hanger is now considered to have been an error.

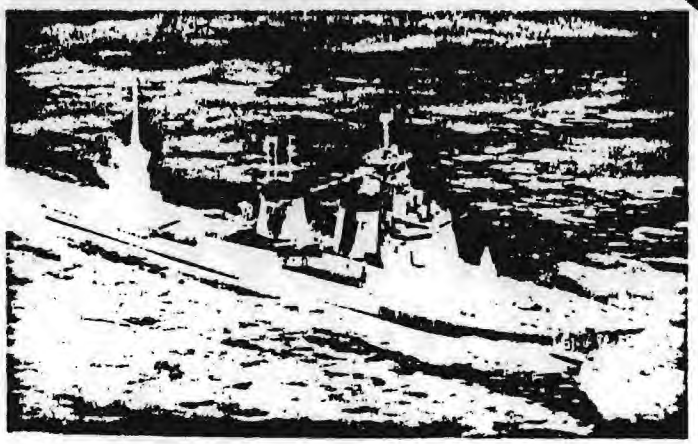

Left: An early artist's impression of the Arleigh Burke, which makes an interesting comparison with the eventual form of the ship shown above. The changes to the after end and the incorporation of the after funnel into a greatly increased superstructure are especially noteworthy. Both the original and current designs, however, lack helicopter hanger facilities, which will be rectified in the follow-on improved Arleigh Burke class.

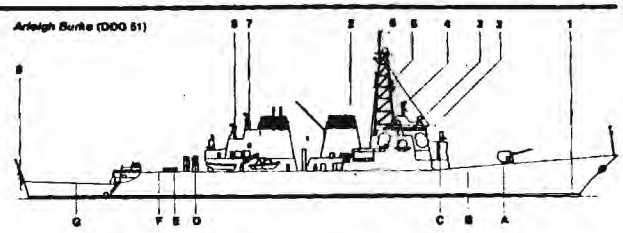

Weapons
A 5in/45 Mk 45 Mod 1 dual-purpose gun (1 x 1)
B Mk 41 Mod 0 32-cell Vertical Launch System (VLS) for Standard SM-2 (MR) SAM, Tomahawk SSM and Asroc ASW missiles
C Mk 15 20mm Vulcan-Phalanx CIWS (1 x 1)
D Harpoon SSM (2 x 4)
E Mk 32 12.75in ASW torpedo tubes (2 x 3)
F Mk 41 Mod 0 64-cell Vertical Launch System
G Landing decks for LAMPS ASW helicopters

Electronics
1 SQS-53C hull-mounted LF sonar
2 SPY-1D phased array radar
3 SLQ-32(V)2 EW system (2 x 2)
4 SPG-62 illuminator (slewed to Aegis system) for Mk 99 Fire Control System
5 SPS-67 surface search radar
6 SRN-25 Tacan antenna
7 SPG-62 illuminator
8 SPG-62 illuminator
9 SQR-19 towed array sonar

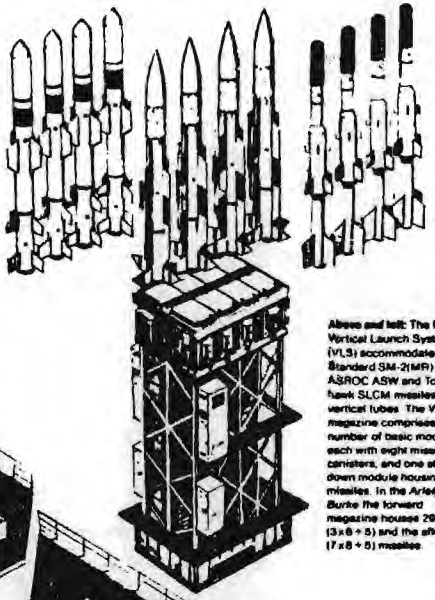

Above and left: The Mk 41 Vertical Launch System (VLS) accommodates Standard SM-2(MR) SAM, ASROC ASW and Tomahawk SLCM missiles in vertical tubes. The VLS magazine comprises a number of basic modules, each with eight missiles in canisters, and one strike-down module housing five missiles. In the *Arleigh Burke* the forward magazine houses 29 (3 x 8 + 5) and the after 61 (7 x 8 + 5) missiles.

FM

Oliver Hazard Perry (FFG 7) class

Origin: USA
Type: Frigate (FFG)
Built: 1975-
Class: (US Navy) 42 in service; 9 building; 1 on order
(Royal Australian Navy) 4 in service; 2 building
(Royal Spanish Navy) 1 in service; 4 building
Displacement: 2,750 tons light; 3,605 tons full load
Dimensions: Length 445ft (135.6m) oa; beam 45ft (13.7m); draught 14.8ft (4.5m) keel, 24.5ft (7.5m) sonar
Propulsion: 1-shaft gas turbine (2 General Electric LM2500), 40,000shp
Performance: Speed 29 knots; range 4,500nm at 20 knots
Weapons: Missiles: 1 Mk 13 launcher for Harpoon SSM (4 carried) and Standard SAM (36 carried)
Guns: 1 3in Mk 75; 1 20mm Phalanx CIWS
Torpedo tubes: 2 x 3 Mk 32
Aircraft: 2 LAMPS helicopters
Sensors: Radar: SPS-49 long-range search; SPS-55 search and navigation; STIR (modified SPG-60) weapon control
Sonar: SQS-56 hull mounted; SQR-19 TACTAS towed array (US Navy FFG 38-43, 45-60).
Complement: 185

Background: The Oliver Hazard Perry (FFG 7) class originated in the Patrol Frigate programme, which was to constitute the cheaper component of a high/low technology mix, providing large numbers of escorts with reduced capabilities and correspondingly reduced price. These were intended to balance the very expensive specialised ASW and AAW ships, whose primary mission was to protect carriers, and strict limitations were placed on cost, displacement and manpower.

The FFG 7s have been built in small yards utilising simple construction techniques, making maximum use of flat panels and bulkheads and ensuring that internal passageways are kept as straight as possible. In addition, the hull structure is prefabricated in modules of varying size (35, 100, 200 or 400 tons), to permit shipyards to select the most convenient size for their capabilities.

As with the US Navy's previous frigate classes, the Perrys have only one screw, but the use of gas turbines means that engine-room layout is much more compact. The gas turbines are of the same model used in the Spruance class, and are located side by side in a single engine room. An unusual feature is that two small retractable propulsion pods are fitted just aft of the sonar dome to provide emergency power and to give assistance in docking; each has a 325hp engine, and the two in combination can propel the ship at a speed of some 10 knots.

The armament is air-defence orientated, including a Mk 13 launcher forward for Standard (MR) SAMs and Harpoon ASMs, and an OTO-Melara 76mm (US Navy Mk 75) gun on top of the superstructure. Aaroc is not fitted, but there is a large hangar aft for the two LAMPS helicopters.

Starting with USS Underwood (FFG 36), the Rapid Haul Down and Traversing System (RAST) is being installed, necessitating an 8ft (2.4m) increase in overall length. This is being achieved by angling out the ship's transom to approximately 45°, and without increasing the waterline length. RAST, TACTAS and LAMPS III support facilities are being installed in all new-build ships from FFG 36 onward. RAST and LAMPS III support facilities will not, at least for the time being, be retrofitted into the earlier ships (FFG 7, 9-16 and 19-34), which will continue to operate LAMPS I (FFG 8 was used as the prototype for the LAMPS III conversion).

The SQS-56 sonar, hull-mounted inside a rubber dome, is a new type, much less sophisticated than the SQS-26. It was planned, however, that the FFG 7 class frigates would operate in company with other frigates equipped with the SQS-26 and would receive target information from sensors on board those ships via data links.

The success of the design can be gauged from the large numbers being built for the US Navy and the fact that it has also been ordered by the Royal Australian and Royal Spanish Navies. The former has already taken delivery of four built in the USA, with another two ordered for construction in Australia, while the latter took delivery of its first two FFG 7 frigates in 1986, when it had a further three on order.

Future: The FFG 7 has been tailored to accommodate only those systems envisaged in the near future, including the SH-60 LAMPS III, SQR-19 towed tactical array, fin stabilizers, Link 11 data transfer system and Phalanx CIWS. Once these have been installed, however, there remains only a further 50-ton margin for additional equipment.

Forty-two of the class are currently in service with the US Navy, with a further nine building and another one on order, to complete the authorized total of 52.

The Royal Australian Navy has ordered two to be built to a slightly modified design in Australia (in addition to four built in the US); these will be completed in 1991 and 1993. Five are being built at Ferrol by Bazan for the Royal Spanish Navy. The first was commissioned in 1986 and the remainder will join the fleet between late 1986 and 1990.

Below: USS **Robert E Bradley (FFG 49) showing her flight deck, large hangars, Vulcan/Phalanx CIWS and SPG-60 STIR search and tracking radar. These ships have good protection against fragmentation and splinter damage, including ¾in (1.9cm) Kevlar over vital compartments.**

Right: The RIM-66B Standard SM-1 (MR) missile has a range of 25nm (46.3km) and uses semi-active homing. The FFG 7 frigates now carry SM-1 (MR) Block 6 missiles with a digital computer and monopulse radar, and 36 are stored in a below-deck magazine. The SM-1 (MR) is fired from a single-arm Mk 13 launcher, which is also capable of firing Harpoon anti-ship missiles (four are carried in the same magazine). The Mk 92 Mod 4 system controls the fire of both the SAMs and the 76mm Mk 75 dual-purpose gun, using a STIR antenna and a US-built HSA WM-28 radar.

Below: USS *Crommelin* (FFG 37). The large box-like nature of the superstructure is clear from the drawing, this was, at least in part, intended to reduce construction costs, but also gives considerable internal volume.

Below: Sikorsky SH-60B Seahawk LAMPS III ASW helicopter, of which two can be carried by the later FFG 7 class frigates. FFG 7 to FFG 35 (less FFG 8) do not have the facilities for LAMPS III and thus retain the Kaman SH-2F Sea Sprite LAMPS I helicopter. FFG 8 (the trials ship) and FFG 36 onwards have the longer stern, fin stabilizers and other systems required for LAMPS III, while the Recovery, Assistance, Securing and Traversing (RAST) system will also be fitted to FFG 50 and later ships. The SH-60B carries 25 sonobuoys and two Mark 46 ASW torpedoes, and is equipped with ASQ-81 (V) 2 MAD and the ALQ-42 ESM system. All sensor displays are repeated back to the controlling ship via a real-time downlink.

Left: Sikorsky on-board ASW weapon system is the Mk 46 torpedo fired from two triple Mk 32 launchers. Mk 46 torpedoes are currently being upgraded to Mod 5 NEARTIP (Near-Term Improvement Program) standard.

Weapons
A Mk 13 Mod 4 single-arm launcher for Harpoon SSM and Standard SM-1 (MR) SAM
B Mk 32 12.75in ASW torpedo tubes (2x3)
C OTO Melara Mk 75 76mm dual-purpose gun
D Mk 15 20mm Vulcan Phalanx CIWS (FFG-27 onward)
E Sikorsky SH-60B Sea Hawk LAMPS III ASW helicopter

Electronics
1 SQS-56 hull-mounted sonar
2 SLQ-32(V)2 EW system antennae (2x1)
3 Mk 92 Mod 2 fire control director
4 SPS-49 long-range air search radar
5 SPS-55 surface search and navigation radar
6 URN-25 Tacan antenna
7 SPG-60 STIR search and tracking radar
8 SQR-19 TACTASS towed sonar array (FFG-36 to FFG-43 and FFG-46 to FFG-60)

Spruance (DD 963) class

Origin: USA
Type: Destroyer (DDG)
Built: 1972-1983
Class: 31 Spruance plus 4 Kidd class in service
Displacement: 5,770 tons light; 7,810 tons full load
Dimensions: Length 563.2ft (171.7m) oa; beam 55.1ft (16.8m); draught 29ft (8.8m) sonar, 19ft (5.8m) keel
Propulsion: 2-shaft gas turbine (4 General Electric LM2500), 80,000shp
Performance: Speed 33 knots; range 6,000nm at 20 knots
Weapons: SSM: 2 x 4 Harpoon launchers
SAM: 1 NATO Sea Sparrow Mk 29 launcher
Guns: 2 x 1 5in/54 Mk 45; 2 20mm Phalanx Mk 15 CIWS
ASW weapons: 1 8-tube Asroc launcher (24 rounds); 2 x 3 Mk 32 torpedo tubes (14 torpedoes)
Aircraft: 1 SH-3 Sea King or two SH-2D LAMPS II helicopters
Sensors: Radar: SPS-55 and SPS-40 search (SPS-49(V) in DD 967); SPG-60 and SPQ-9A fire control
Sonar: SQS-53 or SQS 53C hull-mounted; SQR-19 TACTAS towed array
Complement: 296

Background: One of several post-war classes to arouse considerable controversy, especially in the US Congress, the Spruance class was designed to replace the war-built destroyers of the Gearing and Sumner classes, which, despite modernization programmes, were nearing the end of their useful lives by the early 1970s. The Spruances epitomize the US Navy's design philosophy of the 1970s, with their large hulls and block superstructures maximizing internal volume. They would be fitted with machinery that was easy to maintain or replace and equipped with high-technology weapon systems that could be added to or updated by modular replacement at a later date.

The object was to minimize platform costs in favour of greater expenditure on the weapon systems payload in order to ensure that the ships would remain in the front-line throughout their 30-year life expectancy. In a further attempt to minimize platform costs the entire class was ordered from a single builder (Litton/Ingalls), which invested heavily in a major production facility at Pascagoula, using advanced modular construction techniques.

The only visible weapon systems aboard the Spruances are two single 5in Mk 45 lightweight gun mountings and an Asroc box launcher forward of the bridge. In view of the size and cost of the ships this caused an immediate public outcry. The advanced ASW capabilities of the ships are, however, largely hidden within the hull and the bulky superstructure. The Asroc launcher, for example, has a magazine beneath it containing no fewer than 24 reloads, while the large hangar to port of the after funnel uptakes can accommodate two LAMPS II helicopters and two sliding doors on either side of the superstructure conceal triple Mk 32 torpedo tubes and torpedo handling rooms.

Of even greater significance are the advanced submarine detection features of the class. The SQS-53C bow sonar can operate in a variety of active and passive modes, including direct path, bottom-bounce and convergence zone. This system has proved so successful that the SQS-35 VDS initially scheduled will not now be fitted.

The all-gas turbine propulsion system, with paired General Electric LM2500 gas turbines on echelon, was selected primarily for its ease of maintenance and low manning requirements. Gas turbines also have significant advantages in reducing underwater noise emission and the Spruances are therefore capable of near-silent ASW operations.

The Spruances are fitted with the latest computerized data systems in well designed Combat Information Centres. They also have the most up-to-date digital fire control systems in the Mk 86 Gun Fire Control System and the Mk 116 underwater system.

Besides the weapon systems fitted on completion, the ships of the Spruance class were designed to accept a variety of other systems then at the design stage. All ships have now received the Sea Sparrow Improved Point Defence System (IPDMS) and Harpoon anti-ship missiles (aft of the forward funnel), and three Whiskey-3 (WSC-3) satellite communications transceivers and SLQ-32(V)2 ECM systems have also been fitted.

The inherent flexibility of the Spruance design is such that it has formed the basis for the new Ticonderoga class Aegis cruisers. The Kidd class also stemmed from the Spruance design; originally destined for the Imperial Iranian Navy, and optimized for the general warfare role rather than ASW, the four-ship order was cancelled following the Iranian revolution, and the ships were purchased by the US Navy and completed as designed, making them the most powerful destroyers in the fleet. The major difference from the Spruances is that the Kidds have two twin Mk 26 Standard/Asroc launchers.

Future: Starting from the FY85 overhauls, major improvements being made to the Spruances will enable them to remain effective ASW units well into the next century. Improvements include the installation of the LAMPS III shipboard electronics and the Recovery Assist Secure and Traverse system (RAST) for helicopter handling.

An improved version of the 5in/54 Mk 85 gun is under consideration, and the Tomahawk system will be fitted in all ships of the class, as will the Mk 41 Vertical Launch System with a 61-round magazine in place of the Asroc.

Below: USS Dayo (DD 988). Like many US ships, the Spruance class was subject to ill-informed criticism in their early days, but their merits are now appreciated.

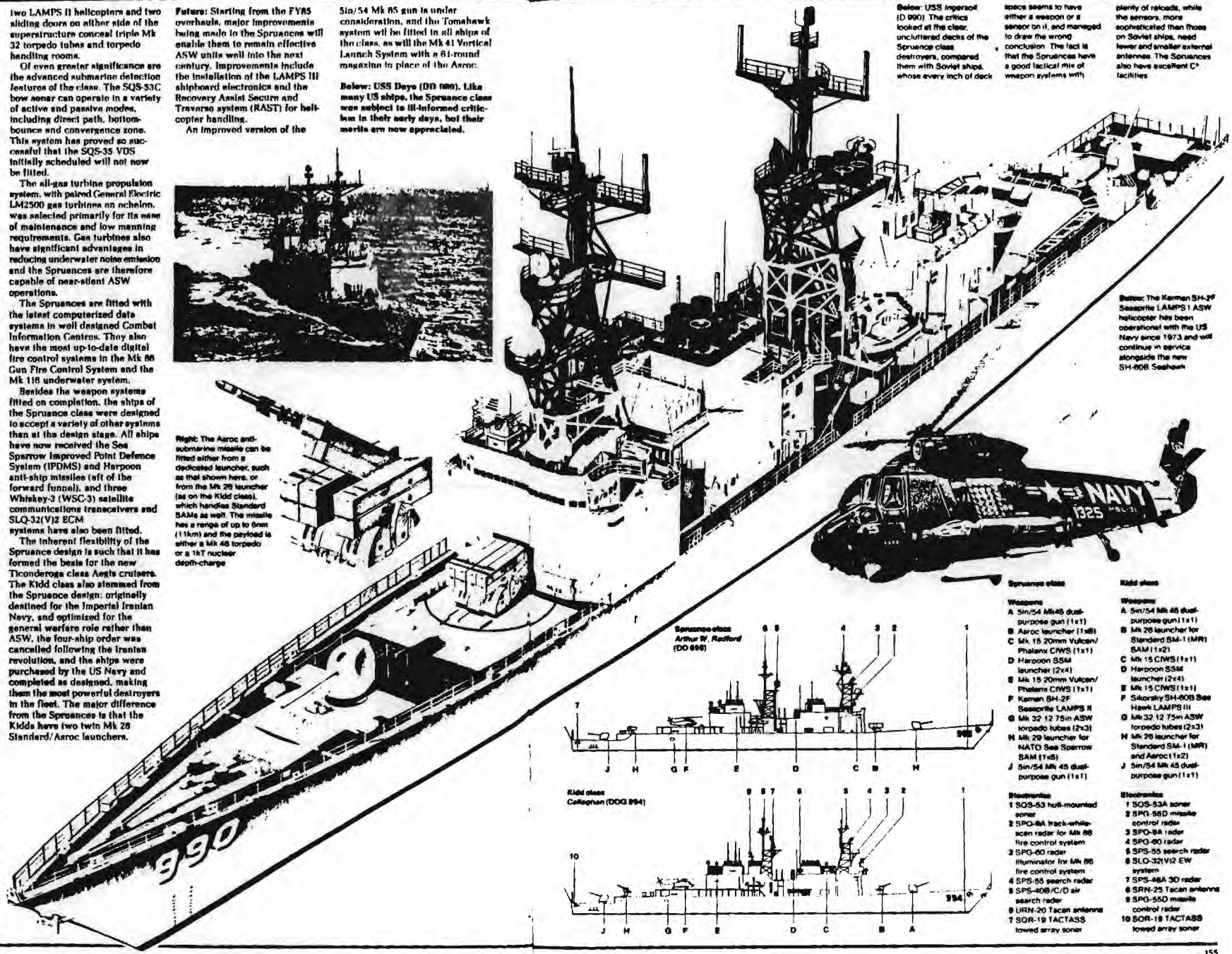

Right: The Asroc anti-submarine missile can be fitted either from a dedicated launcher, such as that shown here, or from the Mk 26 launcher (as on the Kidd class), which handles Standard SAMs as well. The missile has a range of up to 6nm (11km) and the payload is either a Mk 46 torpedo or a 1kT nuclear depth-charge

Below: USS Ingersoll (D 990). The critics looked at the clear, uncluttered decks of the Spruance class destroyers, compared them with Soviet ships, whose every inch of deck space seems to have either a weapon or a sensor on it, and managed to draw the wrong conclusion. The fact is that the Spruances have a good tactical mix of weapon systems with plenty of reloads, while the sensors, more sophisticated than those on Soviet ships, need fewer and smaller external antennae. The Spruances also have excellent C³ facilities

Below: The Kamman SH-2F Seasprite LAMPS I ASW helicopter has been operational with the US Navy since 1973 and will continue in service alongside the new SH-60B Seahawk

Spruance class

Weapons
A 5in/54 Mk45 dual-purpose gun (1x1)
B Asroc launcher (1x8)
C Mk 15 20mm Vulcan/Phalanx CIWS (1x1)
D Harpoon SSM launcher (2x4)
E Mk 15 20mm Vulcan/Phalanx CIWS (1x1)
F Kamen SH-2F Seasprite LAMPS II
G Mk 32 12 75in ASW torpedo tubes (2x3)
H Mk 29 launcher for NATO Sea Sparrow SAM (1x8)
J 5in/54 Mk 45 dual-purpose gun (1x1)

Electronics
1 SQS-53 hull-mounted sonar
2 SPQ-9A track-while-scan radar for Mk 86 fire control system
3 SPG-60 radar illuminator for Mk 86 fire control system
4 SPS-55 search radar
5 SPS-40B/C/D air search radar
6 URN-20 Tacan antenna
7 SQR-19 TACTASS towed array sonar

Kidd class

Weapons
A 5in/54 Mk 45 dual-purpose gun (1x1)
B Mk 26 launcher for Standard SM-1 (MR) SAM (1x2)
C Mk 15 CIWS (1x1)
D Harpoon SSM launcher (2x4)
E Mk 15 CIWS (1x1)
F Sikorsky SH-60B Sea Hawk LAMPS III
G Mk 32 12 75in ASW torpedo tubes (2x3)
H Mk 26 launcher for Standard SM-1 (MR) and Asroc (1x2)
J 5in/54 Mk 45 dual-purpose gun (1x1)

Electronics
1 SQS-53A sonar
2 SPG-58D missile control radar
3 SPQ-9A radar
4 SPG-60 radar
5 SPS-55 search radar
6 SLQ-32(V)2 EW system
7 SPS-48A 3D radar
8 SRN-25 Tacan antenna
9 SPG-55D missile control radar
10 SQR-19 TACTASS towed array sonar

Ticonderoga (CG 47) class

Origin: USA
Type: Guided-missile cruiser (CG)
Built: 1980-
Class: 4 in service; 6 building; 6 ordered; 12 projected
Displacement: 9,600 tons full load
Dimensions: Length 566.8ft (172.8m) oa; beam 55ft (16.8m); draught 31ft (9.5m)
Propulsion: 2-shaft gas turbine (4 General Electric LM2500), 80,000shp
Performance: Speed 30 knots
Weapons: SSM: 8 Harpoon; 30 Tomahawk (CG 52 onward)
SAM: 2 twin Mk 26 launchers with 88 Standard SM-2(MR)/Asroc (CG 47-51); 2 Mk 41 Vertical Launch Systems for 122 Standard SM-2(MR)/Asroc/Tomahawk (CG 52 onward)
Guns: 2 single 5in/54 Mk 45; 2 Phalanx 20mm/76 Mk 16 CIWS; 2 40mm (saluting)
Torpedo tubes: 2 x 3 Mk 32 21in
Aircraft: 2 LAMPS I or III helicopters
Sensors: Radar: SPY-1A 3D phased arrays (CG 47-58); 2 SPY-1B (CG 59 onward); SPS-49(V) air search; SPS-55 surface search; SPQ-9 fire control; LN-66 navigation (CG 47-53); SPS-64 navigation (CG 54 onward)
Sonar: SQS-53A (CG 47-CG 53) bow-mounted; SQS-53B (CG 54 onward); SQR-19 (TACTAS) towed array (CG 54 onwards)
Complement: 375

Background: The US Navy is well used to public criticism of its new ships, especially from Congress, and the Spruance, Oliver Hazard Perry and Virginia classes have all had their fair share. Seldom, however, has so much ill-informed and hostile comment been directed at any one class as that provoked by the Ticonderogas. The ship and her electronics systems have recently vindicated themselves in a series of rigorous tests, backed up by some very successful operational deployments, and they are now among the most potent warships afloat.

The Aegis Combat System, one of the most important breakthroughs in naval technology of recent years, was developed in response to the threat of saturation missile attacks that form the basis of Soviet anti-carrier tactics during the 1980s and beyond. To cope with such tactics, sensors must be able to react virtually instantaneously and have a virtually unlimited tracking capability, but conventional rotating radars are limited both in data-processing capacity and in the number of target tracks they can handle; therefore a new system had to be found.

The solution adopted with the Aegis system is to mount four fixed planar arrays on the superstructure of the ship, two on each of the forward and after deckhouses. Each array has 4,100 radiating elements and is controlled by a UYK-1 digital computer to produce and steer multiple beams for target search, detection and tracking. Targets are automatically tracked, arranged in priority of threat and then engaged, either automatically or with manual override, by a variety of defensive systems. The system also produces target designation data for the Raytheon target illuminating radars which direct the semi-active radar homing Standard SM-2 (ER) missile.

At longer ranges air targets are engaged by the SM-2 missile, fired from one of two Mk 26 launchers. Up to 18 missiles can be kept in the air in addition to four in the terminal phase, and the Mk 99 illuminators switch rapidly from one target to the next under computer control. Close-range defence is provided by two 5in/54 guns, while the final line of defence is provided by two Phalanx CIWS.

It was originally envisaged that this very sophisticated system would be installed in nuclear-powered escorts such as the planned Strike Cruiser (CSGN) or the Modified Virginia (CGN-42) class, but the enormous cost of the system, coupled with that of nuclear propulsion, proved to be prohibitively expensive, especially in the budgetary climate of the later years of the Carter Administration. Since it was considered that two Aegis escorts would be required for each of the 12 carrier battle groups and because not be nuclear powered, it was decided to utilize the growth potential of the gas turbine powered Spruance design to incorporate the necessary electronics.

Ticonderoga and her sisters are designed to serve as flagships and are, therefore, equipped with an elaborate Combat Information Centre, which has an integral flag function and is able to accept and coordinate data from other ships and aircraft in the group. This was found to be invaluable during USS Ticonderoga's deployment off Beirut, and the admiral in command routinely exercised command from this ship because of the excellent facilities. In addition, because the Aegis system worked so well, he was able to reduce the Combat Air Patrol (CAP) cover, a significant contribution to the combat effectiveness of the task group.

Future: Twenty-eight units are currently projected and it is envisaged that they will operate in conjunction with specialized ASW and AAW DDGs of the Spruance

Below: The McDonnell Douglas Harpoon has proved an outstanding success, with well over 2,000 on order for the US and numerous foreign navies. The missile can be fired from aircraft (AGM-84), submarines (UGM-84) and surface ships (RGM-84A), and is propelled by a turbojet, through the surface and submarine versions both have an additional rocket booster; cruise speed is Mach 0.85. Maximum range is 60nm (111km) in the original version and 85nm (157km) in the improved Block 1 missiles, but external targeting systems such as helicopters are required to achieve over-the-horizon ranges.

The shipborne version is usually launched from a simple canister. Despite its ruggedness, the mounting on the Ticonderogas is in an exposed position and must suffer in a seaway.

Right: USS Vincennes (CG 49), her massive superstructure and its two SPY-1A arrays clearly visible. Note also the two Mk 80 illuminator-directors above the bridge with the ball-shaped cover for the SPQ-9 fire control radar antenna above them. The hull of the Ticonderoga class cruisers is identical with that of the Spruance class destroyers, a fact which has produced considerable savings.

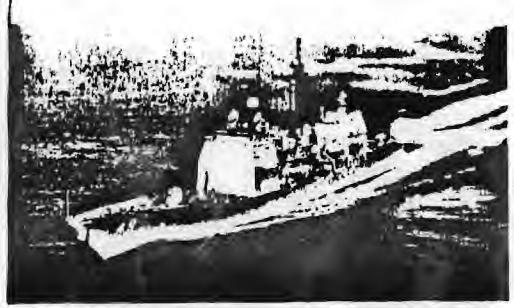

Weapons
A 5in/54 Mk 45 dual-purpose gun (1x1)
B Mk 26 Mod 1 missile launcher (1x2) for Standard SM-2(MR) SAM and Asroc ASW missiles
C 20mm/76 Mk 16 Vulcan/Phalanx CIWS (2x1)
D Sikorsky SH-60B Sea hawk LAMPS III ASW helicopter (2 carried)
E Mk 32 12 75in ASW torpedo tubes (2x3) for Mk 46 torpedoes
F Mk 26 Mod 1 missile launcher (1x2) for Standard SM-2(MR) SAM and Asroc ASW missiles
G 5in/54 Mk 45 dual-purpose gun (1x1)
H Mk 141 launchers for RGM-84A Harpoon SSM (2x4)

Electronics
1 SQS-53 bow-mounted sonar
2 SPY-1A phased array radar forward and starboard arrays (SPY-B from CG 59)
3 WSC-1V satellite communications antenna
4 Mk 80 illuminator-director (SPG-62 radar) (2x1)
5 SPQ-9 gun fire control radar
6 SPS-55 surface search radar
7 URD-1 direction-finding antenna
8 SLQ(V)3 jammer (2x1)
9 Communications antenna
10 UPX-29 IFF interrogator (circular array)
11 SPS-49(V)8 air search radar
12 Mk 80 illuminator-director (SPG-62 radar)
13 Mk 80 illuminator-director (SPG-62 radar)
14 SPY-1A phased array radar aft and port arrays (SPY-1B from CG 59 onward)
15 SQR-19 variable depth sonar (to be installed in Cg 54 onward)

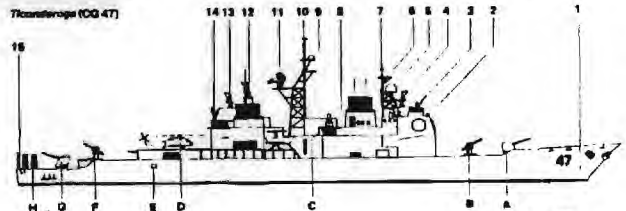

Left: The SH-60B Seahawk LAMPS III is equipped with APS-124 radar, FLIR, sonobuoys and ASQ-81 (V)2 MAD, whose red and yellow bird can be seen under the starboard pylon. Normal weapon load is two Mk 46 torpedoes

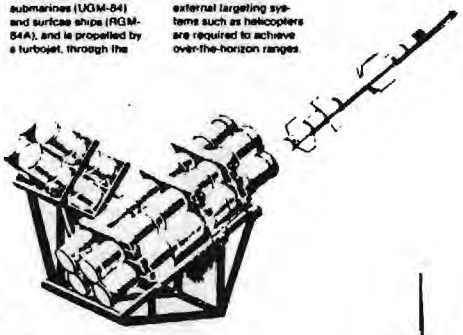

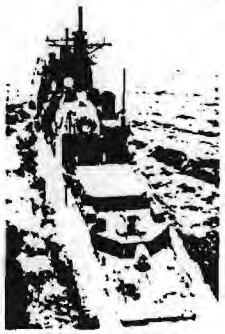

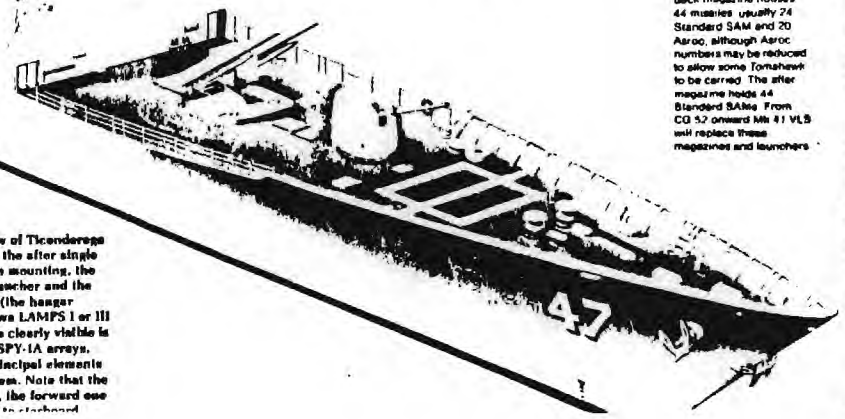

Left: The foredeck of USS Ticonderoga is a typical product of modern US Navy practice, with only one gun mounting and one Mk 26 twin-arm launcher to be seen. The underdeck magazine houses 44 missiles, usually 24 Standard SAM and 20 Asroc, although Asroc numbers may be reduced to allow some Tomahawk to be carried. The after magazine holds 44 Standard SAMs. From CG 52 onward Mk 41 VLS will replace these magazines and launchers.

Left: A stern view of Ticonderoga (CG 47) showing the after single 5in/54 Mk 45 gun mounting, the Mk 26 missile launcher and the large flight deck (the hangar accommodates two LAMPS I or III helicopters). Also clearly visible is the after pair of SPY-1A arrays, which are the principal elements in the Aegis system. Note that the stacks are offset, the forward one

Antenna Measurement

Antennas

Series 28 Broadband Dual Polarized Feeds

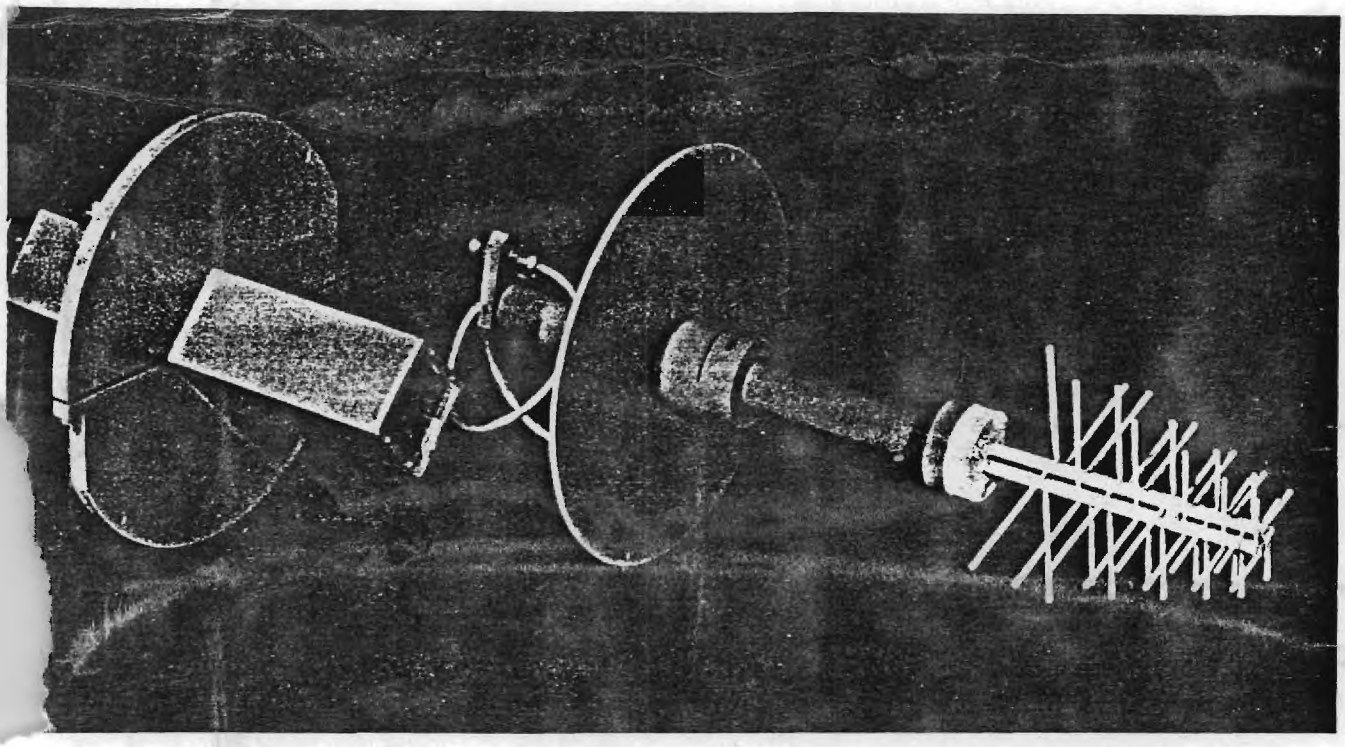

tenna Feeds

es 28 Antenna feeds are dual-polarized feeds intended ıse with Series 22 Reflectors.

es 28C Antenna Feeds utilize a dual-polarized struc- and a 90 degree hybrid, with a 50-ohm termination. -hand circular, right-hand circular, or dual-linear polari- ɔns can be obtained by proper element excitation.

ause of the frequency and polarization versatility of .e antennas, they are particularly useful on antenna ranges. They also have applications in communica- ɜ and monitoring links.

The 28 and 28C Series of antenna feeds are made up of two types of structures. The frequency range from 0.5 GHz to 2.0 GHz is covered with crossed log-periodic dipole arrays. Four-ridged waveguide feeds are used from 2.0 to 18 GHz. All waveguide feeds are treated to resist corrosion and weathersealed with a radome cover. A desiccator in the feeds absorbs any moisture which may accumulate.

All Series 28 and 28C Antenna Feeds are supplied with procedures for mechanically aligning and adjusting the feed in their respective reflectors. Electrical alignment and focusing for optimum radiation patterns can be performed at the factory and copies of the data provided for an additional cost per unit.